

U. S. DEPARTMENT OF COMMERCE

WEATHER BUREAU

TECHNICAL PAPER NO. 47

**PROBABLE MAXIMUM PRECIPITATION
AND RAINFALL-FREQUENCY DATA FOR ALASKA**

**for Areas to 400 Square Miles, Durations to 24 Hours,
and Return Periods from 1 to 100 Years**

Weather Bureau Technical Papers

- | | |
|--|---|
| <p>*No. 1. Ten-year normals of pressure tendencies and hourly station pressures for the United States. 1943.
*Supplement: Normal 3-hourly pressure changes for the United States at the intermediate synoptic hours. 1945.</p> <p>*No. 2. Maximum recorded United States point rainfall for 5 minutes to 24 hours at 207 first order stations. 1947.</p> <p>*No. 3. Extreme temperatures in the upper air. 1947.</p> <p>*No. 4. Topographically adjusted normal isohyetal maps for Western Colorado. 1947.</p> <p>*No. 5. Highest persisting dewpoints in western United States. 1948.</p> <p>*No. 6. Upper air average values of temperature, pressure, and relative humidity over the United States and Alaska. 1945.</p> <p>*No. 7. A report on thunderstorm conditions affecting flight operations. 1948.</p> <p>*No. 8. The climatic handbook for Washington, D.C. 1949.</p> <p>*No. 9. Temperature at selected stations in the United States, Alaska, Hawaii, and Puerto Rico. 1949.</p> <p>No. 10. Mean precipitable water in the United States. 1949. .30</p> <p>No. 11. Weekly mean values of daily total solar and sky radiation. Washington, D.C. 1949. .15. Supplement No. 1, 1955. .05</p> <p>*No. 12. Sunshine and cloudiness at selected stations in the United States, Alaska, Hawaii, and Puerto Rico. 1951.</p> <p>No. 13. Mean monthly and annual evaporation data from free water surface for the United States, Alaska, Hawaii, and the West Indies. 1950. .15</p> <p>*No. 14. Tables of precipitable water and other factors for a saturated pseudo-adiabatic atmosphere. 1951.</p> <p>No. 15. Maximum station precipitation for 1, 2, 3, 6, 12, and 24 hours: Part I: Utah, Part II: Idaho, 1951, each .25; Part III: Florida, 1952, .45; Part IV: Maryland, Delaware, and District of Columbia; Part V: New Jersey, 1953, each .25; Part VI: New England, 1953, .60; Part VII: South Carolina, 1953, .25; Part VIII: Virginia, 1954, .50; Part IX: Georgia, 1954, .40; Part X: New York, 1954, .60; Part XI: North Carolina; Part XII: Oregon, 1955, each .55; Part XIII: Kentucky, 1955, .45; Part XIV: Louisiana; Part XV: Alabama, 1955, each .35; Part XVI: Pennsylvania, 1956, .65; Part XVII: Mississippi, 1956, .40; Part XVIII: West Virginia, 1956, .35; Part XIX: Tennessee, 1956, .45; Part XX: Indiana, 1956, .55; Part XXI: Illinois, 1958, .50; Part XXII: Ohio, 1958, .65; Part XXIII: California, 1959, \$1.50; Part XXIV: Texas, 1959, \$1.00; Part XXV: Arkansas, 1960, .50; Part XXVI: Oklahoma, 1961, .45.</p> <p>*No. 16. Maximum 24-hour precipitation in the United States. 1952.</p> <p>No. 17. Kansas-Missouri floods of June-July 1951. 1952. .60</p> <p>*No. 18. Measurements of diffuse radiation at Blue Hill Observatory. 1952.</p> <p>No. 19. Mean number of thunderstorm days in the United States. 1952. .15</p> <p>No. 20. Tornado occurrences in the United States. Rev. 1960. .45</p> <p>*No. 21. Normal weather charts for the Northern Hemisphere. 1952.</p> <p>*No. 22. Wind patterns over lower Lake Mead. 1953.</p> <p>No. 23. Floods of April 1952—Upper Mississippi, Missouri, Red River of the North. 1954. \$1.00</p> | <p>No. 24. Rainfall intensities for local drainage design in the United States. For durations of 5 to 240 minutes and 2-, 5-, and 10-year return periods. Part I: West of 115th meridian. 1953, .20; Part II: Between 105° W. and 115° W. 1954. .15</p> <p>No. 25. Rainfall intensity-duration-frequency curves. For selected stations in the United States, Alaska, Hawaiian Islands, and Puerto Rico. 1955. .40</p> <p>No. 26. Hurricane rains and floods of August 1955, Carolinas to New England. 1956. \$1.00</p> <p>*No. 27. The climate of the Matanuska Valley. 1956.</p> <p>*No. 28. Rainfall intensities for local drainage design in western United States. For durations of 20 minutes to 24 hours and 1- to 100- year return periods. 1956.</p> <p>No. 29. Rainfall intensity-frequency regime. Part 1—The Ohio Valley, 1957, .30; Part 2—Southeastern United States, 1958, \$1.25; Part 3—The Middle Atlantic Region, 1958, .30; Part 4—Northeastern United States, 1959, \$1.25; Part 5—Great Lakes Region, 1950. \$1.50</p> <p>No. 30. Tornado deaths in the United States. 1957. .50</p> <p>*No. 31. Monthly normal temperatures, precipitation, and degree days. 1956.</p> <p>No. 32. Upper-air climatology of the United States. Part 1—Averages for isobaric surfaces, height, temperature, humidity, and density. 1957, \$1.25. Part 2—Extremes and standard deviations of average heights and temperatures, 1958, .65; Part 3—Vector winds and shear. 1959. .50</p> <p>No. 33. Rainfall and floods of April, May, and June 1957 in the South-Central States. 1958. \$1.75</p> <p>No. 34. Upper wind distribution statistical parameter estimates. 1958. .40</p> <p>No. 35. Climatology and weather services of the St. Lawrence Seaway and Great Lakes. 1959. .45</p> <p>No. 36. North Atlantic tropical cyclones. 1959. \$1.00</p> <p>No. 37. Evaporation maps for the United States. 1959. .65</p> <p>*No. 38. Generalized estimates of probable maximum precipitation for the United States west of the 105th meridian for areas to 400 square miles and durations to 24 hours. 1960.</p> <p>No. 39. Verification of the Weather Bureau's 30-day outlooks. 1961. .40</p> <p>No. 40. Rainfall frequency atlas of the United States for durations from 30 minutes to 24 hours and return periods from 1 to 100 years. 1961. \$1.75</p> <p>No. 41. Meridional cross sections, upper winds over the Northern Hemisphere. 1961. \$4.25</p> <p>No. 42. Generalized estimates of probable maximum precipitation and rainfall-frequency data for Puerto Rico and Virgin Islands. 1961. .50</p> <p>No. 43. Rainfall-frequency atlas of the Hawaiian Islands for areas to 200 square miles, durations to 24 hours, and return periods from 1 to 100 years. 1962. .40</p> <p>No. 44. A catalog of 100 FCC-positioned transosonde flights. 1962. \$2.00</p> <p>No. 45. Snowmelt floods of March-April 1960, Missouri and Upper Mississippi Basins. 1962. \$1.25</p> <p>No. 46. Atmospheric electric measurement results at Mauna Loa Observatory. 1962. \$1.25</p> |
|--|---|

*Out of print.

U.S. DEPARTMENT OF COMMERCE

LUTHER H. HODGES, Secretary

WEATHER BUREAU

F. W. REICHELDERFER, Chief

TECHNICAL PAPER NO. 47

**PROBABLE MAXIMUM PRECIPITATION
AND RAINFALL-FREQUENCY DATA FOR ALASKA**

**for Areas to 400 Square Miles, Durations to 24 Hours
and Return Periods from 1 to 100 Years**

Prepared by

JOHN F. MILLER

**Cooperative Studies Section, Hydrologic Services Division, U.S. Weather Bureau
for**

Engineering Division, Soil Conservation Service, U.S. Department of Agriculture

WASHINGTON, D.C.

1963

PREFACE

Authority. This report was prepared for the Soil Conservation Service to provide generalized rainfall information for planning and design purposes in connection with its Watershed Protection and Flood Prevention Program (authorization: P. L. 566, 83d Congress, and as amended).

Scope. Rainfall data for various hydrologic design problems involving areas up to 400 sq. mi. and durations up to 24 hours are presented. The data consist of generalized estimates of (1) probable maximum precipitation (PMP), and (2) rainfall-intensity-frequency data for return periods from 1 to 100 years.

Accuracy of results. The generalized estimates of probable maximum precipitation presented herein are as accurate as available data and current meteorological and statistical procedures permit. The accuracy of the rainfall-intensity-frequency data is chiefly dependent on the density and distribution of the precipitation network and length of record. The unusually sparse network, relatively short records, the rugged topography of the region, and its varied climatic regimes added to the usual complications. Consequently, the results presented probably have a lower degree of accuracy than those presented in previous reports in this same series for other parts of the United States. As time passes more data will become available through increases in length of records and very likely in station density. Knowledge of precipitation processes is being extended by continuing research. It is therefore only logical to expect that more reliable estimates than those presented herein will be possible in, say, 10 or 15 years.

Acknowledgments. The project was under the supervision of J. L. H. Paulhus, Chief of the Cooperative Studies Section of the Hydrologic Services Division, W. E. Hiatt, Chief. L. L. Weiss assisted in the meteorological and statistical investigations. W. E. Miller and N. S. Foat supervised the collection and processing of the basic data. Drafting was supervised by C. W. Gardner. Coordination with the Soil Conservation Service was maintained through H. O. Ogrosky, Chief, Hydrology Branch, Engineering Division.

CONTENTS

	Page		Page
Preface	ii	Figure No.	
Chapter 1. Basic Data	1	3-11. 1-yr. 30-min. rainfall (in.)	21
Daily data—Hourly data—Six-hourly data—Representativeness of observations		3-12. 2-yr. 30-min. rainfall (in.)	22
Chapter 2. Probable Maximum Precipitation	3	3-13. 5-yr. 30-min. rainfall (in.)	23
Introduction—Maximum observed precipitation—Seasonal distribution of maximum precipitation—Meteorological situations associated with heavy precipitation—Moisture adjustment of storm precipitation—Precipitation-moisture ratio (P/M)—Computation of PMP—Chronological distribution—Appraisal		3-14. 10-yr. 30-min. rainfall (in.)	24
Chapter 3. Rainfall-Frequency Data	14	3-15. 25-yr. 30-min. rainfall (in.)	25
Basic data—Frequency analysis—Isopluvial maps—Smoothing data read from the maps—Depth-area relationships—Seasonal variation		3-16. 50-yr. 30-min. rainfall (in.)	26
References	20	3-17. 100-yr. 30-min. rainfall (in.)	27
		3-18. 1-yr. 1-hr. rainfall (in.)	28
		3-19. 2-yr. 1-hr. rainfall (in.)	29
		3-20. 5-yr. 1-hr. rainfall (in.)	30
		3-21. 10-yr. 1-hr. rainfall (in.)	31
		3-22. 25-yr. 1-hr. rainfall (in.)	32
		3-23. 50-yr. 1-hr. rainfall (in.)	33
		3-24. 100-yr. 1-hr. rainfall (in.)	34
		3-25. 1-yr. 2-hr. rainfall (in.)	35
		3-26. 2-yr. 2-hr. rainfall (in.)	36
		3-27. 5-yr. 2-hr. rainfall (in.)	37
		3-28. 10-yr. 2-hr. rainfall (in.)	38
		3-29. 25-yr. 2-hr. rainfall (in.)	39
		3-30. 50-yr. 2-hr. rainfall (in.)	40
		3-31. 100-yr. 2-hr. rainfall (in.)	41
		3-32. 1-yr. 3-hr. rainfall (in.)	42
		3-33. 2-yr. 3-hr. rainfall (in.)	43
		3-34. 5-yr. 3-hr. rainfall (in.)	44
		3-35. 10-yr. 3-hr. rainfall (in.)	45
		3-36. 25-yr. 3-hr. rainfall (in.)	46
		3-37. 50-yr. 3-hr. rainfall (in.)	47
		3-38. 100-yr. 3-hr. rainfall (in.)	48
		3-39. 1-yr. 6-hr. rainfall (in.)	49
		3-40. 2-yr. 6-hr. rainfall (in.)	50
		3-41. 5-yr. 6-hr. rainfall (in.)	51
		3-42. 10-yr. 6-hr. rainfall (in.)	52
		3-43. 25-yr. 6-hr. rainfall (in.)	53
		3-44. 50-yr. 6-hr. rainfall (in.)	54
		3-45. 100-yr. 6-hr. rainfall (in.)	55
		3-46. 1-yr. 12-hr. rainfall (in.)	56
		3-47. 2-yr. 12-hr. rainfall (in.)	57
		3-48. 5-yr. 12-hr. rainfall (in.)	58
		3-49. 10-yr. 12-hr. rainfall (in.)	59
		3-50. 25-yr. 12-hr. rainfall (in.)	60
		3-51. 50-yr. 12-hr. rainfall (in.)	61
		3-52. 100-yr. 12-hr. rainfall (in.)	62
		3-53. 1-yr. 24-hr. rainfall (in.)	63
		3-54. 2-yr. 24-hr. rainfall (in.)	64
		3-55. 5-yr. 24-hr. rainfall (in.)	65
		3-56. 10-yr. 24-hr. rainfall (in.)	66
		3-57. 25-yr. 24-hr. rainfall (in.)	67
		3-58. 50-yr. 24-hr. rainfall (in.)	68
		3-59. 100-yr. 24-hr. rainfall (in.)	69

LIST OF ILLUSTRATIONS

	Page		Page
Figure No.		Figure No.	
1-1. Precipitation stations	2	3-11. 1-yr. 30-min. rainfall (in.)	21
1-2. Area and station elevation curves	3	3-12. 2-yr. 30-min. rainfall (in.)	22
2-1. Adjusted maximum observed 24-hr. precipitation	4	3-13. 5-yr. 30-min. rainfall (in.)	23
2-2. Surface synoptic map for 1200 GMT, October 28, 1954	5	3-14. 10-yr. 30-min. rainfall (in.)	24
2-3. Surface synoptic map for 1200 GMT, June 13, 1953	5	3-15. 25-yr. 30-min. rainfall (in.)	25
2-4. Surface synoptic map for 1200 GMT, August 29, 1954	6	3-16. 50-yr. 30-min. rainfall (in.)	26
2-5. Surface synoptic map for 1200 GMT, October 28, 1951	6	3-17. 100-yr. 30-min. rainfall (in.)	27
2-6. Comparison of precipitable water estimated from surface dew points with that observed in soundings (maximum dew points)	6	3-18. 1-yr. 1-hr. rainfall (in.)	28
2-7. Comparison of precipitable water estimated from surface dew points with that observed in soundings (maximum moisture)	7	3-19. 2-yr. 1-hr. rainfall (in.)	29
2-8. 50-yr. 12-hr. persisting dew points for mid-July	7	3-20. 5-yr. 1-hr. rainfall (in.)	30
2-9. 50-yr. 12-hr. persisting dew points for mid-October	8	3-21. 10-yr. 1-hr. rainfall (in.)	31
2-10. Variation of P/M ratio with elevation	9	3-22. 25-yr. 1-hr. rainfall (in.)	32
2-11. Moisture inflow barriers	9	3-23. 50-yr. 1-hr. rainfall (in.)	33
2-12. Probable maximum 24-hr. point precipitation	10	3-24. 100-yr. 1-hr. rainfall (in.)	34
2-13. Probable maximum 6-hr. point precipitation	11	3-25. 1-yr. 2-hr. rainfall (in.)	35
2-14. Depth-duration diagram for 6- to 24-hr. PMP	12	3-26. 2-yr. 2-hr. rainfall (in.)	36
2-15. Depth-area-duration diagram for PMP for durations under 6 hours	12	3-27. 5-yr. 2-hr. rainfall (in.)	37
2-16. Depth-area curves for PMP for durations from 6 to 24 hours	12	3-28. 10-yr. 2-hr. rainfall (in.)	38
2-17. Ratio of probable maximum 6-hr. precipitation to 100-yr. 6-hr. rainfall	13	3-29. 25-yr. 2-hr. rainfall (in.)	39
3-1. Duration-interpolation diagram	15	3-30. 50-yr. 2-hr. rainfall (in.)	40
3-2. Return-period-interpolation diagram	15	3-31. 100-yr. 2-hr. rainfall (in.)	41
3-3. Variation of 2-yr. 24-hr. rainfall with elevation—southern California coastal mountains and Cascade Range	15	3-32. 1-yr. 3-hr. rainfall (in.)	42
3-4. Relation for adjusting 2-yr. 24-hr. rainfall data for elevation	16	3-33. 2-yr. 3-hr. rainfall (in.)	43
3-5. Points for which probable maximum precipitation and rainfall-frequency data were computed	16	3-34. 5-yr. 3-hr. rainfall (in.)	44
3-6. Diagram for estimating 2-yr. 1-hr. amounts	17	3-35. 10-yr. 3-hr. rainfall (in.)	45
3-7. Mean annual number of thunderstorm days	17	3-36. 25-yr. 3-hr. rainfall (in.)	46
3-8. Smoothing values read from isopluvial maps	18	3-37. 50-yr. 3-hr. rainfall (in.)	47
3-9. Depth-area curves for rainfall-frequency data	18	3-38. 100-yr. 3-hr. rainfall (in.)	48
3-10. Monthly distribution (in percent) of 24-hr. rainfalls for various return periods	19	3-39. 1-yr. 6-hr. rainfall (in.)	49
		3-40. 2-yr. 6-hr. rainfall (in.)	50
		3-41. 5-yr. 6-hr. rainfall (in.)	51
		3-42. 10-yr. 6-hr. rainfall (in.)	52
		3-43. 25-yr. 6-hr. rainfall (in.)	53
		3-44. 50-yr. 6-hr. rainfall (in.)	54
		3-45. 100-yr. 6-hr. rainfall (in.)	55
		3-46. 1-yr. 12-hr. rainfall (in.)	56
		3-47. 2-yr. 12-hr. rainfall (in.)	57
		3-48. 5-yr. 12-hr. rainfall (in.)	58
		3-49. 10-yr. 12-hr. rainfall (in.)	59
		3-50. 25-yr. 12-hr. rainfall (in.)	60
		3-51. 50-yr. 12-hr. rainfall (in.)	61
		3-52. 100-yr. 12-hr. rainfall (in.)	62
		3-53. 1-yr. 24-hr. rainfall (in.)	63
		3-54. 2-yr. 24-hr. rainfall (in.)	64
		3-55. 5-yr. 24-hr. rainfall (in.)	65
		3-56. 10-yr. 24-hr. rainfall (in.)	66
		3-57. 25-yr. 24-hr. rainfall (in.)	67
		3-58. 50-yr. 24-hr. rainfall (in.)	68
		3-59. 100-yr. 24-hr. rainfall (in.)	69

PROBABLE MAXIMUM PRECIPITATION AND RAINFALL-FREQUENCY DATA FOR ALASKA

for Areas to 400 Square Miles, Durations to 24 Hours,
and Return Periods from 1 to 100 Years.

Chapter I BASIC DATA

1.1 Daily data

1.1.1 *Station data.* Basic precipitation data were obtained from 234 Alaskan and 33 Canadian stations. Table 1-1 groups number of precipitation stations by length of record. Only 223 Alaskan precipitation stations with data subsequent to 1930, when dewpoint data became available, were used in deriving estimates of probable maximum precipitation (PMP). Maximum and near-maximum amounts from other stations were considered in the consistency checks. For the frequency analysis, 184 Alaskan and 33 Canadian stations with at least 5 years of record were used (par. 3.1.1). Figure 1-1 shows the locations of the Alaskan stations, both active and discontinued.

1.1.2 *Network density.* The density of the network available for estimating PMP was about one gage for every 2,600 sq. mi. Elimination of stations with records of less than 5 years reduced the density to about one gage for every 3,200 sq. mi. (The average network density in

TABLE 1-1.—Daily precipitation stations grouped by length of record as of 1960

Length of record (years)	Number of stations for PMP	Number of stations for frequency analysis	
		Alaska	Canada
0-4	50	0	0
5-9	46	51	6
10-14	33	38	8
15-19	33	34	6
20-24	19	19	3
25-29	13	13	3
30-34	7	7	4
35-39	8	8	3
40-44	11	11	0
45-49	2	2	0
50-54	1	1	0

TABLE 1-2.—Distribution of daily precipitation stations by latitude

Latitude	Area (sq. mi.)	Number of stations		
		All	For PMP	For frequency
South of 62°N.	227,000	157	148	123
62°N. to 65°N.	137,000	49	48	36
North of 65°N.	222,000	28	27	25

the contiguous United States is about one station per 250 sq. mi.) The distribution of gages throughout Alaska was far from uniform. Table 1-2 groups stations with suitable data by latitude. Two-thirds of the precipitation stations were south of 62°N. in an area of 227,000 sq. mi., about 39 percent of the total area. Approximately 38 percent of the area of Alaska, or about 222,000 sq. mi., is north of 65°N., roughly the latitude of Fairbanks, while only 13 percent of the stations were in this region. The precipitation-network density decreased from about one gage per 1,500 sq. mi. in the south for PMP and one per 1,800 sq. mi. for frequency analysis to one per 8,300 sq. mi., and one per 8,900 sq. mi., respectively, north of 65°N.

1.1.3 The distribution of precipitation stations with respect to elevation was very poor. While about 18 percent of Alaska is above 3,000 ft., there was only one station above that level, and it had but a 3-year record. Only 12 percent of the stations were above 1,000 ft., whereas 54 percent of the area is above that elevation. Fifty-five percent of the stations were located at elevations below 100 ft. while only about 7 percent of the area is below that elevation. Figure 1-2 shows the station-elevation and area-elevation curves side by side for comparison.

1.2 Hourly data

1.2.1 *Station data.* Only nine Alaskan stations were equipped with recording gages. Three had records of 20 years or longer, one had 19 years, and three had between 10 and 15 years. The remaining two gages had 1 and 3 years, respectively. The recording gages are indicated by the solid symbols on figure 1-1.

1.2.2 *Network density.* The density of the recording-gage network was about one gage per 62,000 sq. mi. Elimination of gages with less than 5 years of record reduced the density to about one per 80,000 sq. mi., roughly one-hundredth that of the contiguous United States, which has about one recording gage per 860 sq. mi. There were no recording-gage stations above 500 ft., and only two over 100 ft.

1.3 Six-hourly data

1.3.1 Some stations take observations at 6-hour intervals for inclusion in the regular synoptic reporting network. These data were surveyed for 18 stations in Alaska. The stations were selected to provide as nearly as possible a balanced geographical distribution (fig. 1-1) for the testing of empirical relationships developed with data from other regions.

1.4 Representativeness of observations

1.4.1 *Sampling.* The more intense rainfall rates measured by the existing network were obviously a very small sample of the heavy rainfalls that have occurred in Alaska. The sampling was particularly poor for local showers or thunderstorms, whose areal extent is limited to a few square miles. The chance that the most intense

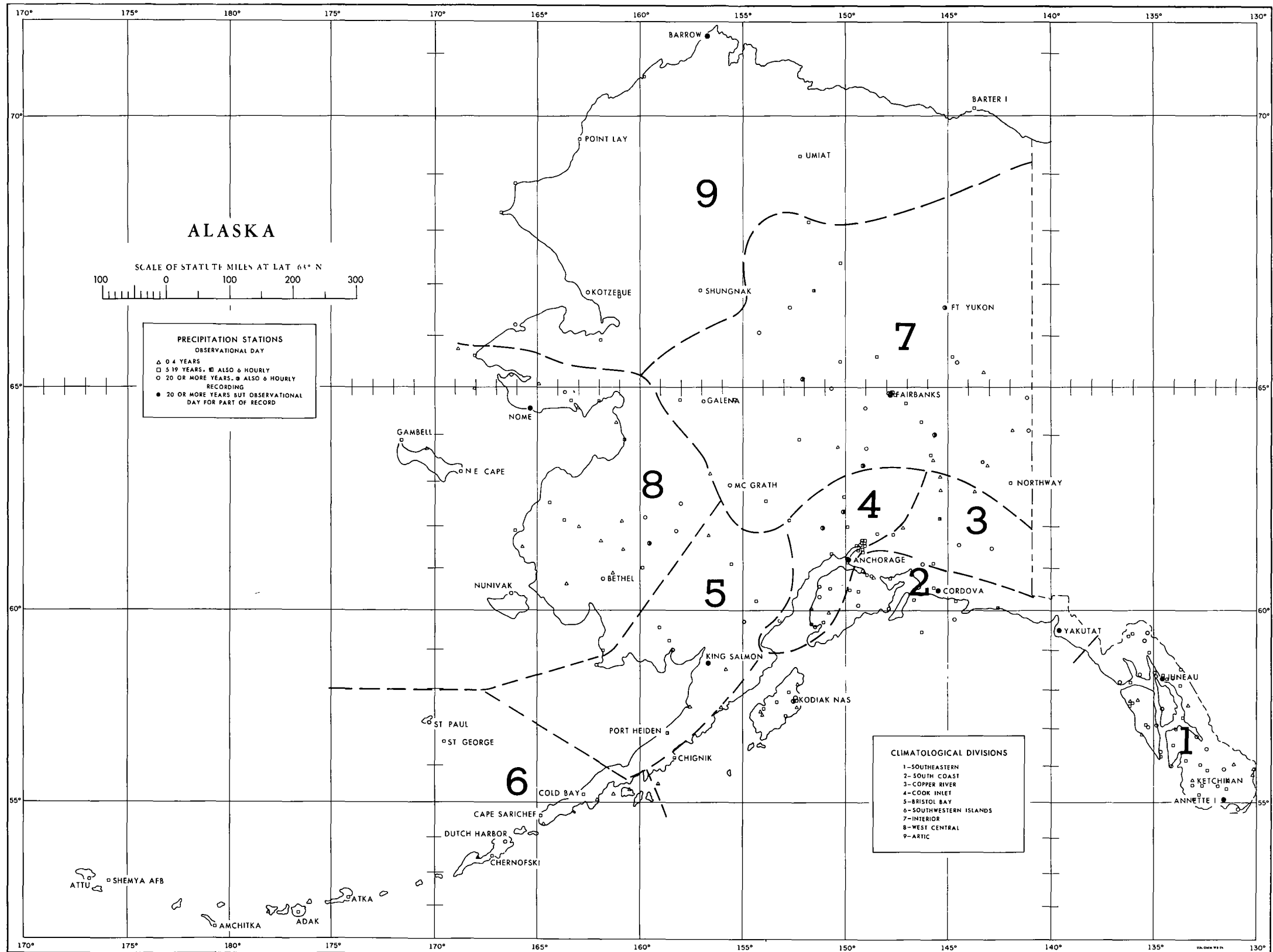


FIGURE 1-1.—Precipitation stations.

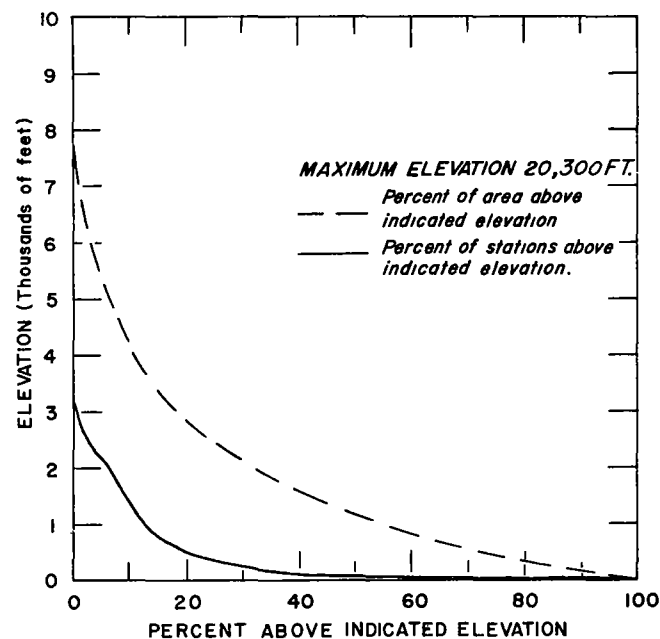


FIGURE 1-2.—Area and station elevation curves.

rainfall in a thunderstorm would center over a gage is extremely remote. This type of precipitation is important because it provides maximum intensities for short durations over small areas. The more uniform rainfall rates in large, or general, storms, often extending over several thousand square miles, were naturally somewhat better represented by the gage sampling. On the basis of past experience [1], it is ventured that a more uniformly distributed network with a density like that of the contiguous 48 states (about 10 times the present density in Alaska) would in, say, 10 years yield enveloping rainfall values over twice the present maxima.

1.4.2 *Measurement errors.* The most serious error in precipitation measurements is that resulting from wind effect. The gage obstructs the horizontal flow of the air,

which is forced around and over the gage. The upward component of the wind passing over the gage deflects precipitation that would otherwise fall into the gage, resulting in a deficient catch. The deficiency is greater for snow than for rain because snow has a lower density and is therefore more easily affected by wind [2]. Since many severe storms are accompanied by relatively strong winds, measurements of heavy rainfall and snowfall intensities are likely to be appreciably deficient. This effect is particularly important in exposed areas such as the Aleutians and coastal regions. In this study, as in previous ones, no attempt has been made to correct for wind errors as there are no data on wind speeds at gage-orifice level on which to base such an adjustment.

Chapter 2

PROBABLE MAXIMUM PRECIPITATION

2.1 Introduction

2.1.1 Most heavy storm-precipitation amounts in the southern coastal areas are the result of large-area, or general, fall and winter storms. In the interior and Arctic regions heavy rainfalls occur in the late spring and summer, generally as showers associated with the passage of frontal systems.

2.2 Maximum observed precipitation

2.2.1 Figure 2-1 shows observed or estimated maximum 24-hour rainfalls for Alaska. The true maximum 24-hour amounts were plotted for stations having these data. Observational-day amounts for other stations were adjusted upward to approximate the true maximum 24-hour amounts by one of the two following methods. The adjustment most commonly used consisted of adding to the maximum observational-day value one-half of the higher of the amounts for the adjoining days, i.e., the preceding or following day. Tests made in various regions of the United States indicate that, on the average, this procedure yields satisfactory approximations of the true 24-hour maxima.

2.2.2 The other adjustment used consisted of multiplying the maximum observational-day amounts by 1.13. This procedure is a result of studies of precipitation data for various regions of the contiguous United States. Tests using Alaskan data showed good agreement with the previous work. This method yields generally reliable results when applied to rainfall-frequency data. When applied to individual amounts, however, the factor might yield appreciably erroneous estimates which are nevertheless generally more nearly correct than estimates based on the assumption that the observational-day maxima are also true 24-hour maxima. The 1.13 factor was used only when precipitation amounts for days adjoining the date of maximum precipitation were not available. A few of the amounts shown on figure 2-1 were adjusted by this method.

2.2.3 Maximum rainfall amounts for durations under 24 hours were also of interest. Table 2-1 lists the nine recording-gage stations (par. 1.2.1), their periods of record, and their maximum observed amounts for 1, 2, 3, and 6 hours.

TABLE 2-1.—Maximum observed rainfall amounts for short durations

Station	Amount (in.) Date	Duration (hours)			
		1	2	3	6
Anchorage 1942-61	0.40 8/18/59	0.54 7/31/56	0.68 7/31/56	0.88 7/31/56	
Annette-Ketchikan 1941-60*	1.05 10/29/58	1.62 10/29/58	1.92 10/29/58	2.72 11/30/59	
Barrow 1960	0.15 8/10/60	0.25 8/10/60	0.32 8/10/60	†0.59 6/26/55	
Cordova 1948-60	0.62 11/2/57	0.95 7/31/56	1.24 7/31/56	2.12 10/16/57	
Fairbanks 1931-61*	0.99 7/13/39	1.06 7/13/39	1.09 7/13/39	1.11 7/13/39	
Juneau 1931-61*	0.72 8/3/56	0.94 8/3/56	1.35 8/3/56	1.87 10/10/46	
King Salmon 1958-60	0.28 9/1/60	0.52 9/1/60	0.73 9/1/60	1.11 9/1/60	
Nome 1942-56	0.56 8/9/56	0.87 8/9/56	0.97 8/9/56	1.25 8/9/56	
Yakutat 1952-61	0.67 9/18/61	1.14 10/5/55	1.47 10/5/55	2.18 10/5/55	

* Breaks in record

† From a synoptic report prior to installation of recording gage.

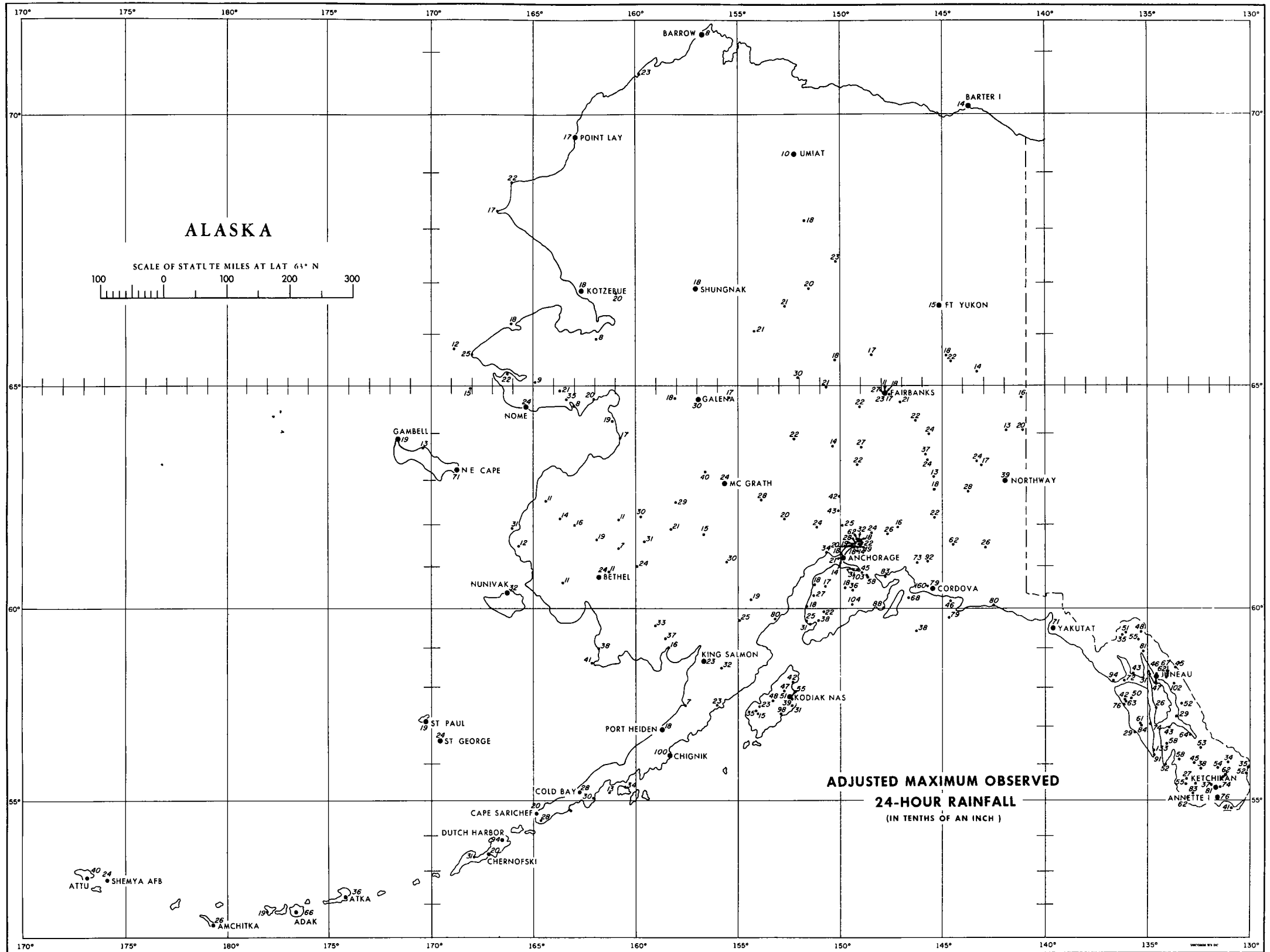


FIGURE 2-1.—Adjusted maximum observed 24-hr. precipitation for Alaska.

TABLE 2-2.—Monthly distribution of large daily precipitation amounts (percent)

Region	J	F	M	A	M	J	J	A	S	O	N	D
South Coast and Southeastern	7	6	2	1	1	1	3	6	17	38	9	9
Interior and Arctic	2	0	2	0	0	20	30	33	8	3	2	0
West Central and Bristol Bay	4	2	3	3	4	5	9	39	11	11	8	1
Copper River and Cook Inlet	6	7	2	1	1	9	4	21	18	13	10	8
Southwestern Islands	0	6	3	3	6	6	8	20	17	8	17	6

2.3 Seasonal distribution of maximum precipitation

2.3.1 Table 2-2 shows by climatological regions [3] the monthly distribution of the three highest daily precipitation amounts for each station. These regions are delineated in figure 1-1. For the Southeastern and South Coast regions the maximum values occur in the fall and winter. In the Interior and Arctic regions summertime maxima predominate. The Copper River, Cook Inlet, West Central, and Bristol Bay regions are transitional regions with the more southerly stations having primarily winter maxima with summer maxima more frequent in the northern part. The Southwestern Islands are influenced by a primary storm track through all seasons [4]. This is reflected by the more uniform seasonal distribution of large precipitation amounts.

2.4 Meteorological situations associated with heavy precipitation

2.4.1 *South Coast and Southeastern Regions.* These regions have a predominantly maritime climate. The heaviest precipitation in Alaska occurs in these regions. Slight variations in temperature determine whether the precipitation falls as rain or snow. Winter rainfall is relatively common except at high elevations. The maximum observational-day amount for Alaska (14.13 in.) was measured at Cordova on December 29, 1955. The precipitation began as snow on the 27th but changed to rain during the period of maximum intensity.

2.4.2 Maximum amounts of precipitation in these regions usually occur with widespread precipitation from low-pressure centers which develop in or cross the Gulf of Alaska. The flow aloft is usually either southerly or southwesterly as a result of a trough moving eastward over the Alaska Peninsula area into the Gulf. The synoptic map of October 28, 1954 is a good example of this storm type (fig. 2-2).

2.4.3 *Interior and Arctic Regions.* The northern and central sections of Alaska are sheltered by orographic

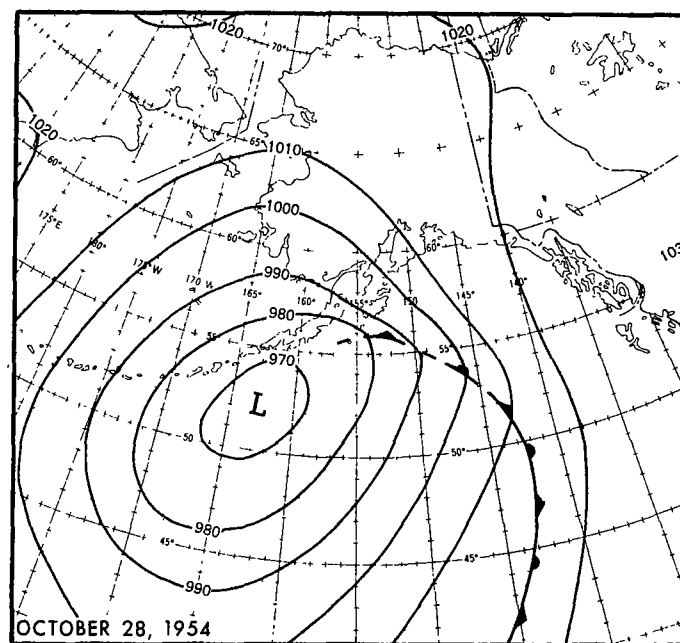


FIGURE 2-2.—Surface synoptic map for 1200 GMT, October 28, 1954.

barriers or long overland distances from the warm maritime air which predominates over the southern coastal regions. Winter precipitation is almost entirely in the form of snow. The largest daily precipitation amounts occur during the summer months. Summer precipitation is predominantly of the shower type, particularly in the interior. Thunderstorms are quite frequent in summer throughout the Yukon Valley, occurring almost weekly at some stations (fig. 3-7). The incidence of thunderstorms decreases from the Brooks Range northward. Characteristic of the storms associated with heavy precipitation in these regions is that of June 13, 1953 (fig. 2-3). Precipitation in this storm was of the showery type with some stations receiving near-maximum amounts of rain while others reported little or none.

2.4.4 *West Central and Bristol Bay Regions.* These regions are a transitional zone between the maritime influence along the coast and the continental characteristics of the interior. Though open to the ocean, the waters of the Bering Sea are cooler than the open water areas of the North Pacific. This, coupled with the lack of major orographic barriers, precludes any sharp boundary between maritime and continental influences. During the winter a large part of the Bering Sea is ice-covered, and the region loses much of the effects of maritime influence.

2.4.5 Heavy daily precipitation amounts are primarily associated with low-pressure systems that move north-

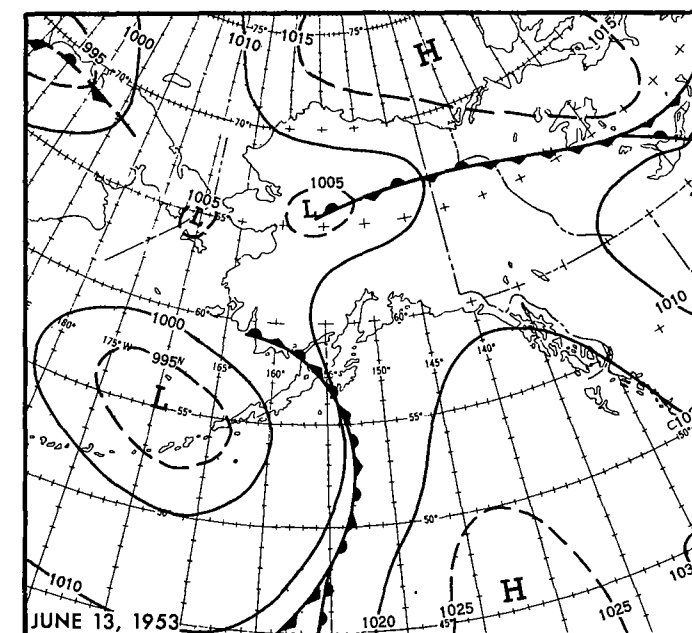


FIGURE 2-3.—Surface synoptic map for 1200 GMT, June 13, 1953.

eastward across the Bering Sea. In winter most cyclones move eastward south of these regions into the Gulf of Alaska. In late winter and early spring the storm track begins a shift to the northeast. By midsummer the cyclones move northeastward from the western Aleutian Islands across the Bering Sea toward the Seward Peninsula. These cyclones provide a southerly flow of air across the region and cause widespread precipitation. As winter approaches, the storm track shifts back southward toward the Gulf. The Bristol Bay region continues to receive heavy precipitation well into the fall until the primary storm track is south of the Alaska Peninsula. Figure 2-4 shows the synoptic map for August 29, 1954. This storm is typical of those associated with heavy precipitation over this region.

2.4.6 *Copper River and Cook Inlet.* These regions are also transitional areas between the maritime and continental regions. The major orographic barriers on the southern edge of the region make the transition more abrupt than in the West Central and Bristol Bay areas. In winter heavy daily precipitation amounts are associated with large, general storms that also cause widespread precipitation in the maritime regions to the south. During the summer shower-type precipitation becomes predominant as in the interior.

2.4.7 *Southwestern Islands.* The primary storm track across the North Pacific lies along the Aleutian Islands and

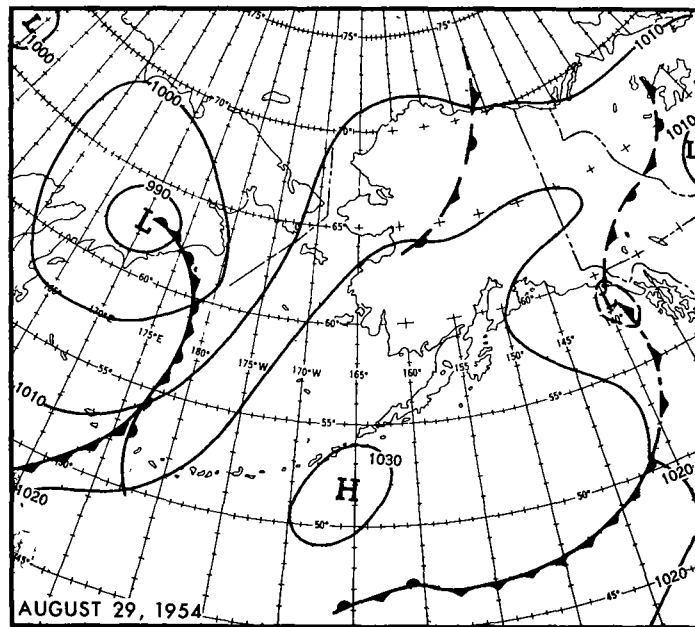


FIGURE 2-4.—Surface synoptic map for 1200 GMT, August 29, 1954.

the western portion of the Alaska Peninsula with a resultant high level of cyclonic activity in all seasons. The cyclonic systems usually have steep pressure gradients with resultant strong winds, introducing considerable error in precipitation measurements (par. 1.4.2). Typical of these storms is that of October 28, 1951 (fig. 2-5).

2.5 Moisture adjustment of storm precipitation

2.5.1 Procedures for maximizing storm data involve adjustment for maximum moisture charge. In some procedures, the moisture adjustment is the only maximizing factor. The adjustment for maximum moisture charge is made for the purpose of estimating what the storm precipitation would have been had the moisture supply for the storm been at the maximum. The adjustment usually consists of multiplying the storm-precipitation amounts by the ratio of the probable maximum atmospheric moisture for the time of year to that observed or estimated during the actual storm.

2.5.2 *Measurements of atmospheric moisture.* The amount of water vapor, or moisture charge, can be expressed in several ways, but the term commonly used in hydrometeorology is precipitable water. *Precipitable water*, or W_p , is the depth of water, in inches, that would be realized over a given area if all the water vapor in the air column above that area were to be precipitated on that area without loss. There is, of course, no process that will completely remove all water vapor from the atmosphere.

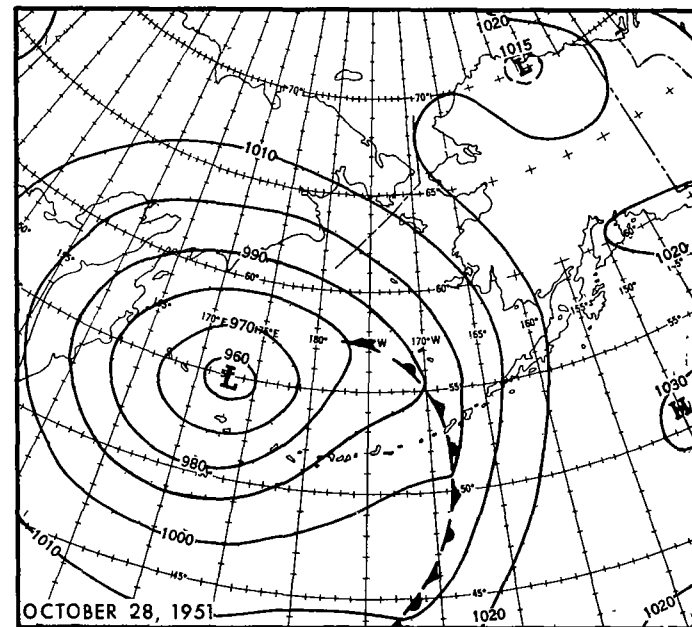


FIGURE 2-5.—Surface synoptic map for 1200 GMT, October 28, 1951.

2.5.3 Measurements of W_p are generally obtained from radiosonde data, and in the United States may range from a small fraction of an inch to about 3 inches. Measurements of precipitable water are rarely used for maximizing observed storms for three reasons: (1) the radiosonde network is relatively sparse, the moist air current flowing into a storm is often between stations, and the radiosonde data are then not representative of the moisture flow into the storm; (2) some storms to be maximized occurred before 1940 when installation of the radiosonde network was started; and (3) W_p is not computed regularly for all soundings so that it is a laborious task to determine the maximum observed W_p values of record required for maximization. For these reasons W_p is usually estimated from surface dew point temperatures.

2.5.4 *Estimates of storm W_p .* Studies of major storms in the United States and other parts of the world have indicated that the air carrying the main supply of W_p into a storm is saturated or nearly so. Tests have been conducted showing that reasonably accurate estimates of W_p for storm or high-moisture conditions can be made by using the surface dew point and computing W_p on the assumption that saturation and pseudoadiabatic conditions prevail. There are more stations making dew point observations than there are radiosonde stations, so finding a dew point station in the path of moist-air inflow into a storm is generally less difficult. Furthermore, dew point observations are usually made on an hourly or 6-hourly

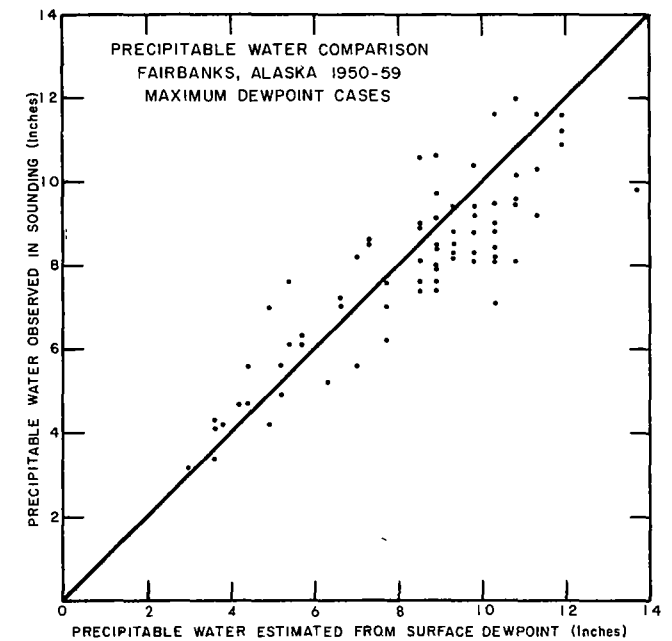


FIGURE 2-6.—Comparison of precipitable water estimated from surface dew points for a saturated pseudoadiabatic atmosphere with that observed in soundings at Fairbanks, Alaska, in the period 1950-59, using maximum dew point cases only.

basis whereas soundings are made at 12-hour intervals. Also, dew point records generally cover a longer period than do radiosonde observations, which are a relatively recent innovation (1940).

2.5.5 Dew point data represent instantaneous conditions. Since the storm-rainfall data of primary interest are usually for durations of one or more hours, there arises the problem of what dew point or dew points would be most representative of moisture inflow during the duration of the storm. Various tests made in previous studies have indicated that the *12-hour persisting storm dew point*, which is the highest dew point that has been equalled or exceeded for a period of at least 12 hours during the storm, is most suitable for computing W_p representative of moisture inflow into storms of durations up to several days.

2.5.6 *Representativeness of Alaskan surface dew points.* Tests were made to determine if surface dew points in Alaska were representative of moisture aloft. Surface and upper-air data for Fairbanks were selected for the months of maximum precipitation during the period 1950-1959. The first test was for representativeness of high surface dew points. W_p in the layer from the surface to the 500-mb. level was computed from radiosonde observations made at the time of the maximum 12-hour persisting dew point for each half month of each

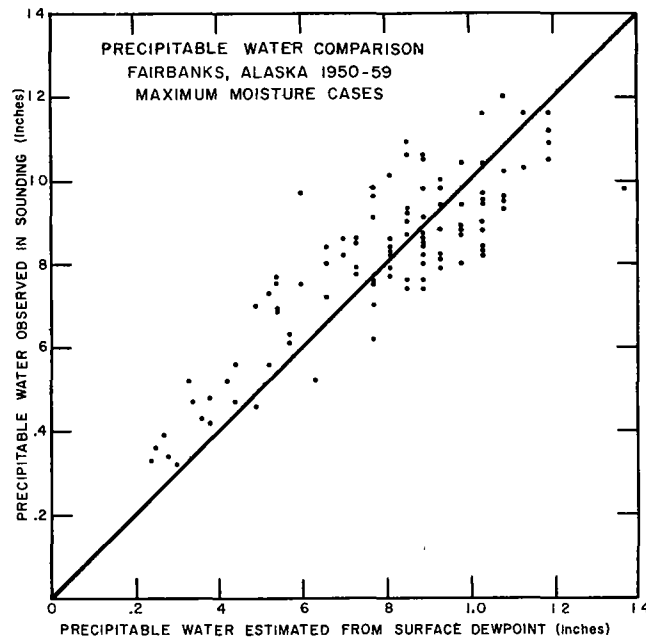


FIGURE 2-7.—Comparison of precipitable water estimated from surface dew points for a saturated pseudoadiabatic atmosphere with that observed in soundings at Fairbanks, Alaska, in the period 1950-59, using maximum moisture cases only.

year. These observed values were compared (fig. 2-6) with those estimated from the 12-hour persisting surface dew points.

2.5.7 A second test was made for representativeness of surface dew points at times of high moisture aloft. For each half-month interval during the 1950-59 period, the maximum observed W_p values obtained from the soundings were compared (fig. 2-7) with those estimated from the 12-hour persisting surface dew point for the period centered as closely as possible to the time of the sounding.

2.5.8 The diagrams of figures 2-6 and 2-7 indicate that estimates of W_p based on 12-hour persisting dew points and a pseudoadiabatic lapse rate provide satisfactory approximations of W_p for high-moisture conditions at Fairbanks. Similar tests for Anchorage, Juneau, and other radiosonde stations representative of the various climatic regimes of Alaska also showed that the surface dew points, with pseudoadiabatic conditions assumed, provided satisfactory estimates of W_p for high-moisture conditions.

2.5.9 The representativeness of surface dew points during storm situations was also investigated. Moisture patterns (W_p maps) were constructed for dates on which two or more stations recorded maximum daily precipitation amounts. The data consisted of both observed W_p values from radiosonde stations and of estimated values

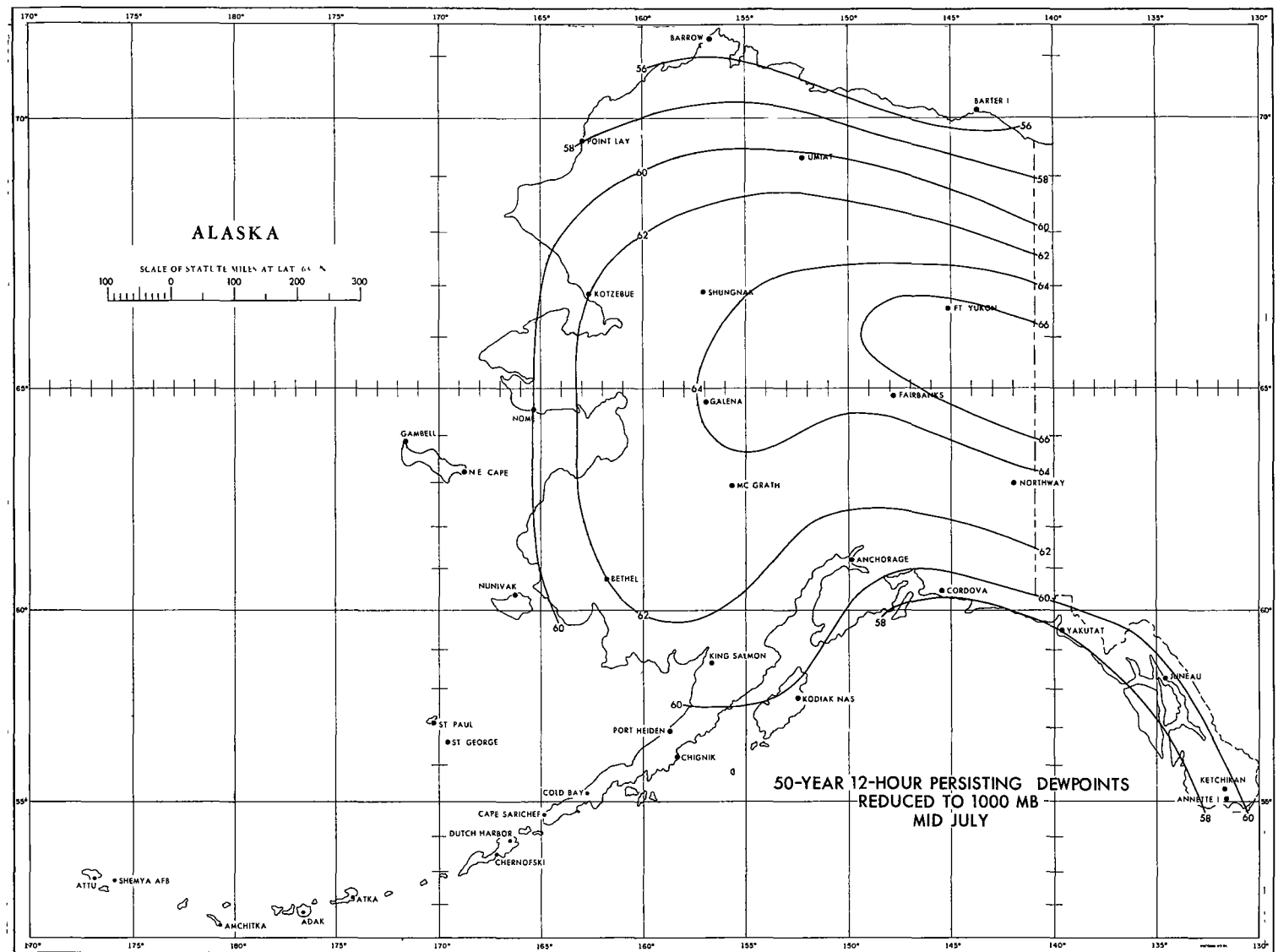


FIGURE 2-8.—50-yr. 12-hr. persisting dew points for mid-July.

from dew point stations. The maps showed no inconsistencies that might have resulted had there been appreciable differences between W_p values obtained from the two sources.

2.5.10 *Maximum moisture charge.* The manner in which W_p could be estimated from surface dew points was discussed in paragraphs 2.5.4-2.5.9. The upper limit of the moisture charge was determined from surface dew points also. Where long dew point records, say, 50 or more years, are available, W_p is usually based on the maximum 12-hour persisting dew points of record. The envelope of these maximum values has been found to approximate the 50-year dew points. The records for each Alaskan dew point station were surveyed for the

highest 12-hour persisting dew points of record in each half-month of each year of record. These annual maxima for each half-month period were analyzed for frequency. The maximum 12-hour persisting dew points from the relatively short Alaskan records were found to have return periods generally between 25 and 50 years. The curve showing the seasonal variation of the maximum 12-hour persisting dew points was therefore constructed to envelop the 50-year values which exceeded the maxima of record in all cases. The mid-month dew point values for July and October for each station were obtained from its seasonal variation curve and plotted on maps (figs. 2-8 and 2-9). The reason for using these two maps only is discussed later.

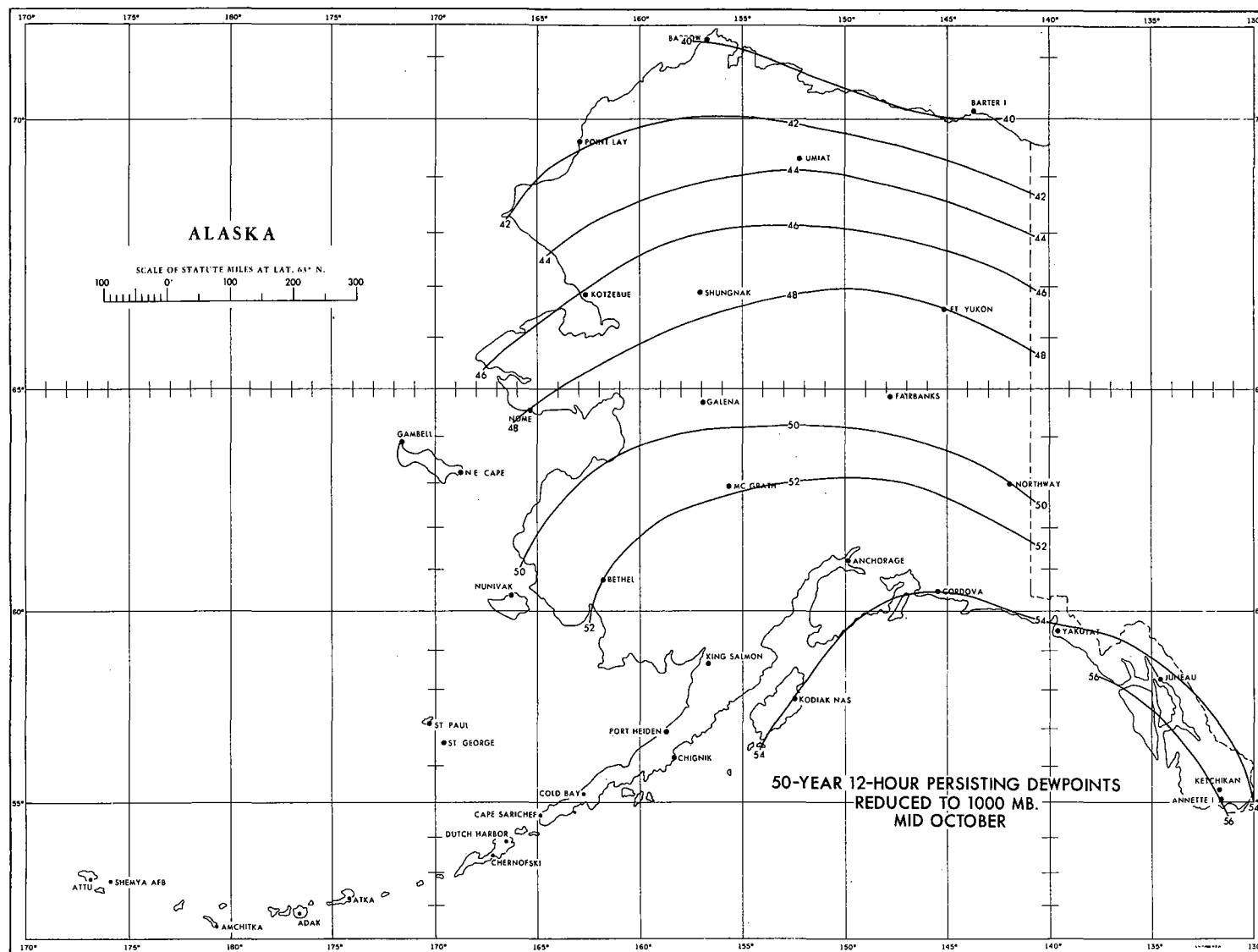


FIGURE 2-9.—50-yr. 12-hr. persisting dew points for mid-October.

2.6 Precipitation-moisture ratio (P/M)

2.6.1 Precipitation over relatively flat areas results from the lifting of warm moist air by atmospheric processes. An indication of the relative efficiency of different storms can be obtained by dividing the observed precipitation by the available moisture charge, or precipitable water. This P/M ratio has been discussed in *Hydrometeorological Report No. 36* [5].

2.6.2 *Determination of P/M ratios for Alaska.* A survey of Alaskan precipitation was made to determine the three highest observational-day values for each station (par. 1.1.1). The moisture supply associated with each pre-

cipitation amount was determined by selecting a representative 12-hour persisting dew point and estimating W_p . The precipitation amount was then divided by the corresponding W_p . These ratios (P/M), or storm-efficiency indices, would be about the maxima for Alaska since 1930.

2.6.3 *Orographic variations.* The lack of high elevation stations in Alaska (par. 1.1.3) necessitated the development of relationships for regions with similar physiographic characteristics and with adequate data to determine the orographic effects on storm efficiency. In order to define completely the orographic effects on the P/M ratio it was necessary to investigate its variations

due to the effect of orographic barriers of different crest elevations in maritime and continental regions.

2.6.4 For the maritime regions four orographic barriers were chosen: (1) the Cascade Range of western Washington with an average crest elevation of 7,000 ft., (2) the Coast Ranges of northern California with an average crest elevation of 4,000 ft., (3) the Coast Ranges of southern California with an average crest elevation of 8,000 ft., and (4) the Sierra Nevada with an average crest elevation of 10,000 ft. These average elevations represent the lowest levels to which moisture inflow into a storm is forced to rise in crossing over the barrier. Individual peaks may exceed these average elevations by several thousand feet.

2.6.5 The first step in developing these relationships was a survey of the three highest observational-day precipitation amounts at each station on the four barriers and in the adjacent level areas. Precipitable water was estimated for the storm associated with each precipitation amount, and P/M ratios were computed. The maximum ratio for each station was plotted against station elevation, and mean curves were drawn for windward and leeward slopes of each of the four barriers. The curves were then converted from actual P/M values into percentages of the mean ratio at 1,000 ft. on the windward slope. Curves for other barrier-crest elevations were determined by interpolation. These curves are identified as "maritime" in figure 2-10.

2.6.6 The Salmon River and Bitterroot Ranges of southern Idaho and southwestern Montana with an average crest elevation of 10,000 ft., and the Strawberry and Blue Mountains of eastern Oregon with an average crest elevation of 7,000 ft. were used to investigate the variation of the P/M ratio with elevation in the continental or interior region (fig. 2-10). The procedure was similar to that described in the preceding paragraph. There was considerable scatter of plotted data about the mean lines, but introduction of other parameters did not significantly improve the relationship.

2.6.7 *Enveloping P/M ratio map.* The largest values of the P/M ratio for all stations in Alaska with elevations less than 1,000 ft. were plotted on a map together with the month of occurrence. The largest values for those stations with an elevation in excess of 1,000 ft. were then adjusted by use of the relationships of figure 2-10. The resulting map thus depicted a pattern of maximum P/M ratios representative of elevations up to 1,000 ft., m.s.l. Examination of month of occurrence permitted delineation of a boundary between those regions where maximum ratios occurred in fall or winter and those where they occurred in late spring or summer.

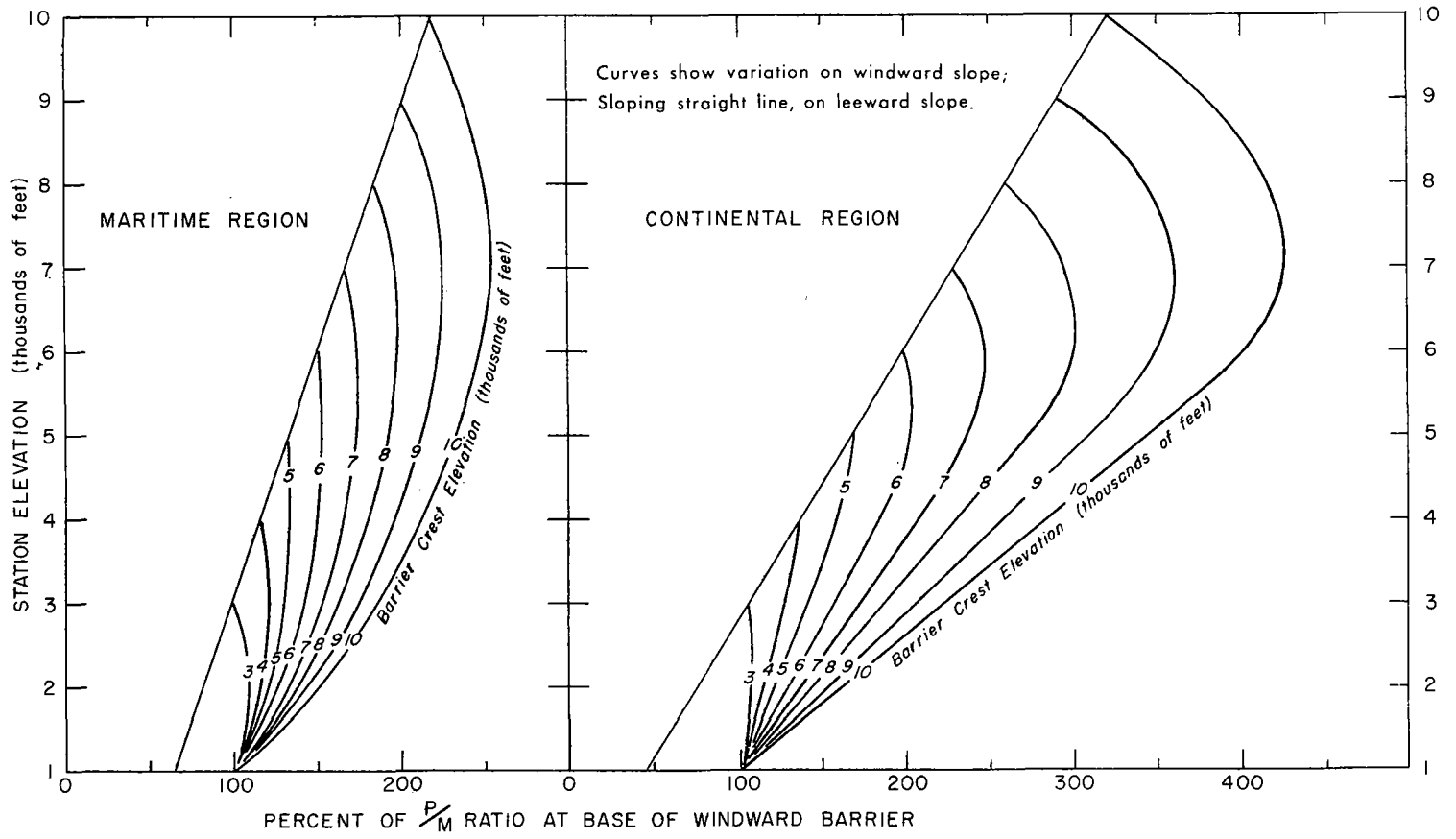


FIGURE 2-10.—Variation of P/M ratio with elevation in continental and maritime regions for various barrier-crest elevations.

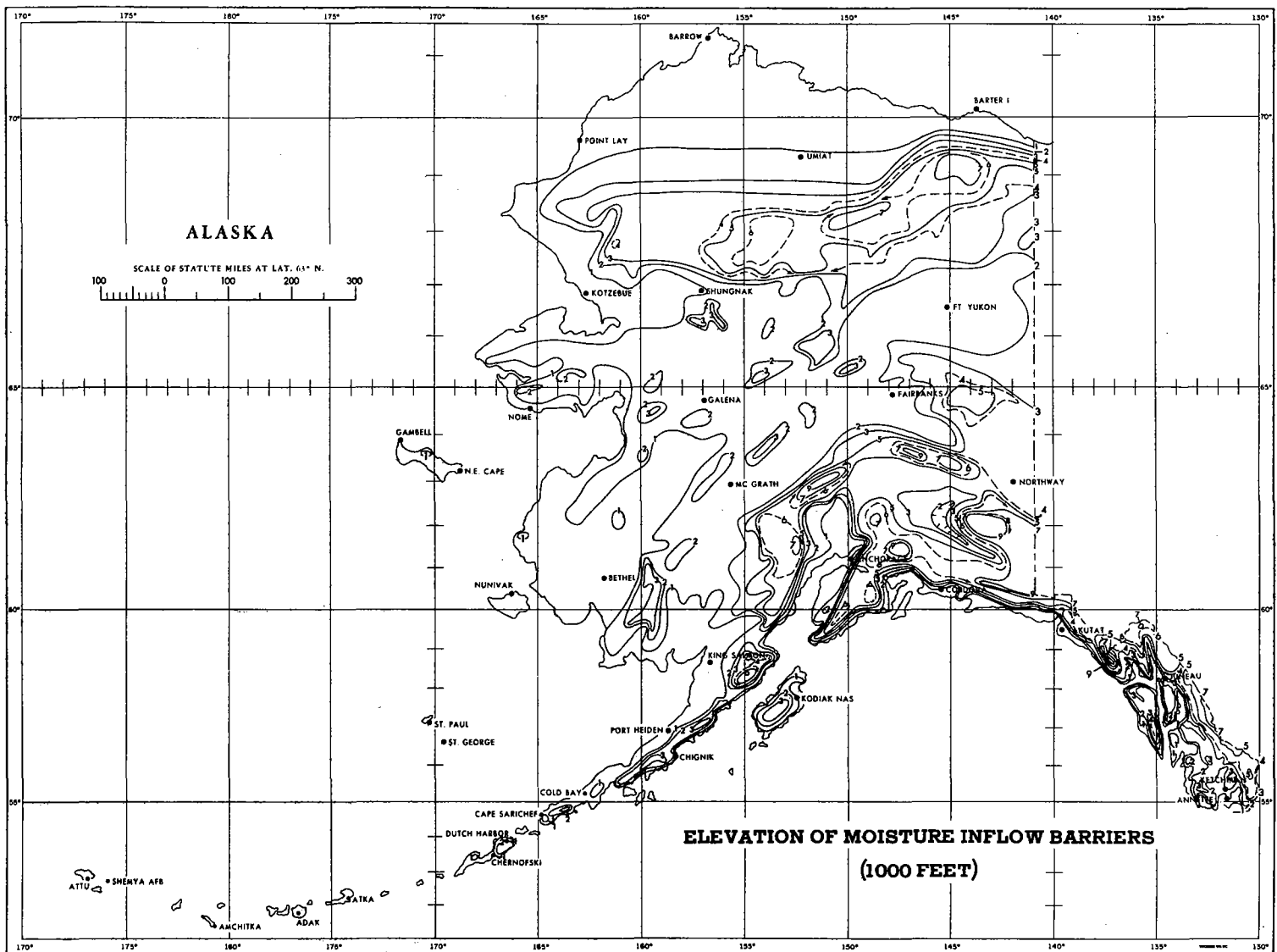


FIGURE 2-11.—Elevations of moisture inflow barriers in major storms, in thousands of feet above mean sea level.

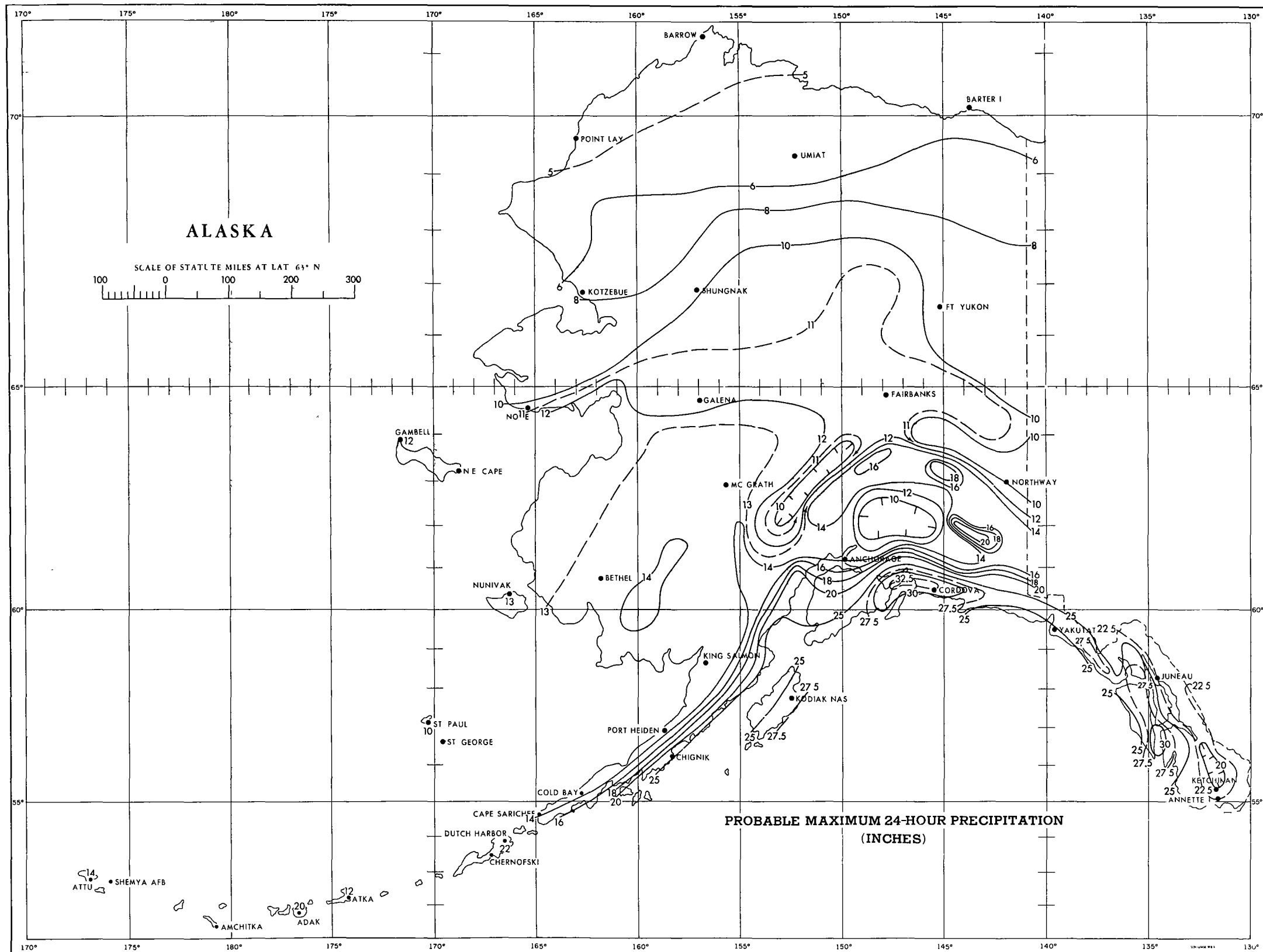


FIGURE 2-12.—Probable maximum 24-hr. point precipitation, in inches.

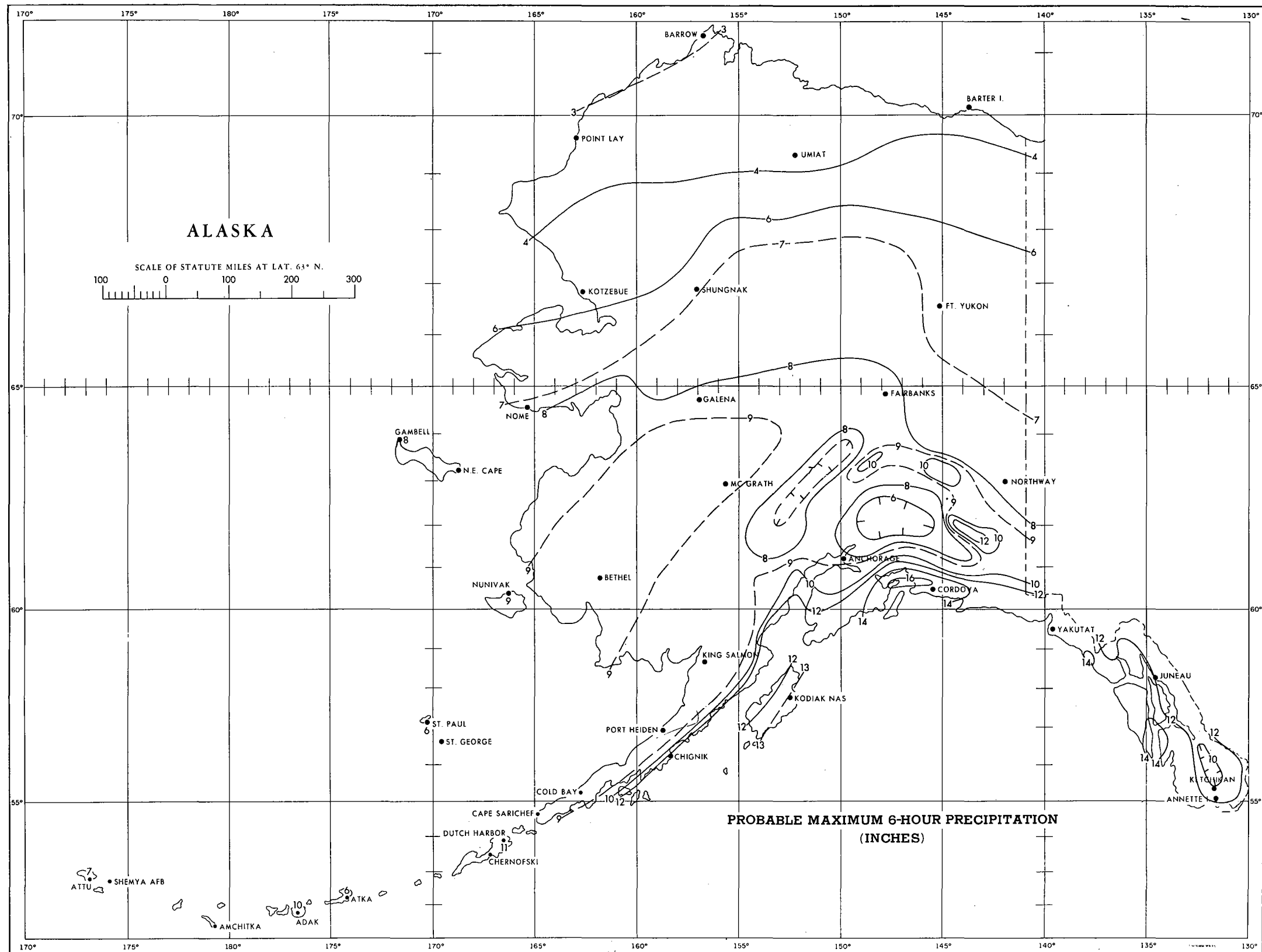


FIGURE 2-13.—Probable maximum 6-hr. point precipitation, in inches.

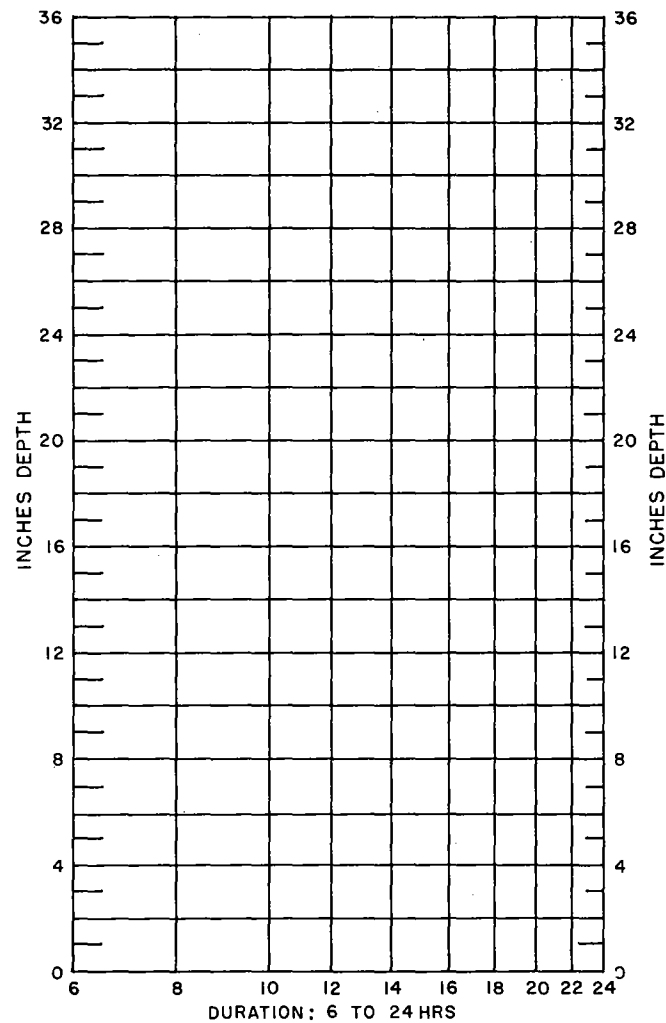


FIGURE 2-14.—Depth-duration diagram for 6- to 24-hr. PMP. (See fig. 2-16 for example of use.)

2.7 Computation of PMP

2.7.1 24-hour PMP. The 24-hour PMP at any point was obtained from the product of the maximum storm-efficiency index multiplied by the maximum W_p . The maximum index for any point in Alaska was obtained from the P/M ratio map (par. 2.6.7). Ratios for all points on lee slopes and for points with elevations over 1,000 ft. on windward slopes were adjusted by the ratio-elevation curves (fig. 2-10), the barrier-crest elevations being estimated from the map of figure 2-11. P/M ratios were thus obtained for the grid of figure 3-5. The seasonal variation curves of 50-year 12-hour persisting dew points (par. 2.5.10) showed the maximum moisture for summer was in mid-July (fig. 2-8) and for winter, in mid-October (fig. 2-9). Mid-July or mid-October W_p was

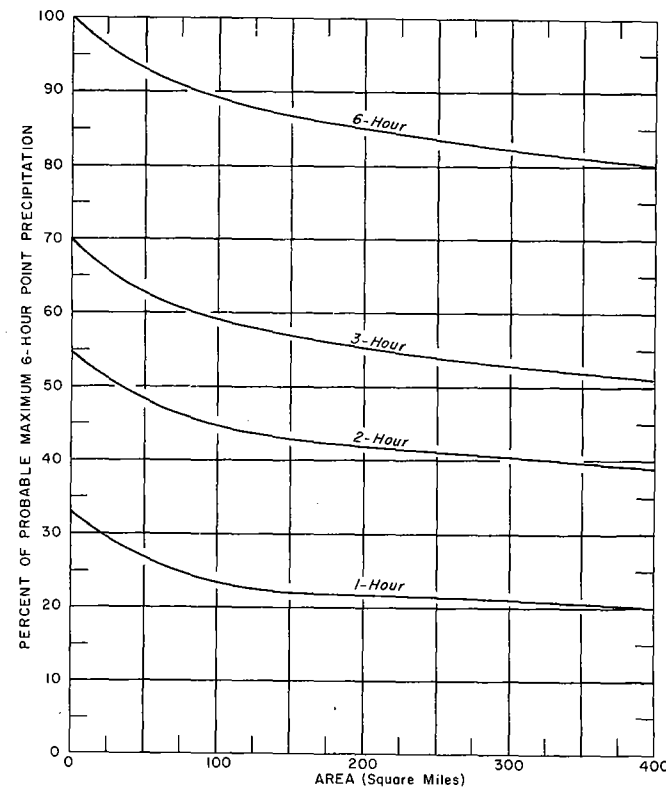


FIGURE 2-15.—Depth-area-duration diagram for PMP for durations under 6 hours for use with figure 2-13. (See fig. 2-16 for example of use.)

estimated for each grid point and combined with the corresponding cold or warm season P/M ratio to yield 24-hour PMP (fig. 2-12).

2.7.2 6-hour PMP. Data were inadequate for developing the 6-hour PMP directly. The ratio of 6-hour to 24-hour precipitation is a relatively stable value and may show little variation over relatively large meteorologically homogeneous regions. The 6:24-hour ratios were determined in two different ways. One value was computed on a within-storm basis, i.e., 6- and 24-hour amounts from the same storm. The other was obtained from 6- and 24-hour amounts not necessarily from the same storm. In general, the differences between these two ratios show a small random variation. Examination of the 6:24-hour ratios obtained indicated a mean value of 50 percent over southern and southeastern Alaska to be reasonable. An average value of 60 percent was more appropriate for the region north of the southern coastal areas and south of the interior continental areas. For the continental and Arctic regions a mean 6:24-hour ratio of 70 percent was used. Examination of 6:24-hour ratios for other climato-

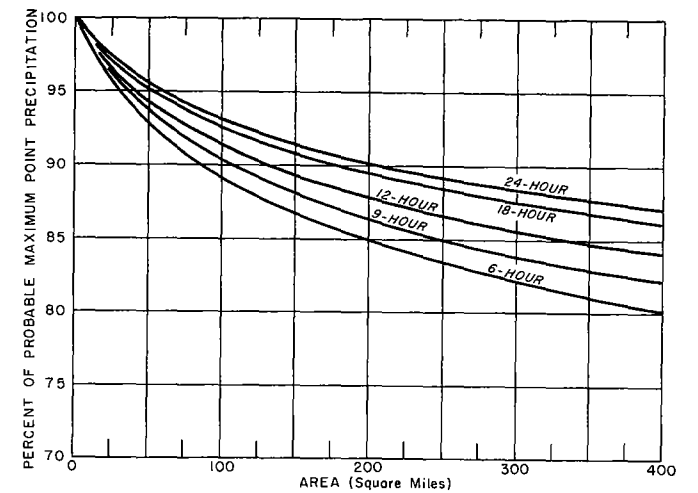


FIGURE 2-16.—Depth-area curves for PMP for durations from 6 to 24 hours for use with figure 2-12.

EXAMPLE: Determine the hourly increments of 12-hr. PMP for a 100 sq. mi. watershed centered at $60^{\circ}00'N$, $153^{\circ}30'W$. The 6- and 24-hr. point PMP for that location are found to be 10.0 and 20.0 in., respectively. Plot the 6- and 24-hr. value on the depth-duration diagram of fig. 2-14 and draw a straight line between the two plotted points. The point PMP values for 9- and 12-hr. from the line drawn on the diagram are: 12.8 and 15.0 in. Figure 2-16 indicates 100 sq. mi. reduction factors of 89, 90, and 91 percent for the 6-, 9-, and 12-hr. durations, respectively. Application of these factors to the point PMP for the corresponding durations yields 8.9, 11.5, and 13.7 in. for the 6-, 9-, and 12-hr. 100 sq. mi. PMP, respectively. Figure 2-15 indicates adjustments of 24, 44, and 58 percent, to be applied to the 6-hr. point PMP to yield the 100 sq. mi. 1-, 2-, and 3-hr. PMP. These computations will result in values of 2.4, 4.4, and 5.8 in. for the 1-, 2-, and 3-hr. 100 sq. mi. PMP. The adjusted values, 2.4, 4.4, 5.8, 8.9, 11.5, and 13.7, are then plotted against duration and a curve is drawn through the points. Values for every duration up to 12 hr. are obtained from this curve and are used to compute the required hourly increments.

logically similar regions indicated that the Alaskan ratios were of the proper magnitude for their respective areas. The ratios were then applied to corresponding 24-hour PMP values (fig. 2-12) at the grid points of figure 3-5 to obtain the 6-hour PMP (fig. 2-13). Discontinuities at the boundaries of regions with different ratios were smoothed subjectively.

2.7.3 PMP for durations between 6 and 24 hours. Figure 2-14 shows a generalized duration-interpolation diagram for determining precipitation amounts for intermediate durations when the 6- and 24-hour values are known. This diagram is the same as that used in Weather Bureau *Technical Paper No. 38* [6] and *No. 42* [7]. While

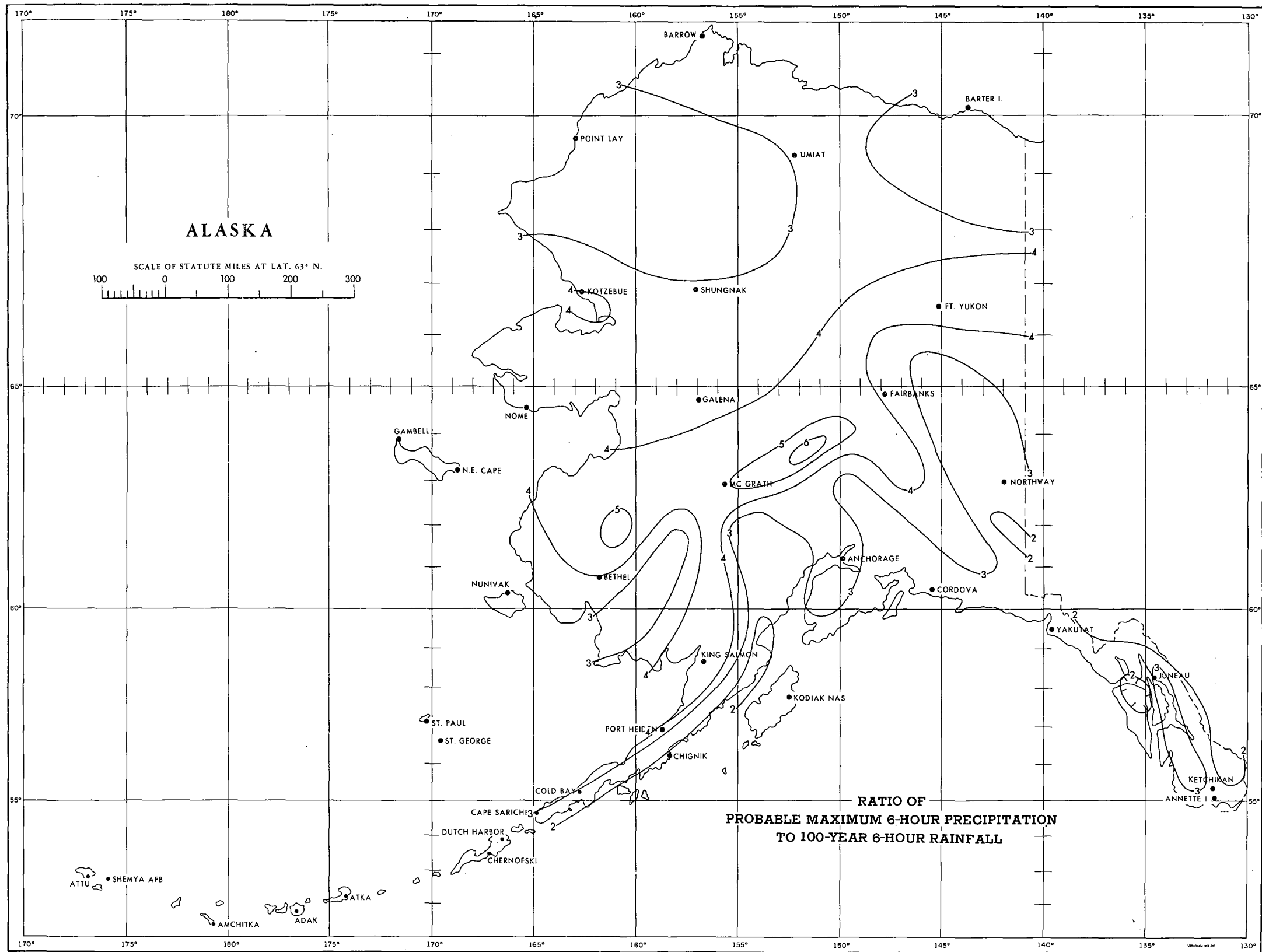


FIGURE 2-17.—Ratio of probable maximum 6-hr. precipitation to 100-yr. 6-hr. rainfall (figs. 2-13 and 3-45).

there may be regional variations in this type of relation, it was not possible to evaluate them. To use the diagram, a straightedge is laid across the values for 6 and 24 hours obtained from the maps of figures 2-12 and 2-13, and the values for intermediate durations are read at the proper intersections.

2.7.4 *PMP for durations less than 6 hours.* PMP values for durations from 1 to 6 hours can be read from the depth-area-duration diagram of figure 2-15, which shows the values in terms of percentage of the 6-hour amount. The 1-hour point value on this diagram is an average 1:6-hour ratio for stations in Alaska, California, Oregon, and Washington. Percentage values for other durations were obtained from relationships based on data used in previous studies.

2.7.5 *Depth-area reductions.* All mention of PMP thus far applied to point values. In order to reduce these point values for size of area, it is necessary to refer to the diagrams of either figure 2-15 or 2-16. Figure 2-15 is used for reducing point values for durations up to 6 hours, and figure 2-16, for durations from 6 to 24 hours. The latter depth-area diagram is the same as presented in Weather Bureau *Technical Paper No. 38* [6], except that the curves for durations under 6 hours have been integrated in figure 2-15.

2.8 Chronological distribution

2.8.1 For durations up to 24 hours there is no consis-

tent or typical chronological distribution of precipitation in outstanding storms. In the absence of any observed definite order within the maximum 24-hour period, it is suggested that the PMP increments be distributed in the most critical sequence.

2.9 Appraisal

2.9.1 There is only one way in which the accuracy of PMP estimates can be definitely established and that is in the negative sense only. In other words, if a PMP estimate is exceeded by an observed rainfall, the estimate is undeniably too low. If it is equalled by an observed rainfall, the estimate may be adequate but there is greater probability that it is too low. A PMP estimate may be excessive, i.e., it is beyond the limits of meteorological possibility. These limits are what PMP evaluation procedures attempt to establish, of course, but the required data and procedures are only barely adequate to provide approximate solutions to the problems involved.

2.9.2 Statistical methods of estimating PMP have been suggested by Hershfield [8]. This and other statistical procedures utilized are severely limited by the quality and quantity of the basic precipitation data available. An additional 20 years of records and an adequate network of favorably located recording gages would have done much to increase the reliability of the statistical approach. The statistical estimates of PMP were used as an aid in determining the extreme values of PMP, i.e., the highest

and lowest values considered possible. They also aided in establishing the general level of PMP.

2.9.3 The ratio of 6-hour PMP to 100-year 6-hour rainfall provides a rough index of the geographic consistency and relative probability of the PMP estimates. In the contiguous United States the ratio for 6-hour rainfall has been found [9] to range generally from 2 to 9. The low ratios are usually found in the wetter regions where the occurrence of high intensity rainfalls is relatively common. The highest ratios are found in arid or semi-arid regions where high intensity rainfalls are possible, but the probability is extremely low. This trend is found in Alaska. The ratio map of figure 2-17 indicates the PMP estimates to be reasonable. The ratios range from about 2 to 6. The lowest ratios are found in southeastern and southern Alaska while the highest ratios are found in the interior and Bering Sea regions of Alaska.

2.9.4 The estimates given in figures 2-12 and 2-13 are much greater than the maximum observed amounts (fig. 2-1). This does not necessarily indicate that the estimates are excessive. The period of rainfall observations was relatively short, and the station distribution was far from ideal for sampling maximum precipitation rates. In spite of the relative inadequacy of the basic data and the shortcomings of the procedures used in computing PMP, the estimates appear reasonable.

Chapter 3

RAINFALL-FREQUENCY DATA

3.1 Basic data

3.1.1 Only stations with at least 5 years of record were used in the frequency analysis. These are listed in table 1-1 by length of record. Stations with records of 20 years or more were used to define the frequency relationships, and those with records between 5 and 19 years were used to help establish the regional pattern. The Canadian stations, which bordered Alaska, were used to aid in the definition of the regional pattern in the eastern portion of the State. The seven recording gages with periods of record in excess of 10 years were used to aid in developing statistics for rainfall durations under 6 hours.

3.1.2 *True maximum n-minute amounts.* Analysis of hundreds of station-years of precipitation data has produced a factor of 1.13 for converting observational-day

and clock-hour data into true maximum 1440- and 60-minute rainfalls. This empirical factor was tested for several stations in Alaska and found to be valid.

3.2 Frequency analysis

3.2.1 *Two types of data series.* The *partial-duration series*, which includes all values above a selected base even though several may have occurred in the same year, was required for this study. However, the processing of partial-duration data is very laborious. Furthermore, there is no theoretical basis for extrapolating these data beyond the length of record. For these reasons an alternate procedure was used. The annual maximum event was collected for each year to form the *annual series*. After analysis for frequency, the annual series statistics

were converted to partial-duration statistics for corresponding return periods, and the rainfall-frequency maps presented in this report thus, in effect, represent the results of a partial-duration series analysis. Table 3-1, based on a sample of 50 widely scattered stations in the United States, gives the empirical factors for converting the partial-duration series to the annual series for return

TABLE 3-1.—*Empirical factors for converting partial-duration series to annual series*

Return period	Conversion factor
2-yr	0.88
5-yr	0.96
10-yr	0.99

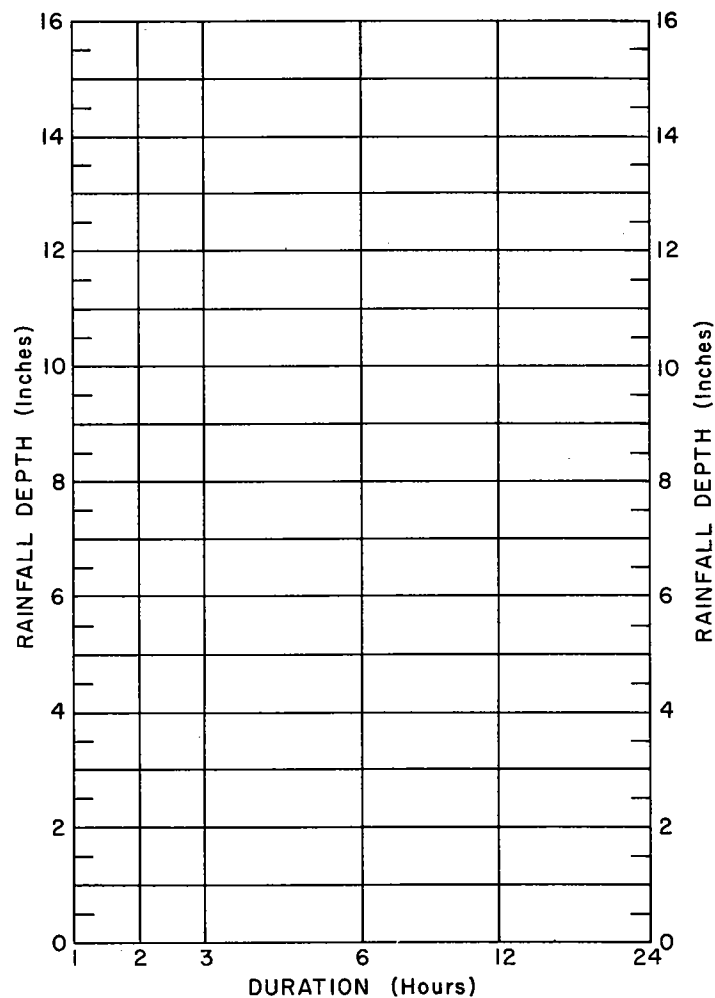


FIGURE 3-1.—Duration-interpolation diagram.

periods up to 10 years. The two types of data series show no appreciable differences for return periods greater than 10 years.

3.2.2 Duration-interpolation diagram. The generalized depth-duration relation presented in figure 3-1 provides a means for computing rainfall depth for any duration between 1 and 24 hours if the 1- and 24-hour amounts for a particular return period are given. The generalization was obtained by the method described by Weiss [10]. This relationship was compared with the diagram developed from data for 200 U.S. Weather Bureau first-order stations for use in "Rainfall Frequency Atlas of the United States" [9]. The two methods produce identical results.

3.2.3 Rainfall values for durations between 1 and 24 hours are obtained by plotting the 1- and 24-hour values for the same return period on the corresponding duration

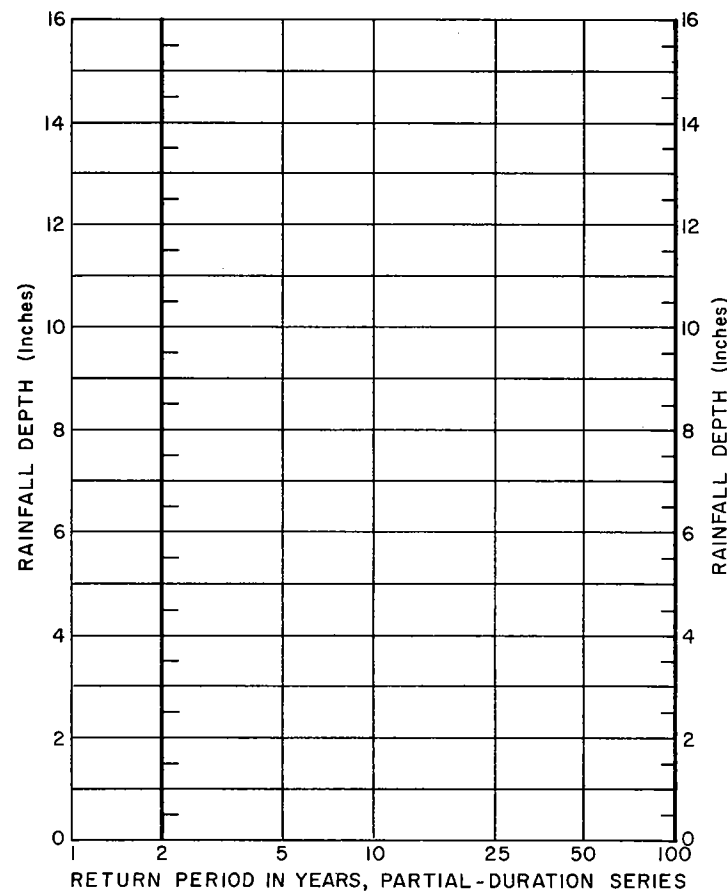


FIGURE 3-2.—Return-period-interpolation diagram.

lines and laying a straightedge between the two points. Intersections of the straightedge and intermediate duration lines yield corresponding rainfall values. Tests with recording-gage data showed that the depth-duration diagram yielded reasonably accurate values. The 30-minute rainfall values for a particular return period were obtained by multiplying the 1-hour rainfall for that return period by 0.79. Amounts for 5, 10, and 15 minutes can be obtained by applying the factors of table 3-2 [9] to the 30-minute values.

3.2.4 Return-period-interpolation diagram. The return-period diagram of figure 3-2 is obtained by the method described in [10]. Comparison of this relation-

TABLE 3-2.—Average relationship between 30-minute rainfall and shorter duration rainfall for same return period.

Duration (min.).....	5	10	15
Ratio.....	0.37	0.57	0.72

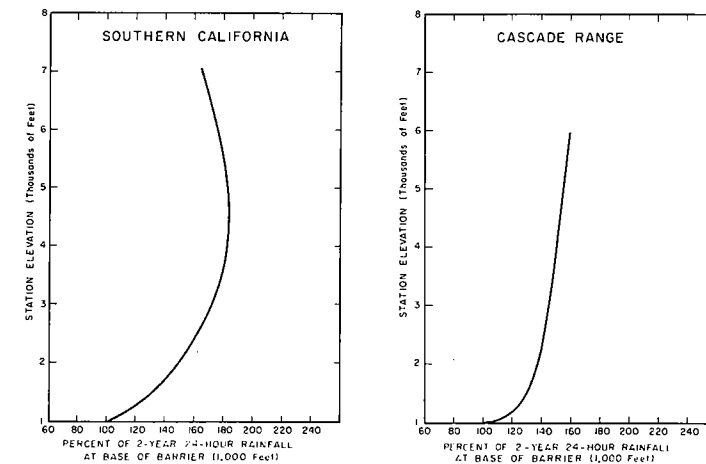


FIGURE 3-3.—Variation of 2-yr. 24-hr. rainfall with elevation for stations on the windward slopes of the southern California coastal mountains and Cascade Range.

ship with one developed from data for 200 Weather Bureau first-order stations [9] showed negligible differences. If values for return periods between 2 and 100 years are read from the return-period diagram, then converted to annual series values and plotted on either Gumbel or log-normal probability paper, the points will very nearly define a straight line.

3.2.5 Tests for secular trend. The use of short-record data introduces the question of possible secular trend and biased sample. Routine tests with data from records of equal length but for different periods showed no secular trend. The use of short-record data thus appeared justified.

3.3 Isopluvial maps

3.3.1 Rainfall-frequency-elevation relationship. Of the 184 stations available for the Alaskan area, 88 percent have an elevation of less than 1,000 ft. (fig. 1-2). Only two stations had an elevation above 2,500 ft. To define the rainfall-frequency regime over the wide range of elevation in Alaska, it was necessary to determine the variation of rainfall-frequency data with elevation in other parts of the United States with similar climatic regimes. Two criteria were used in the selection of suitable regions: (1) similar rainfall-frequency characteristics for low-elevation stations; and (2) similar topography. The areas which most nearly met these criteria were the Cascade Range of western Washington and the Salmon River Mountains and Bitterroot Range of southern Idaho and Montana.

3.3.2 Initial attempts to show the variation of the rainfall-frequency regime in the Cascade region of Wash-

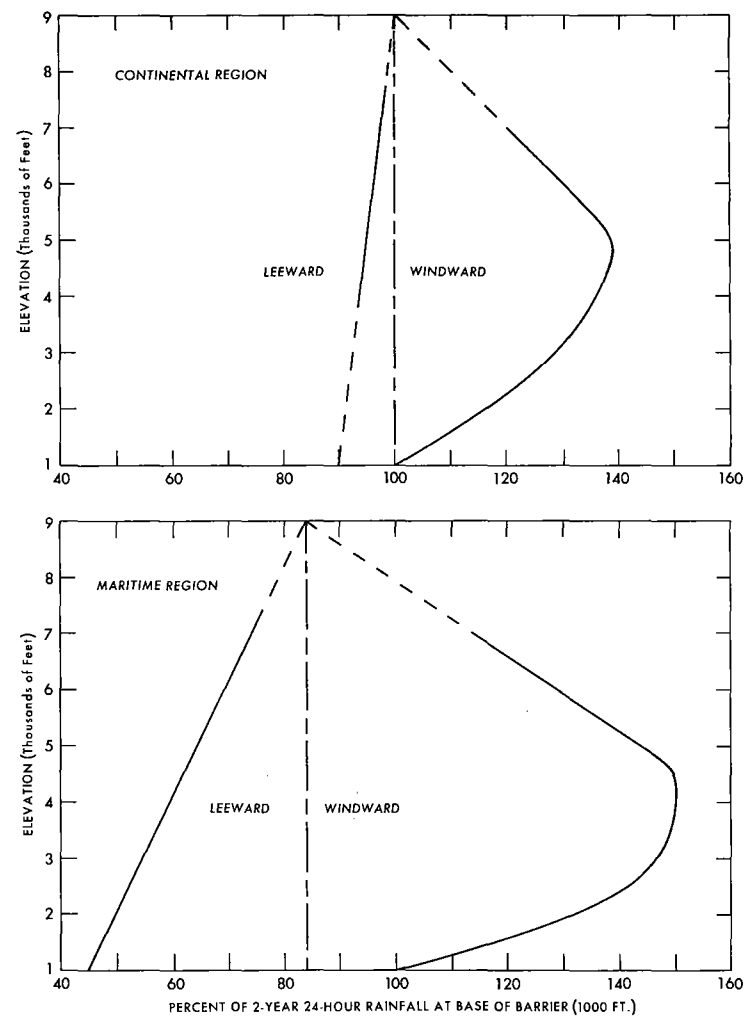


FIGURE 3-4.—Relation for adjusting 2-yr. 24-hr. rainfall data for elevation.

ington were based on data used in the preparation of "Rainfall Frequency Atlas of the United States" [9]. With the exception of two stations between 6,000 and 6,500 ft., the data were restricted to stations below 4,500 ft. Since this sample did not adequately cover the wide range of elevations required, data for another region were studied. The coastal mountains in southern California have had for several years an extensive precipitation network with a wide range of elevations. The rainfall-frequency data from this network were used to develop an elevation relationship for the windward slopes. The curve (fig. 3-3) is expressed in percent of the value at the base of the barrier to facilitate comparison between regions with different 2-year 24-hour values. A similar curve for the Cascade Range in Washington is shown also. The two curves suggest that the variation of the rainfall-

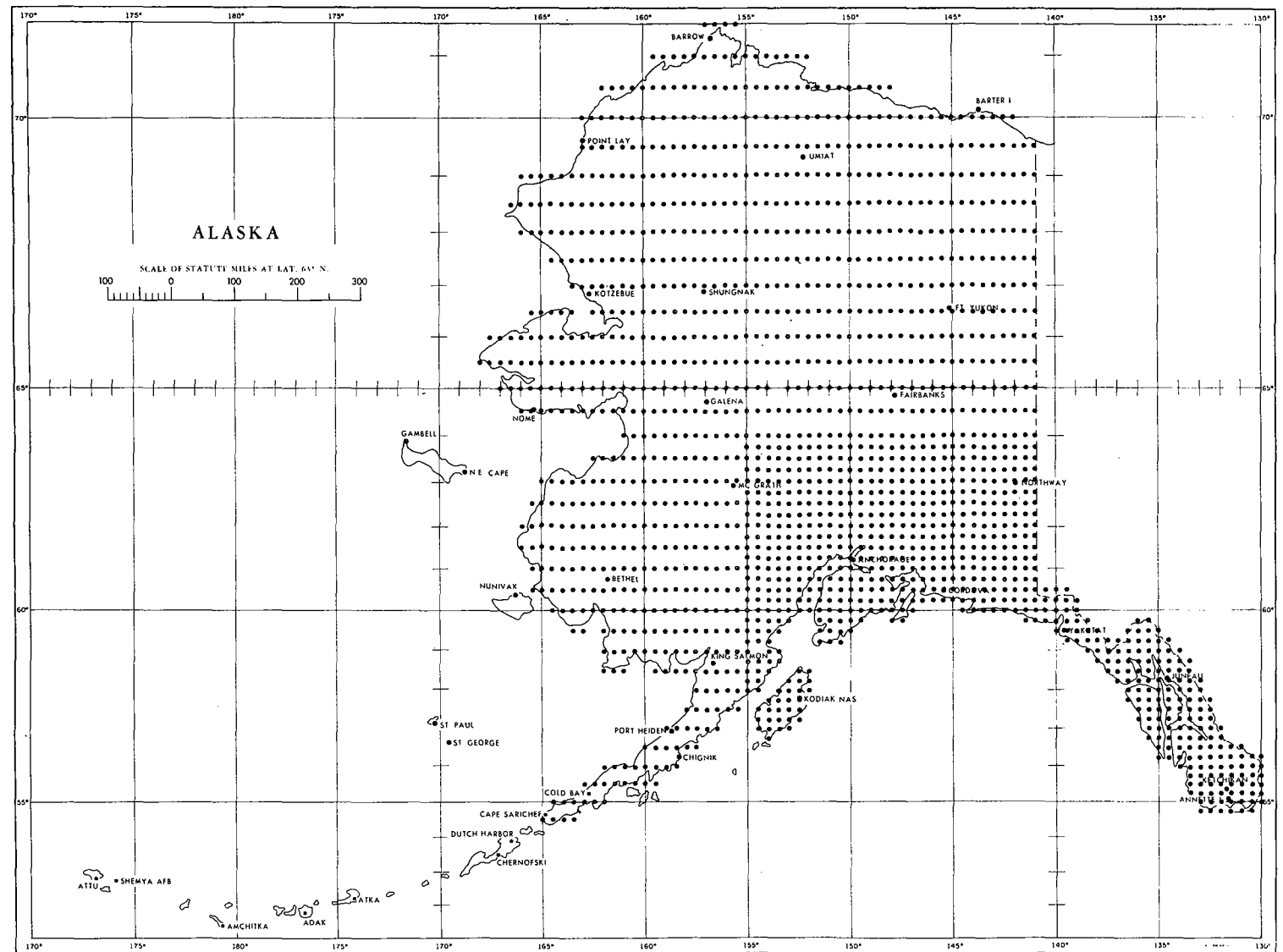


FIGURE 3-5.—Points for which probable maximum precipitation and rainfall-frequency data were computed.

frequency regime with elevation is about the same for these two regions.

3.3.3 In order to depict the entire range of elevation, a 15-minute grid was used on the 2-year 24-hour map of Weather Bureau *Technical Paper No. 28* [11] for the Cascade Range. This relationship, which is shown as the maritime curve in figure 3-4, is considered applicable to the mountainous regions of southern and southeastern Alaska. Although there was considerable scatter of the data about the curves, attempts to introduce other parameters, such as orientation, exposure, distance to moisture source, etc., failed to produce any improvement.

3.3.4 Another relation was developed for the interior

regions of Alaska. The region extending northeastward from the Snake River between Boise and Pocatello was selected as most nearly meeting the established criteria. Sufficient station data were available for this region to show the variation of the rainfall-frequency regime. The relationship is shown as the continental curve in figure 3-4. As with the maritime regions introduction of other parameters did not improve the relation.

3.3.5 *2-year 24-hour map (fig. 3-54).* Because of the greater quantity of 24-hour data available and the smaller error associated with the estimates of the shorter return periods, the 2-year 24-hour map was constructed first. The initial step required analysis of the map for the low-

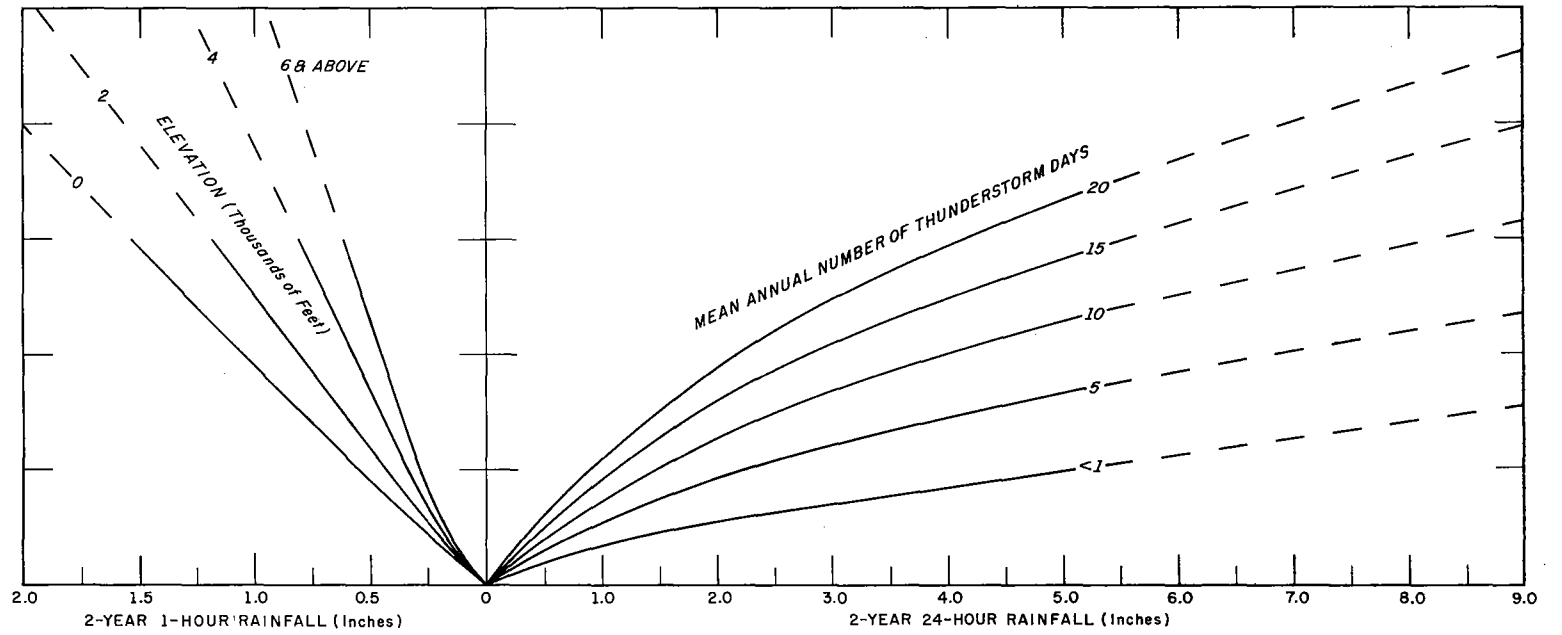


FIGURE 3-6.—Diagram for estimating 2-yr. 1-hr. amounts.

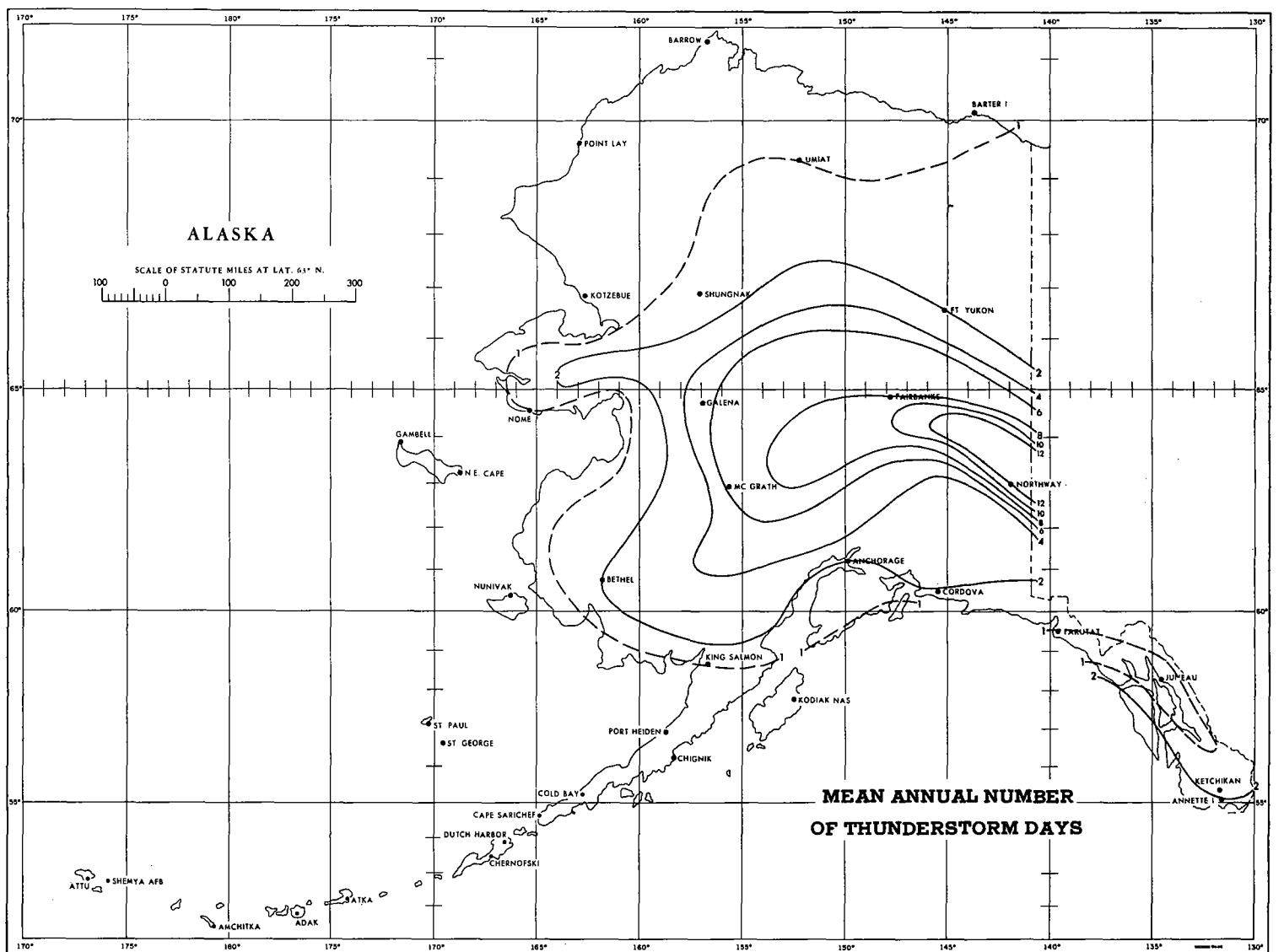


FIGURE 3-7.—Mean annual number of thunderstorm days.

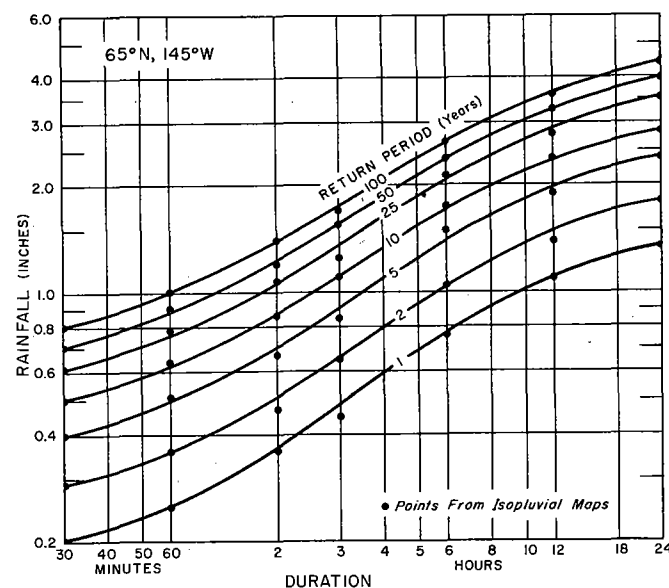


FIGURE 3-8.—Example of smoothing values read from rainfall-frequency maps.

elevation stations, which, in effect, provided a map from which the 2-year 24-hour values at the bases of the various barriers could be obtained. A grid (fig. 3-5) was then placed over the mountainous regions, and elevations at the grid points were determined from the generalized contour map of figure 2-11. The 2-year 24-hour values for various elevations were then obtained from the base values adjusted by means of the relation of figure 3-4. The values estimated from figure 3-4 and those computed for stations with elevations in excess of 1,000 ft. were plotted on the map, and the analysis over the mountainous regions was revised.

3.3.6 *100-year 24-hour map (fig. 3-59).* Relatively few stations had records of sufficient length to be used directly in the determination of the 100-year map. An indirect method of arriving at the 100-year map was thus deemed appropriate. The 100-year to 2-year ratio is subject to less variation due to orographic effects than are the frequency values themselves. A ratio map will generally show less geographic variation, with more easily definable regional patterns. The 100- to 2-year ratios were therefore plotted on a map, and isolines were drawn. The 100-year map was then constructed by applying the ratio at each of the points on the grid of figure 3-5 to the corresponding 2-year value from figure 3-54.

3.3.7 *Estimating 1-hour data.* The paucity of recording-gage data necessitated the synthesis of an hourly rainfall regime based partly on Alaskan data and partly on relationships based on data from other regions of the

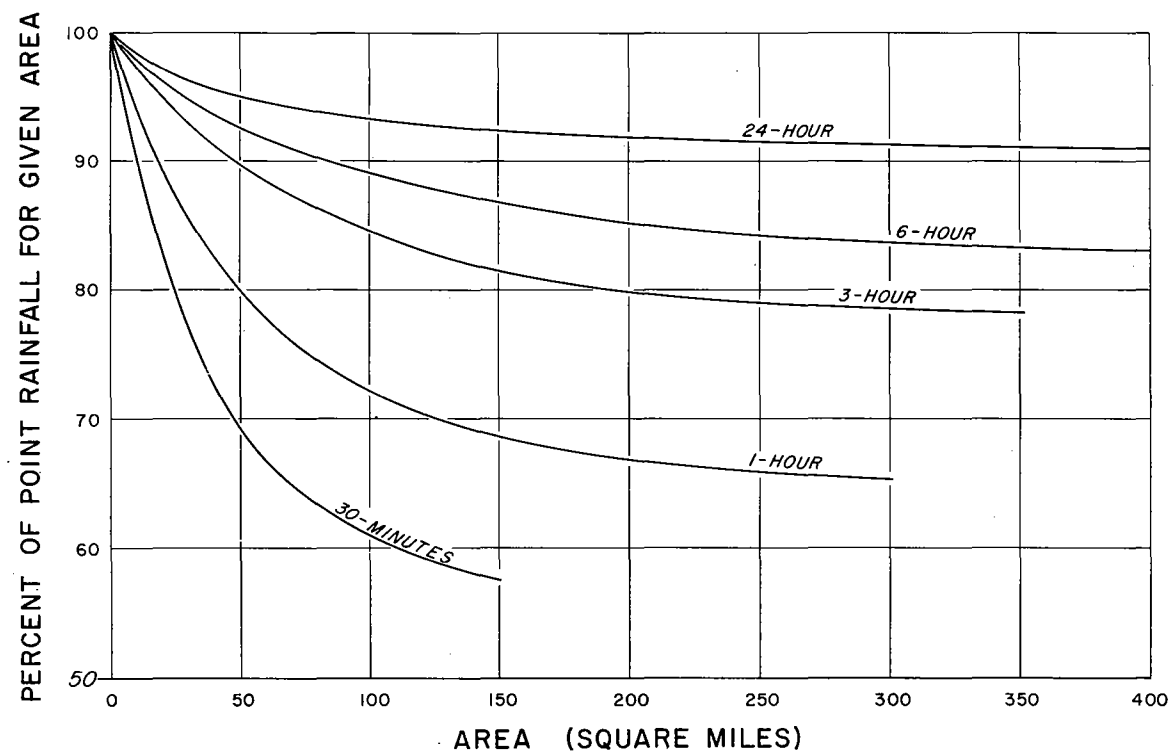


FIGURE 3-9.—Depth-area curves for rainfall-frequency data for use with figures 3-11 to 3-59.

United States and Canada. The frequency regime of short-duration precipitation can be reasonably estimated from climatic and topographic parameters. In the present study three parameters were used to synthesize the 1-hour rainfall-frequency regime: (1) the 2-year 24-hour precipitation; (2) mean annual number of thunderstorm days; and (3) elevation. Figure 3-6 shows the relationship developed from data for 59 stations in Canada and the United States.

3.3.8 The use of figure 3-6 necessitated the development of a map showing the mean annual number of thunderstorm days (fig. 3-7). The map is based on 127 stations, having from 5 to 40 years of record. Only 36 stations had records in excess of 20 years.

3.3.9 *2-year 1-hour map (fig. 3-19).* Values of the 2-year 24-hour precipitation, mean annual number of thunderstorm days, and elevation were determined for the grid of figure 3-5. The 1-hour amounts were then estimated from figure 3-6. These values together with those from the seven recording gages were plotted on a map, and isopluvials were drawn. At a few points the 1:24-hour ratio was found to be less than 10 percent. On the basis of tests with Alaskan and other data indicating such low

ratios to be unrealistic, the 1-hour map was adjusted where necessary so the minimum ratio was 10 percent.

3.3.10 *100-year 1-hour map (fig. 3-24).* The 100- to 2-year ratios were computed for the seven recording-gage stations with more than 10 years of record. The ratios were plotted on a map, and isolines were drawn. Ratios for the grid of figure 3-5 were read from the map and combined with the corresponding 2-year 1-hour values to provide the 100-year 1-hour map. The 1:24-hour ratio was computed for the 100-year return period and plotted on a map as a consistency check. The ratios were compared with a similar map for the 2-year return period to determine if the ratios were everywhere consistent. Some minor adjustments were made in regions where the 100-year 1:24-hour ratio was less than 10 percent.

3.3.11 *Additional isopluvial maps.* The 2-year 1-hour, 2-year 24-hour, 100-year 1-hour, and 100-year 24-hour maps were then used in conjunction with the duration and return-period relations of figures 3-1 and 3-2 to obtain 38 isopluvial maps for intermediate durations and return periods. The computations were made by a digital computer. Values were computed for and plotted on the grid of figure 3-5, and the isopluvials were then drawn with

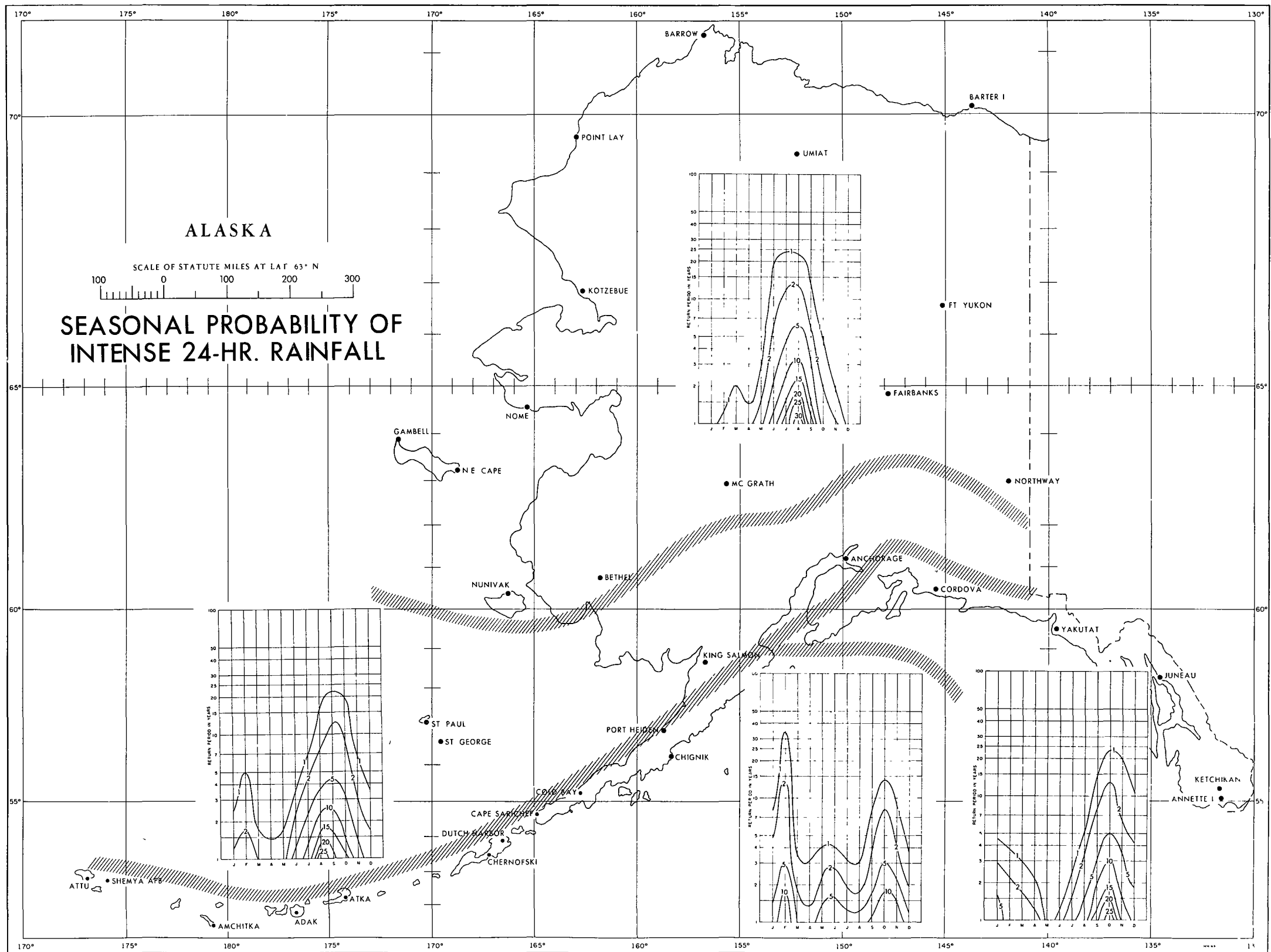


FIGURE 3-10.—Monthly distribution (in percent) of 24-hr. rainfalls for various return periods.

reference to these grid values. The seven 30-min. maps were developed from the relationship 0.79 times the values on the 1-hour maps for corresponding return periods [9]. The 49 rainfall-frequency maps are presented at the end of this chapter (figs. 3-11 to 3-59).

3.4 Smoothing data read from the maps

3.4.1 The complex patterns and steep gradients of the isopluvials combined with the difficulties of interpolation and accurate location of a point on a series of maps might result in inconsistencies in data read from the maps. Such inconsistencies can be minimized by fitting smooth curves to a plot of the data obtained from the maps. Figure 3-8 illustrates a set of curves on logarithmic paper for the point at 65°N., 145°W. The interpolated values for a particular duration should very nearly approximate a straight line on the return-period diagram of figure 3-2.

3.5 Depth-area relationships

3.5.1 There are two basic types of depth-area relationships: (1) storm-centered relations, and (2) geographically fixed relations. The depth-area curves of figures 2-15 and 2-16 are storm-centered, i.e., they were developed from rainfall data in storm centers. The frequency-derived, geographically fixed, depth-area curves of figure 3-9 are based on data from different parts of different storms instead of on the highest amounts surrounding the storm centers. Since the area is geographically fixed, its precipitation stations measure rainfall sometimes near the storm center, sometimes on the outer edges, and sometimes in between the two. The averaging process results in the geographically fixed curves being flatter than storm-centered curves. Each type of curve is appropriate for its respective application—the storm-centered for PMP, and the geographically-fixed for frequency data.

3.5.2 The depth-area curves of figure 3-9 are based on data from 20 dense precipitation networks and are identical to those of Weather Bureau *Technical Paper No. 29* series [12].

3.6 Seasonal variation

3.6.1 The frequency analysis discussed followed the conventional procedures of using only the annual maxima (annual series) or the n maximum events for n years of record (partial-duration series). Obviously, some months contribute more events to these series than do other months, and some months may not contribute at all. As a matter of interest the annual maximum 24-hour data were analyzed to determine their monthly distribution. The data for all Alaskan stations with 15 or more years of record were used. This provided a total of 2,464 station-years of record. These data were then classified according to month of occurrence and return period. Examination of the data disclosed four regions with different seasonal characteristics. After the stations were grouped by region the frequencies were computed for each month by determining the ratio (in percent) of the number of occurrences of amounts equal to or greater than the value for a particular return period to the total number of occurrences (total years of record). Cases of nonoccurrence as well as occurrence of rainfall events were considered in order to arrive at numerical probabilities. The probabilities were then plotted as a function of return period and season and smoothed isopleths fitted to the probabilities. Figure 3-10 shows the monthly distribution for each region. The boundaries for these zones cannot be considered as a sharp line but rather as a diffuse zone of transition from one region to another.

EXAMPLE: Determine the monthly probabilities of 5-yr. 24-hr. rainfalls for June through October for Umiat and for August through December for Juneau. Figure 3-10 shows the required probabilities for the region in which Umiat is located are 2, 5, 6, 3, and 1; for Juneau they are 1, 3, 5, 3, and 2. In other words, the probability of a 5-yr. 24-hr. rainfall in June of any year for Umiat is 2 percent; for July, 5 percent, etc. For Juneau in August the probability of a 5-yr. 24-hr. rainfall is 1 percent; for September, 3 percent; etc.

References

1. U.S. Weather Bureau, "Maximum Recorded United States Point Rainfall," *Technical Paper No. 2*, April 1947, 36 pp.
2. L. L. Weiss and W. T. Wilson, "Precipitation Gage Shields," *Comptes Rendus et Rapports—Assemblée Générale de Toronto*, International Union of Geodesy and Geophysics, Gentbrugge, vol. 1, 1958, pp. 462-484.
3. U.S. Weather Bureau, "Climates of the States—Alaska," *Climatology of the United States No. 60-49*, Sept. 1959, 24 pp.
4. U.S. Weather Bureau and U.S. Navy Hydrographic Office, *Climatological and Oceanographic Atlas for Mariners, Volume II—North Pacific Ocean*, 1961, 6 pp., 159 charts.
5. U.S. Weather Bureau, "Interim Report, Probable Maximum Precipitation in California," *Hydrometeorological Report No. 36*, Oct. 1961, 202 pp.
6. U.S. Weather Bureau, "Generalized Estimates of Probable Maximum Precipitation for the United States West of the 105th Meridian," *Technical Paper No. 38*, 1959, 66 pp.
7. U.S. Weather Bureau, "Generalized Estimates of Probable Maximum Precipitation and Rainfall-Frequency Data for Puerto Rico and Virgin Islands," *Technical Paper No. 42*, 1961, 94 pp.
8. D. M. Hershfield, "Estimating the Probable Maximum Precipitation," *Journal of the Hydraulics Division, Proceedings of the American Society of Civil Engineers*, vol. 87, No. HY5, Sept. 1961, pp. 99-116.
9. U.S. Weather Bureau, "Rainfall-Frequency Atlas of the United States," *Technical Paper No. 40*, May 1961, 115 pp.
10. L. L. Weiss, "A General Relation Between Frequency and Duration of Precipitation," *Monthly Weather Review*, vol. 90, No. 3, March 1962, pp. 87-88.
11. U.S. Weather Bureau, "Rainfall Intensities for Local Drainage Design in Western United States," *Technical Paper No. 28*, Nov. 1956, 46 pp.
12. U.S. Weather Bureau, "Rainfall Intensity-Frequency Regime, Part I—The Ohio Valley," *Technical Paper No. 29*, June 1957, 44 pp.

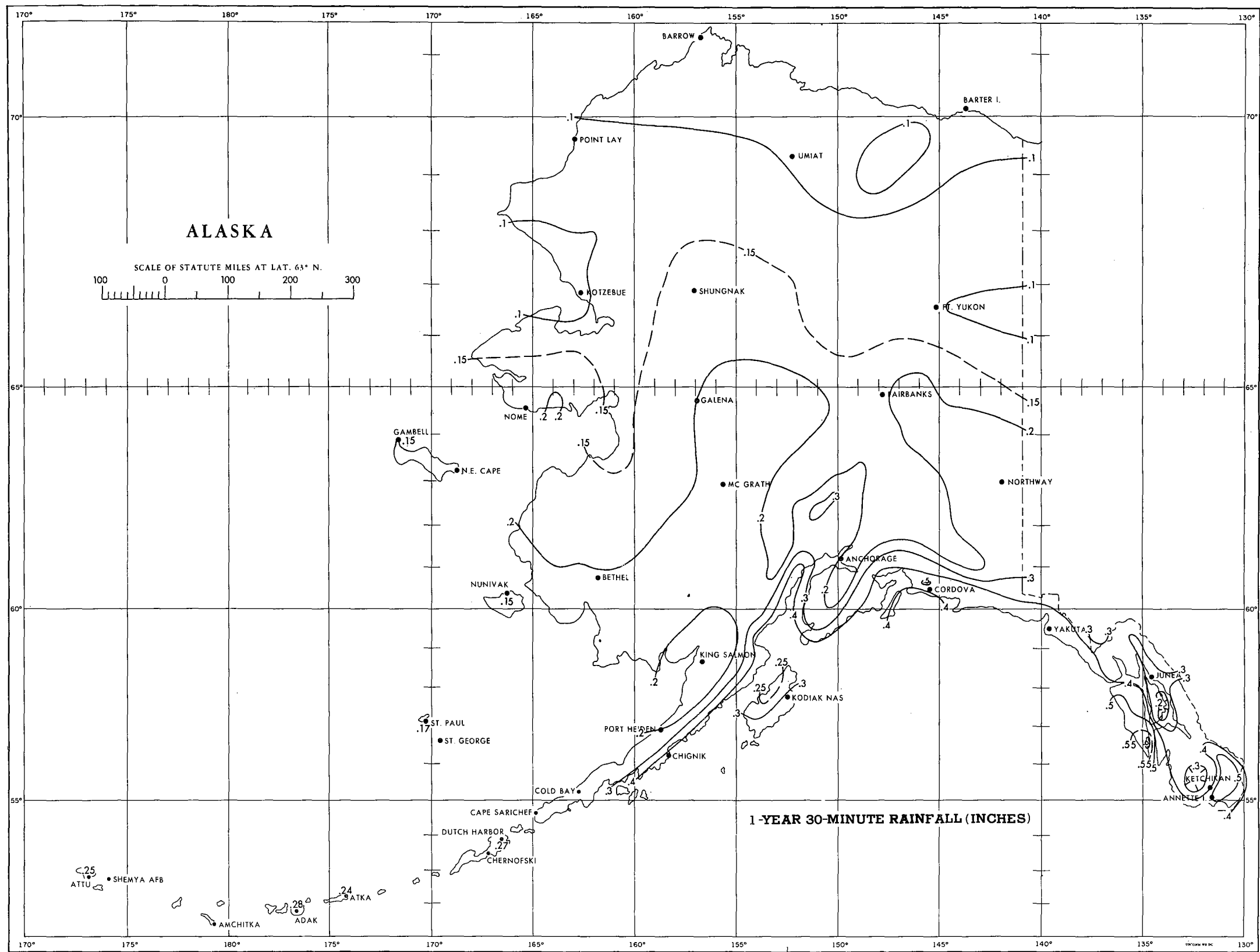


FIGURE 3-11.—1-yr. 30-min. rainfall (in.).

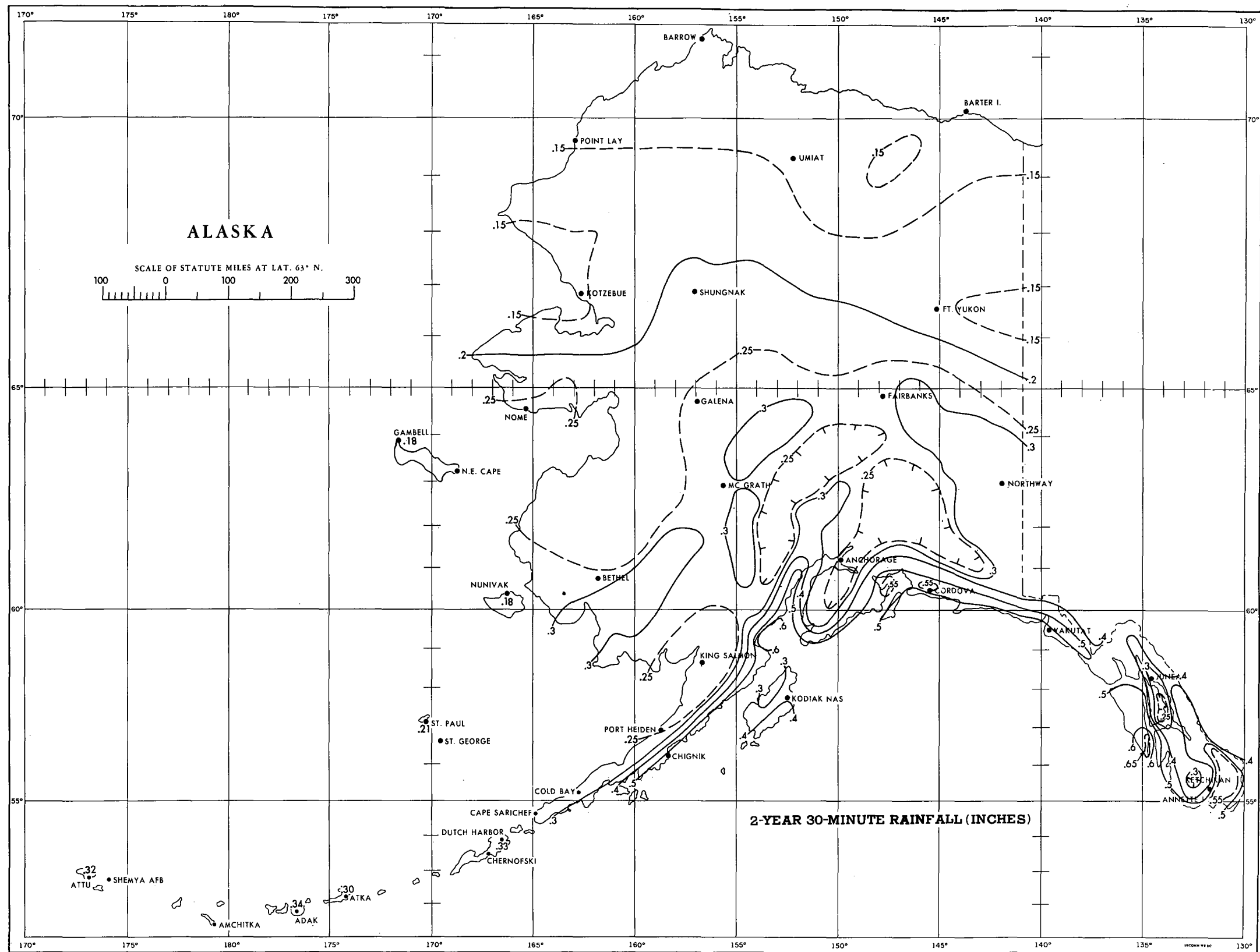


FIGURE 3-12.—2-yr. 30-min. rainfall (in.).

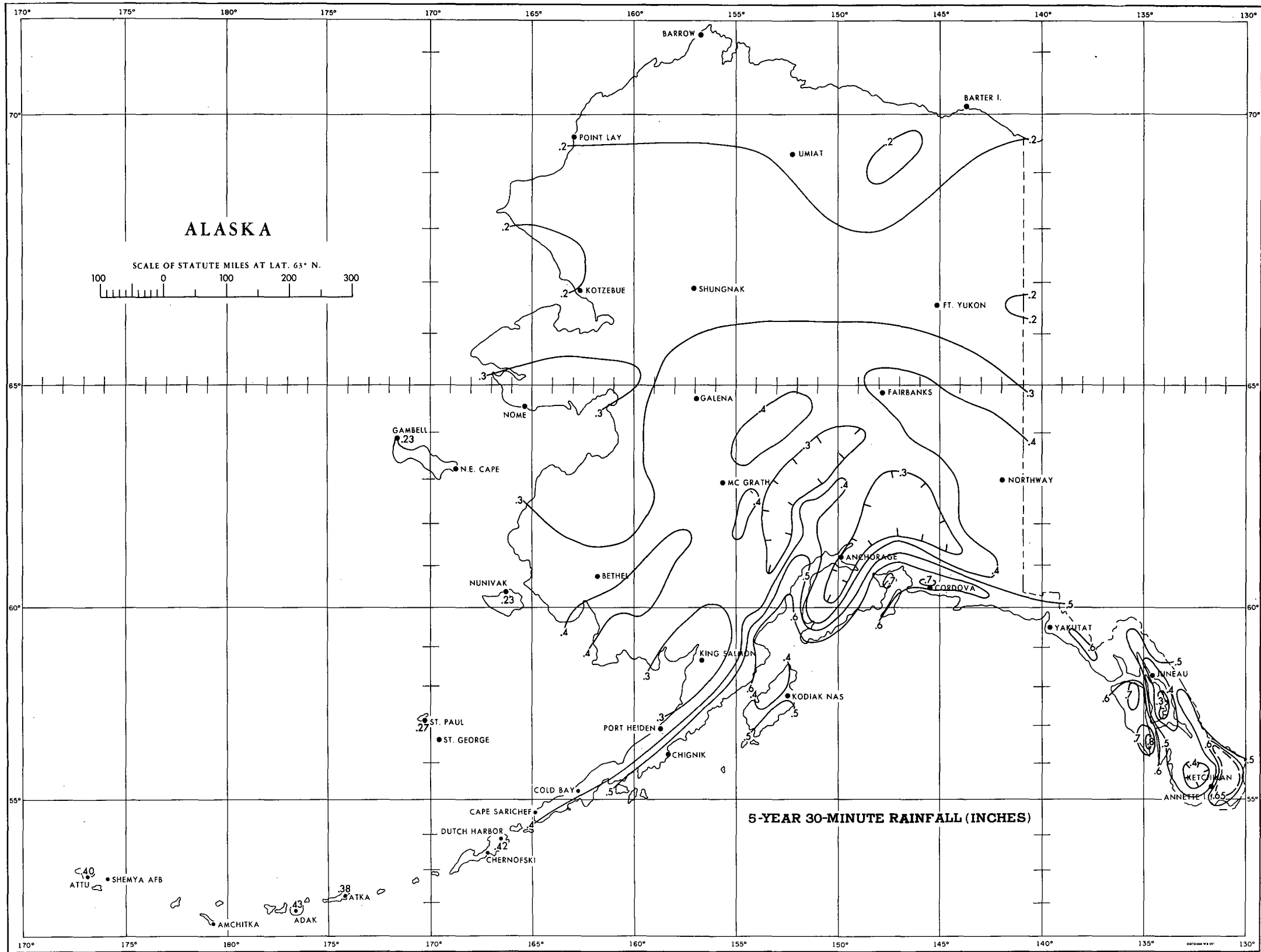


FIGURE 3-13.—5-yr. 30-min. rainfall (in.).

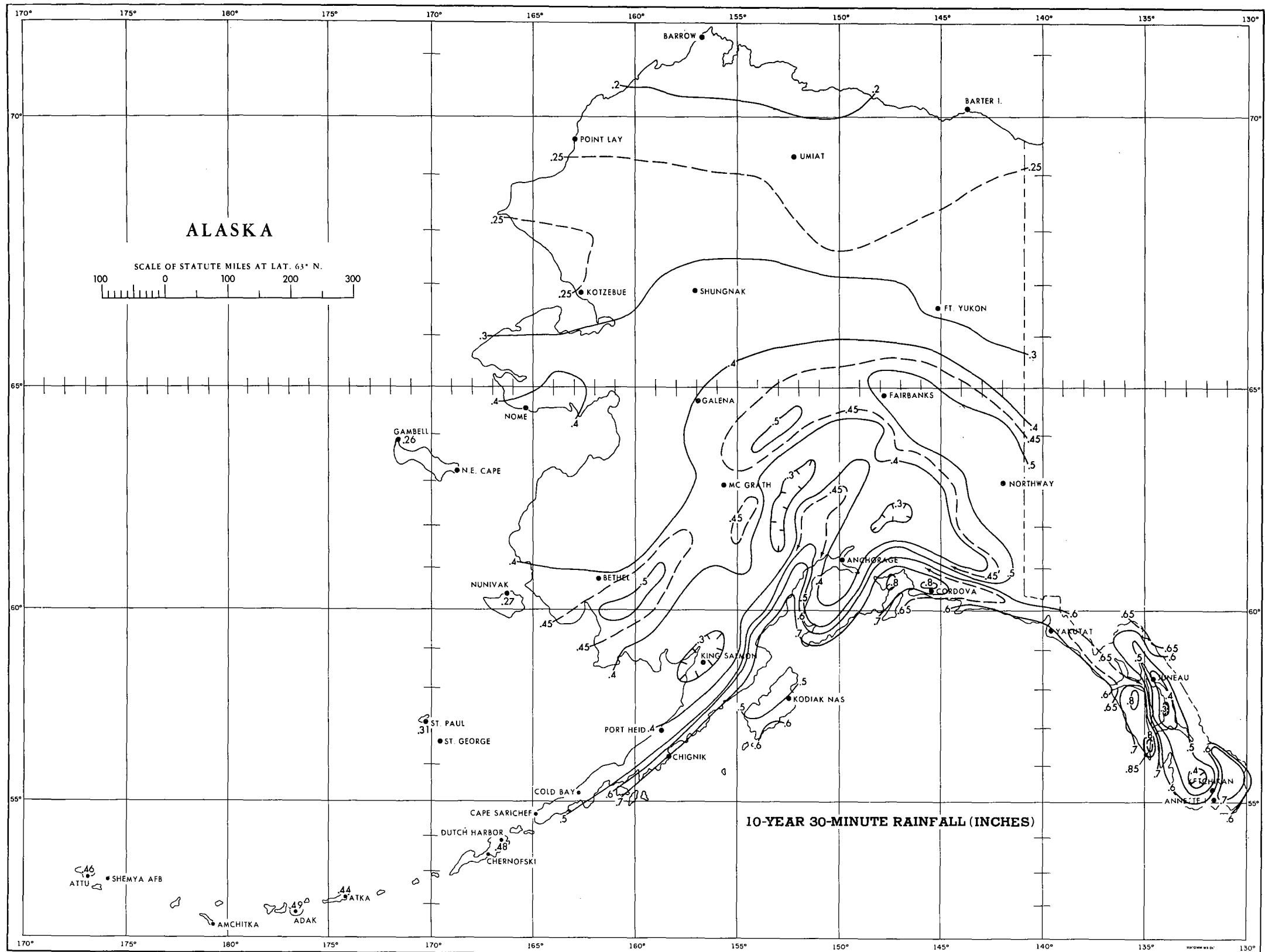


FIGURE 3-14.—10-yr. 30-min. rainfall (in.).

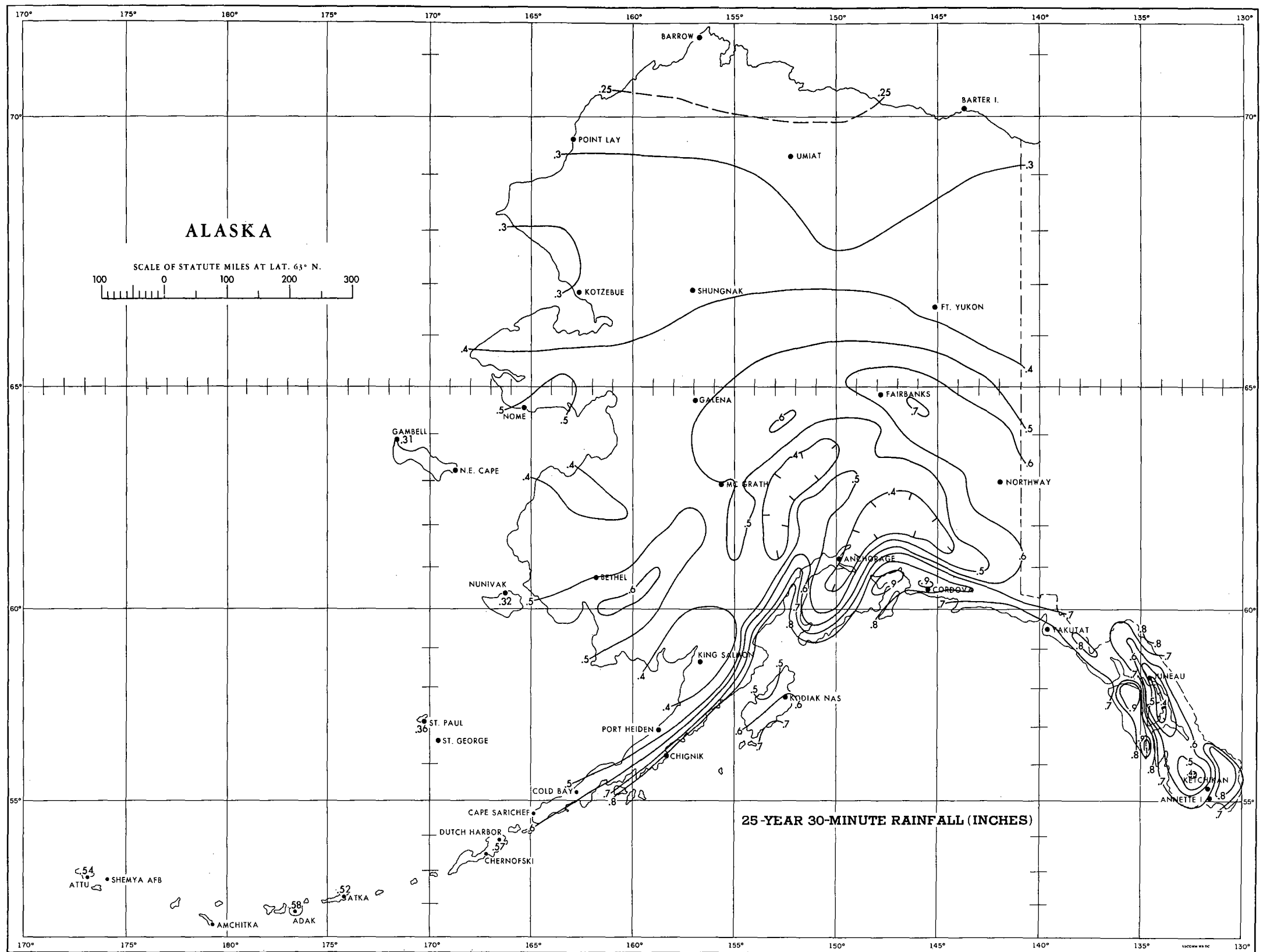


FIGURE 3-15.—25-yr. 30-min. rainfall (in.).

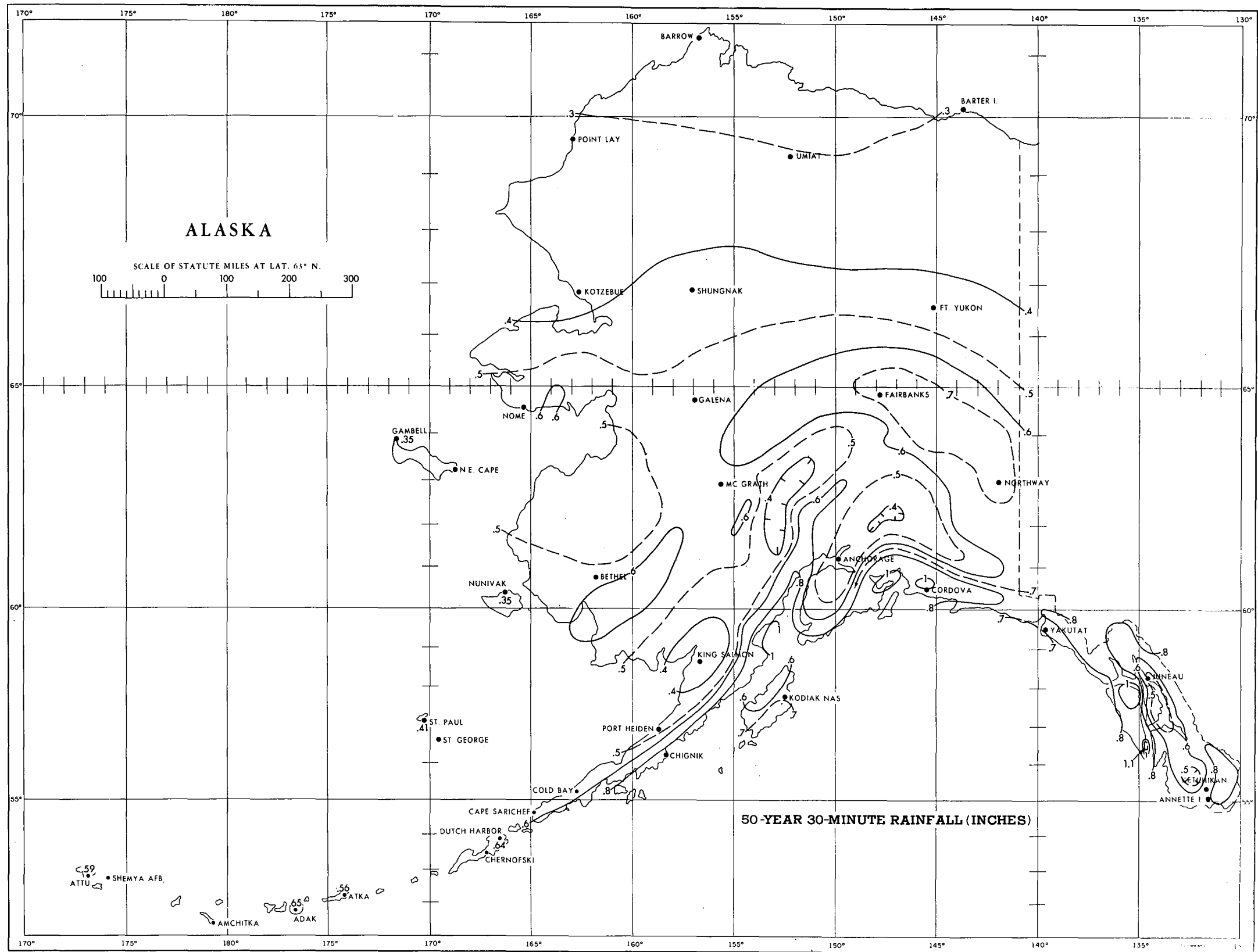


FIGURE 3-16.—50-yr. 30-min. rainfall (in.).

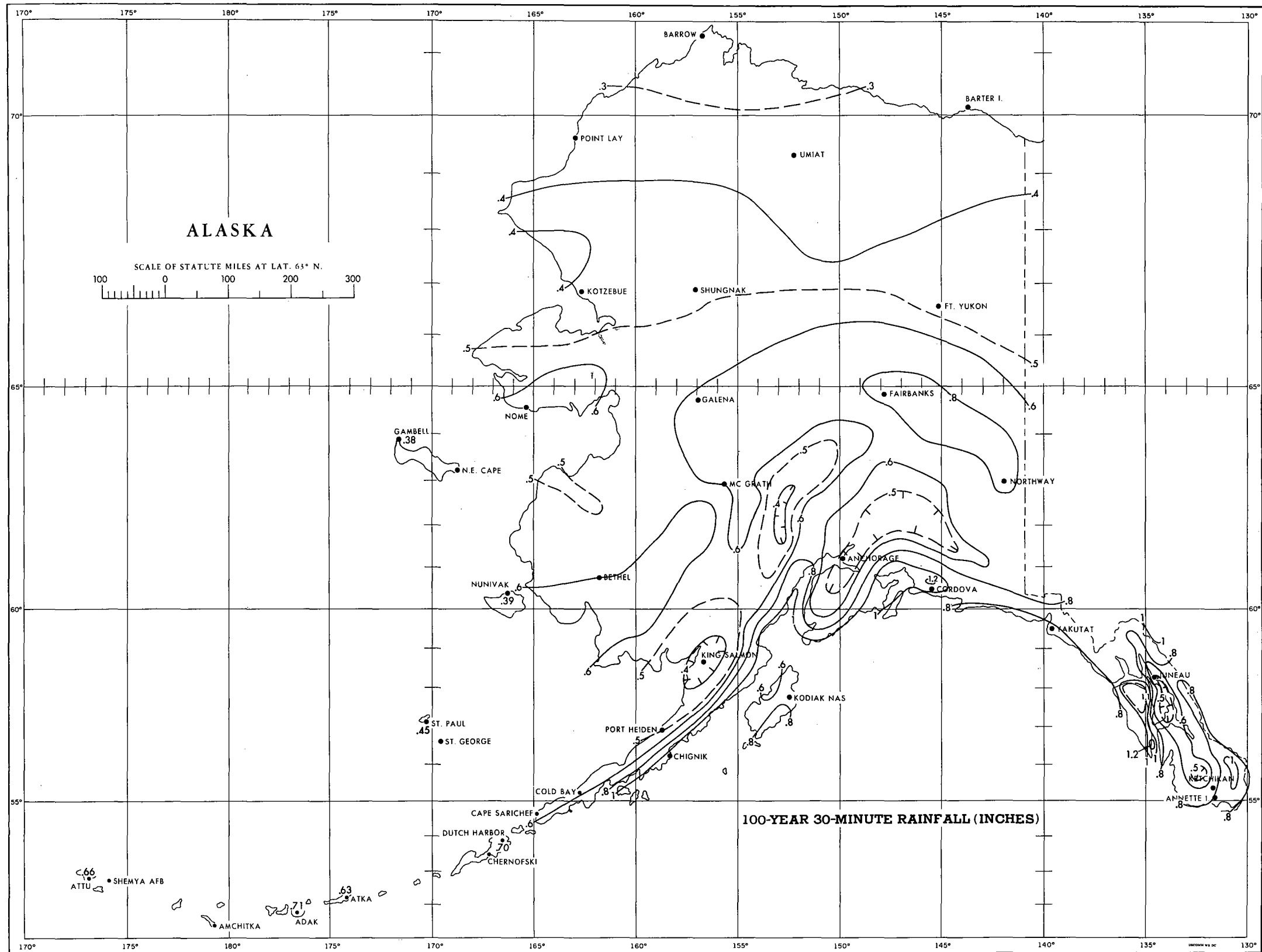


FIGURE 3-17.—100-yr. 30-min. rainfall (in.).

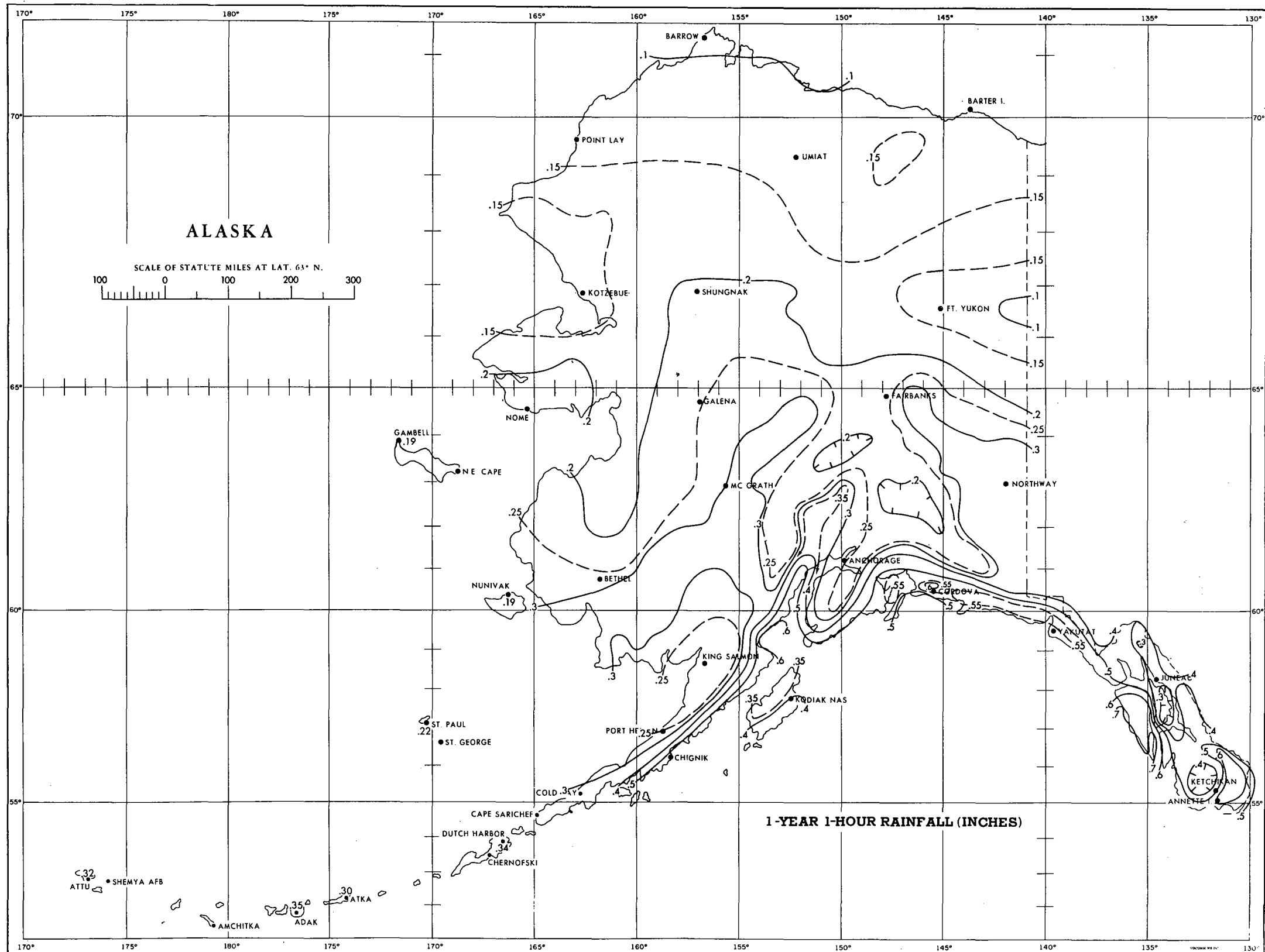


FIGURE 3-18.—1-yr. 1-hr. rainfall (in.).

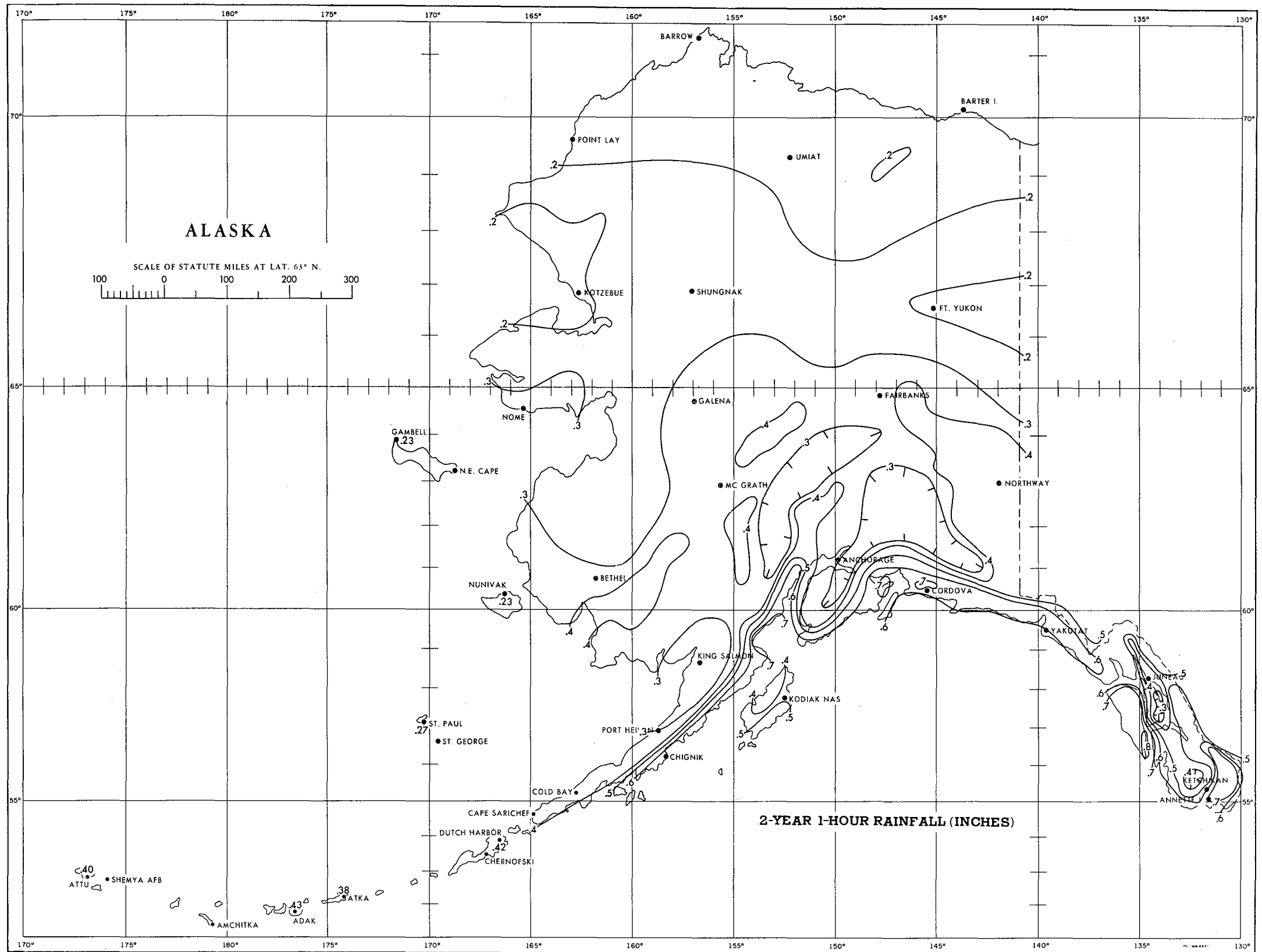


FIGURE 3-19.—2-yr. 1-hr. rainfall (in.).

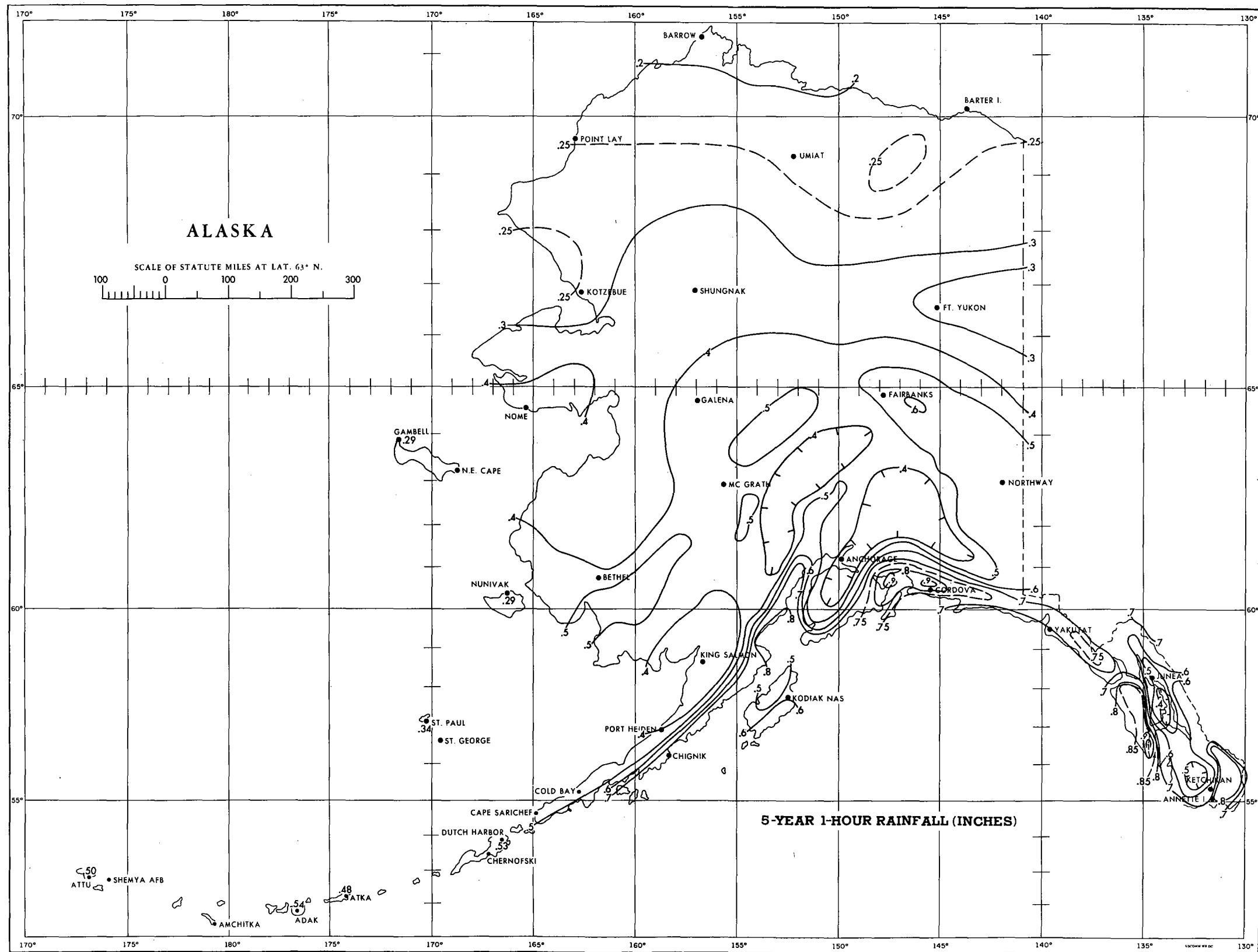


FIGURE 3-20.—5-yr. 1-hr. rainfall (in.).

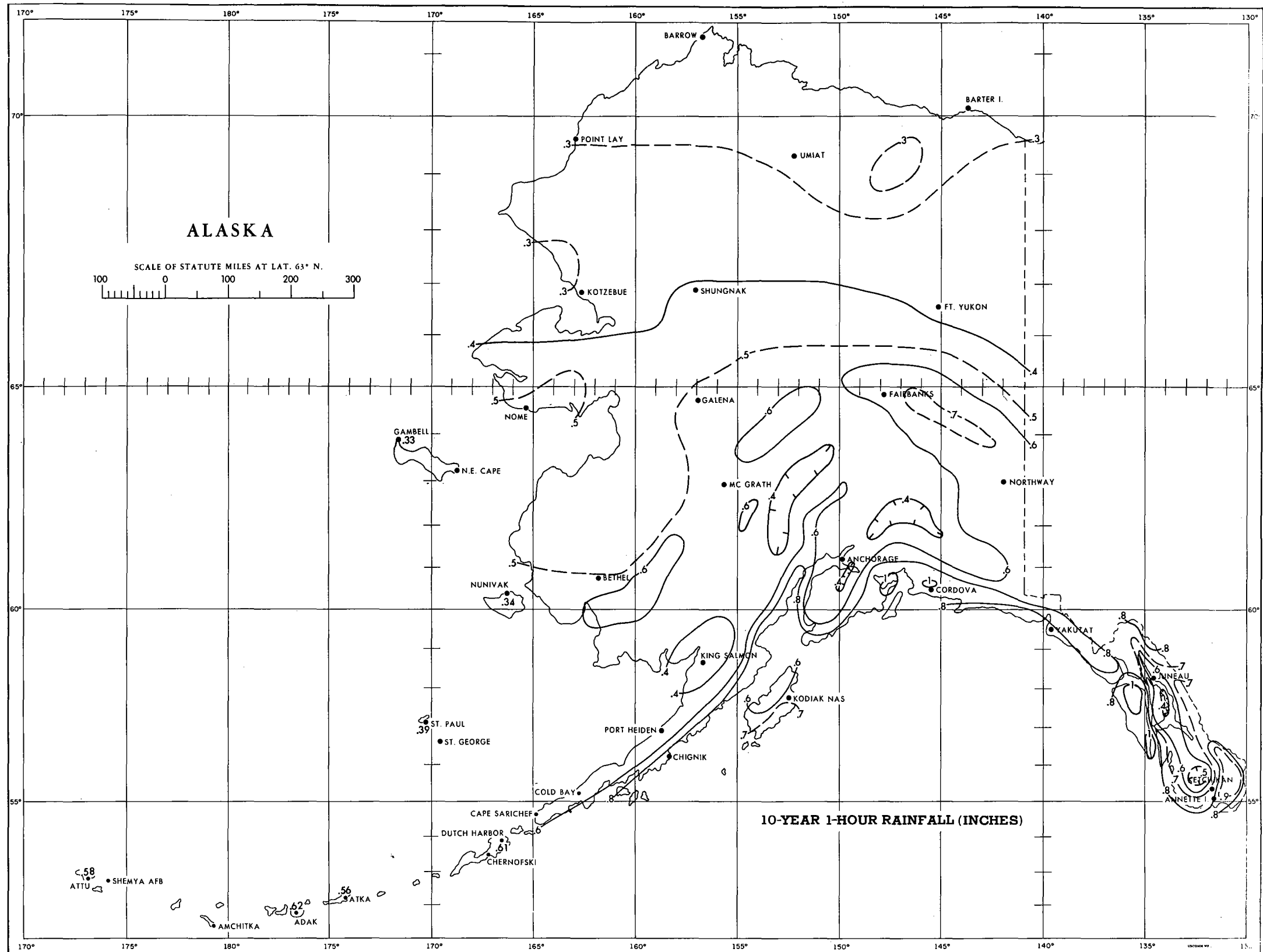


FIGURE 3-21.—10-yr. 1-hr. rainfall (in.).

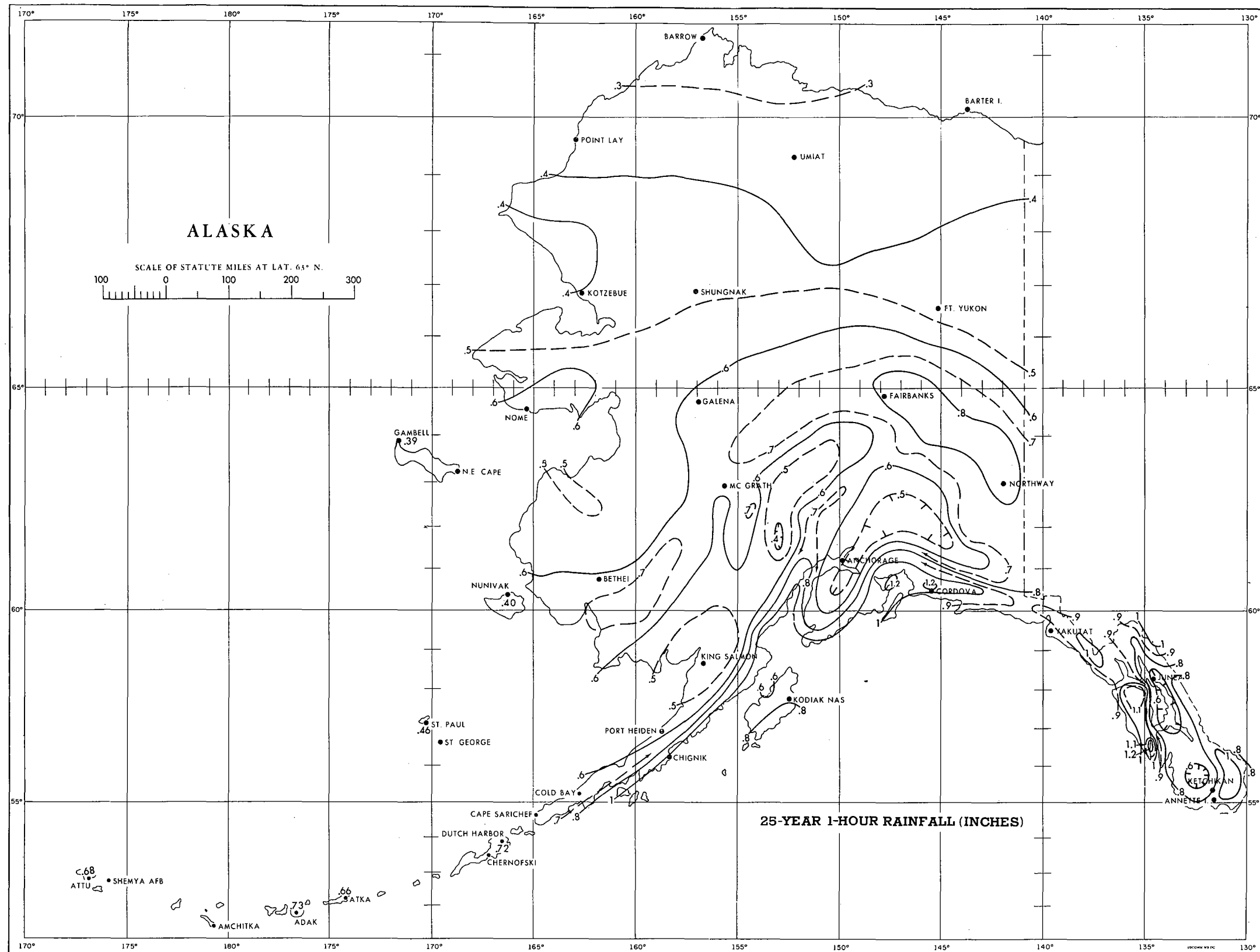


FIGURE 3-22.—25-yr. 1-hr. rainfall (in.).

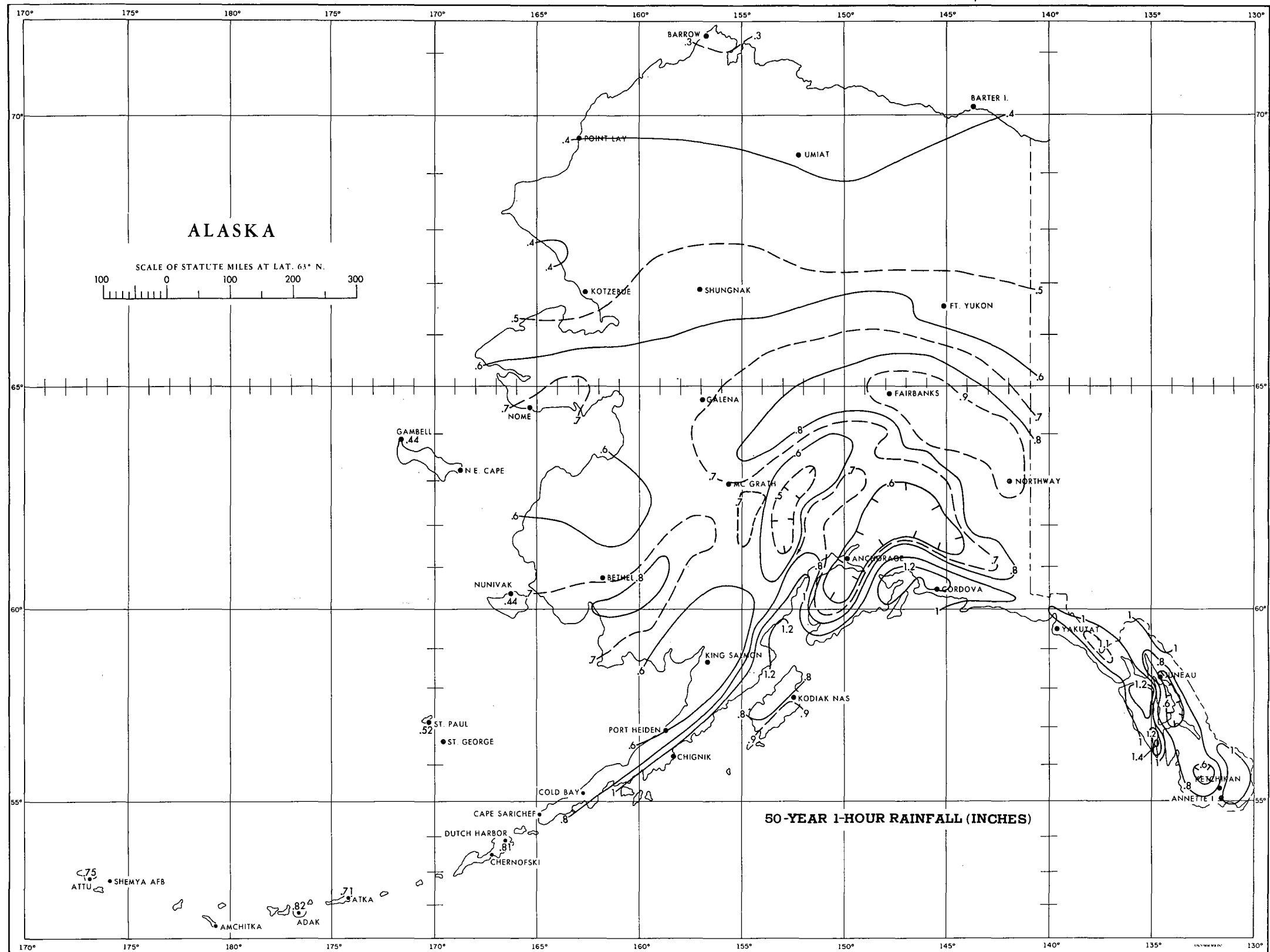


FIGURE 3-23.—50-yr. 1-hr. rainfall (in.).

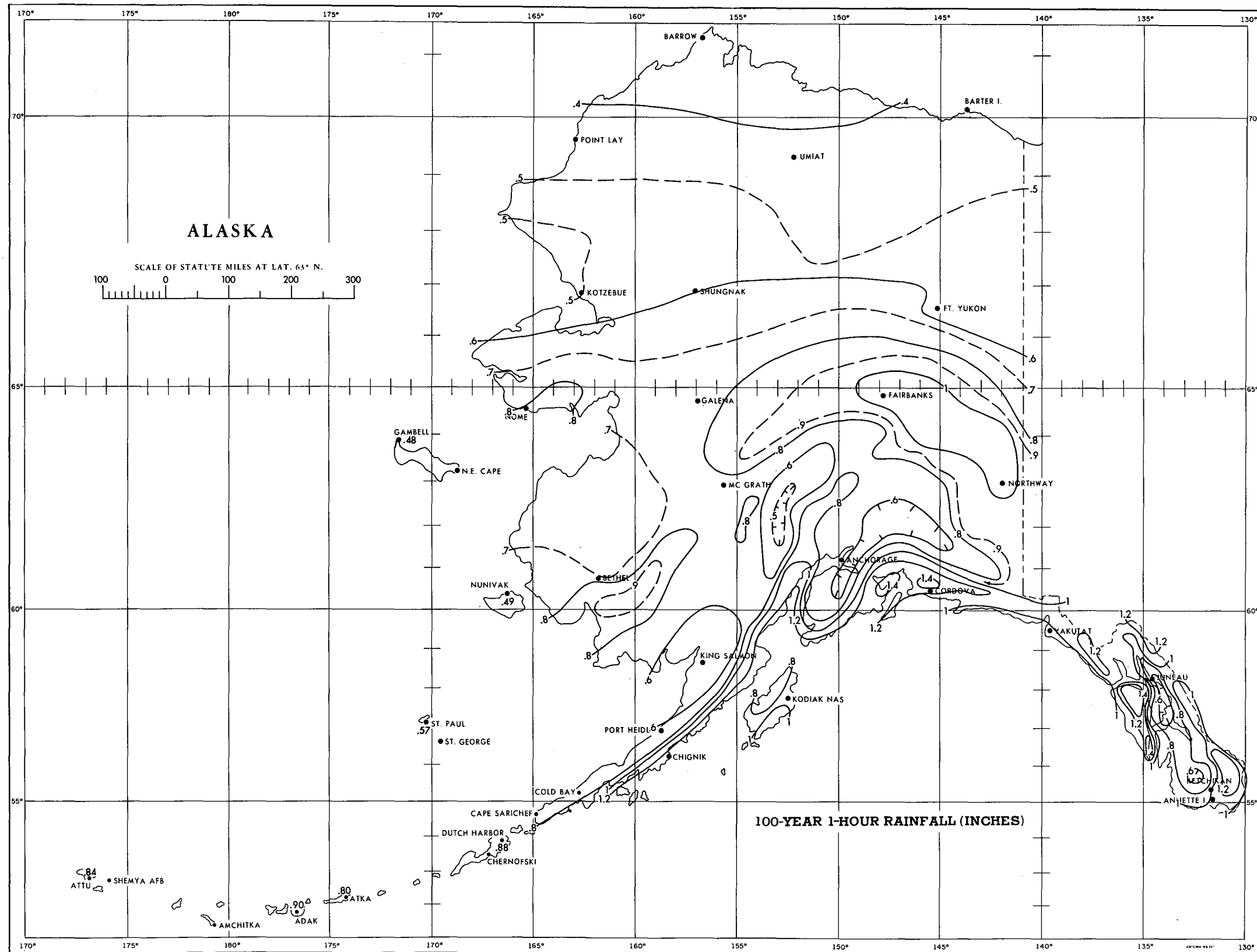


FIGURE 3-24.—100-yr. 1-hr. rainfall (in.).

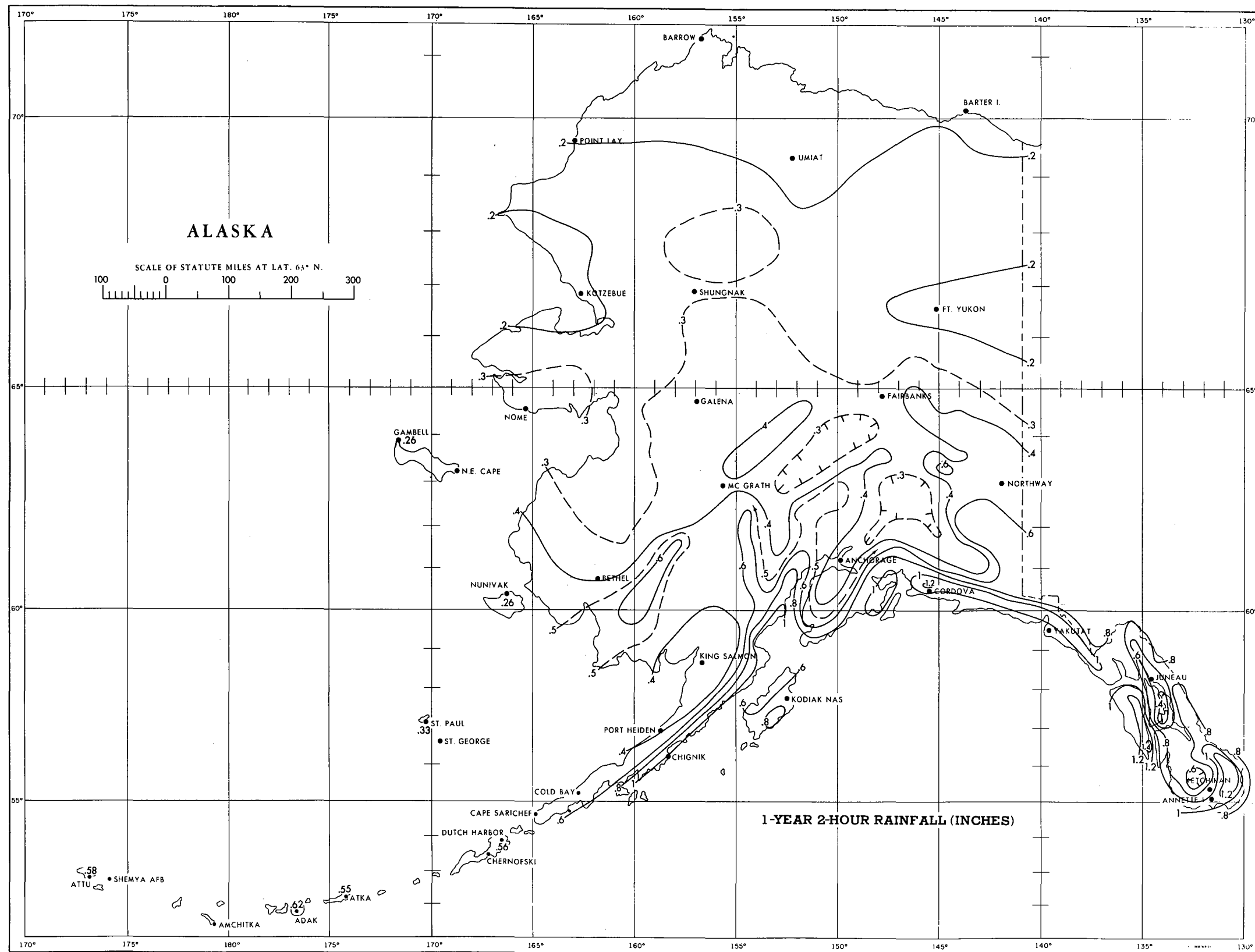


FIGURE 3-25.—1-yr. 2-hr. rainfall (in.).

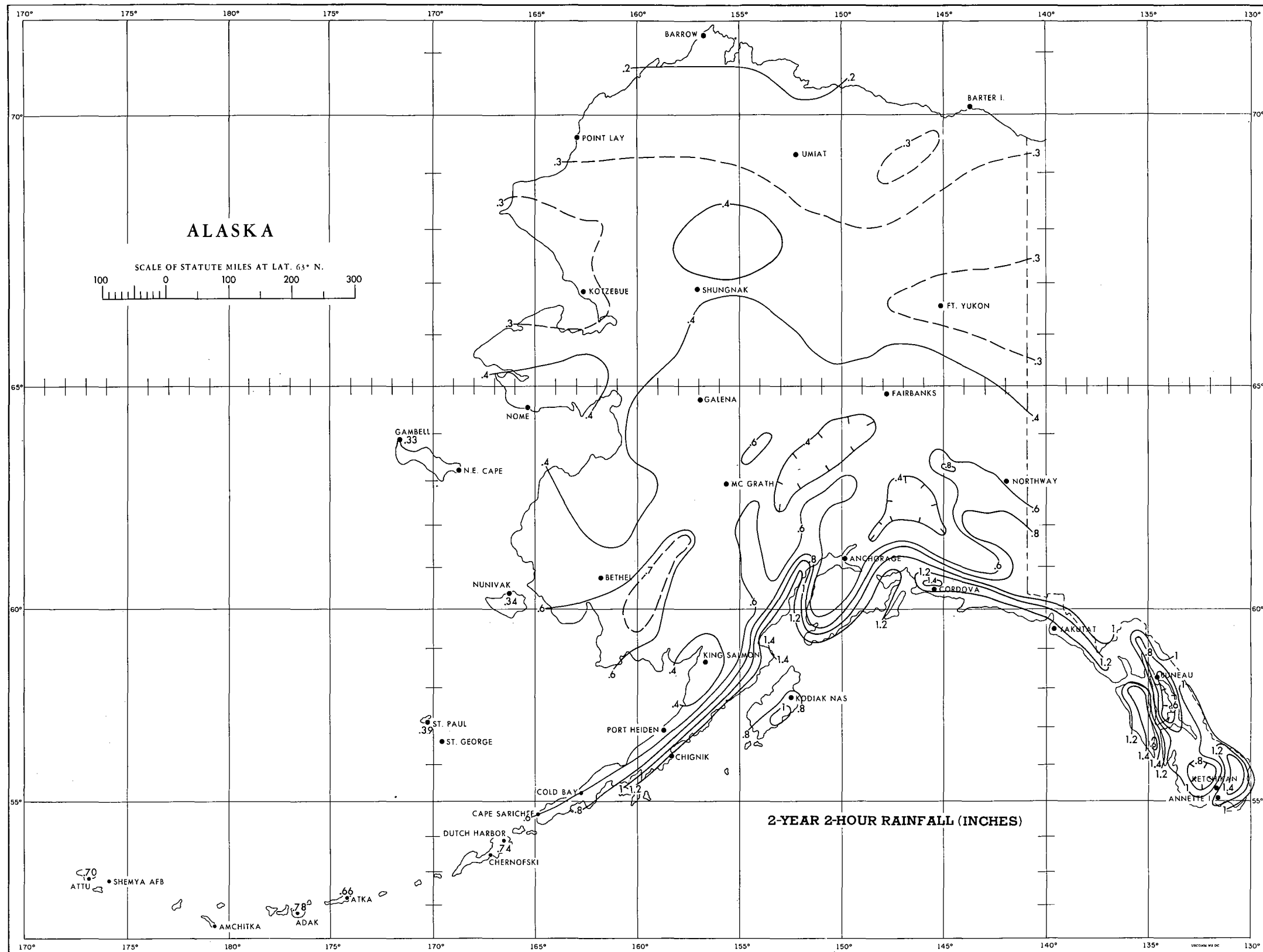


FIGURE 3-26.—2-yr. 2-hr. rainfall (in.).

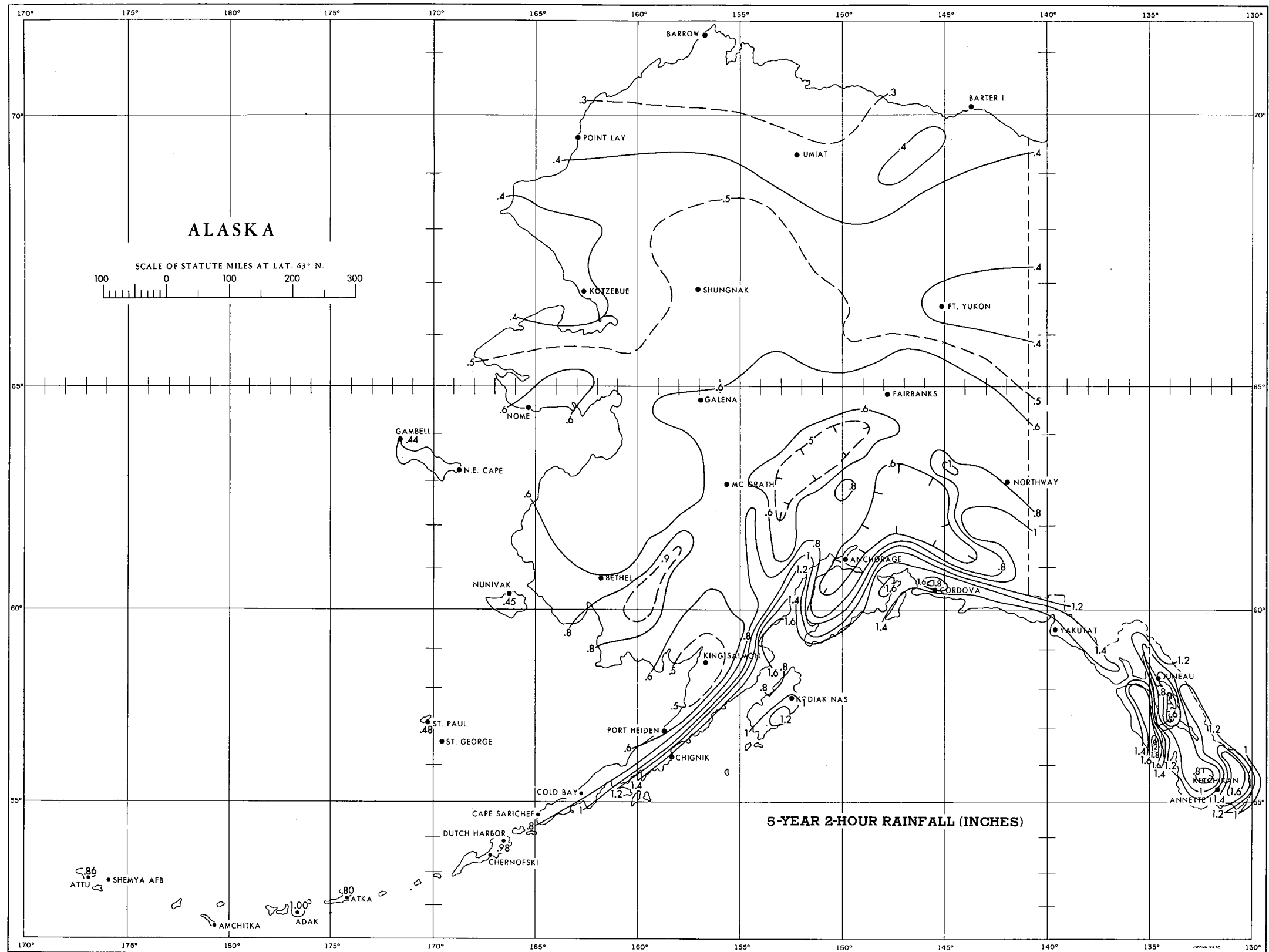


FIGURE 3-27.—5-yr. 2-hr. rainfall (in.).

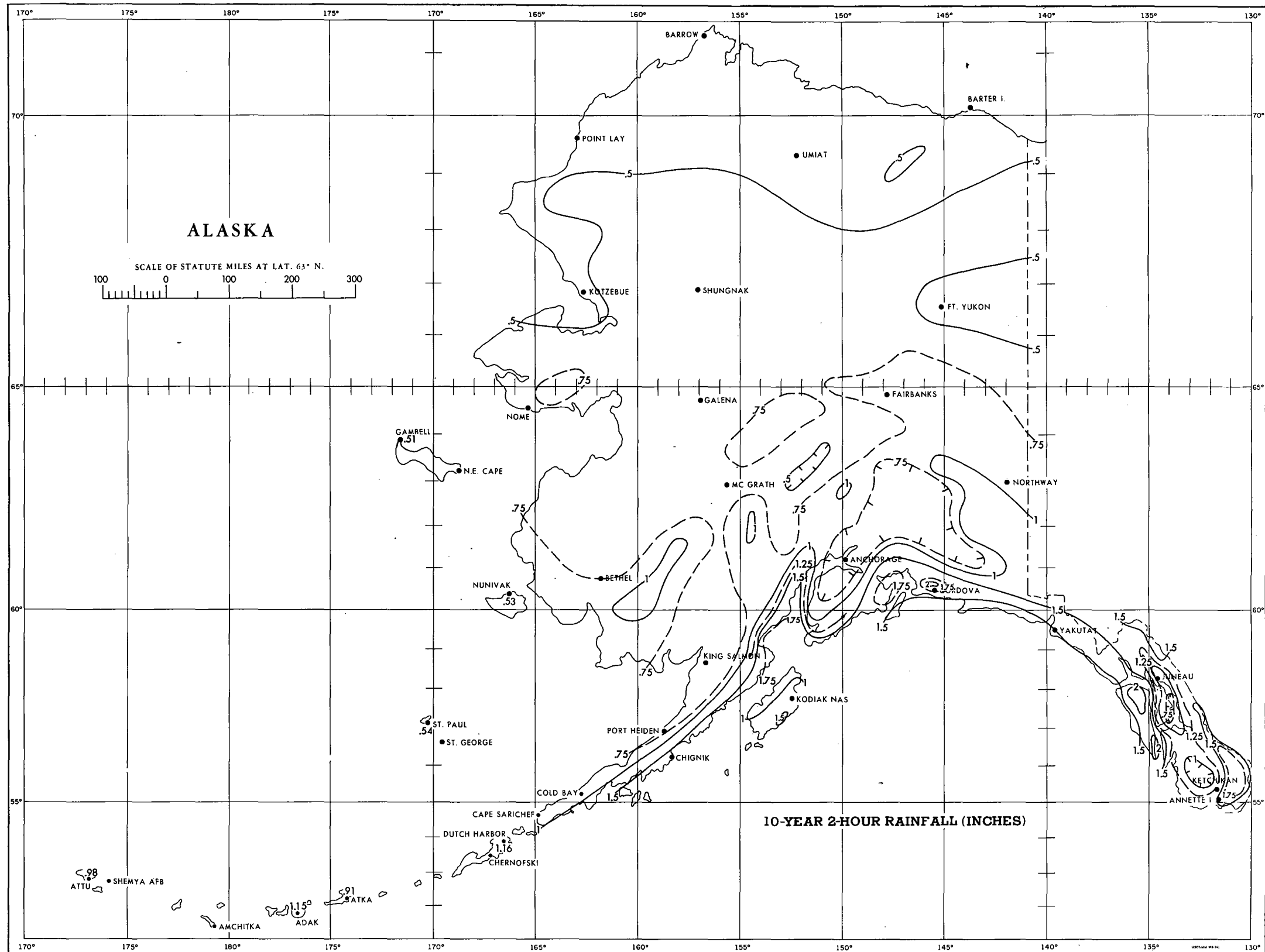


FIGURE 3-28.—10-yr. 2-hr. rainfall (in.).

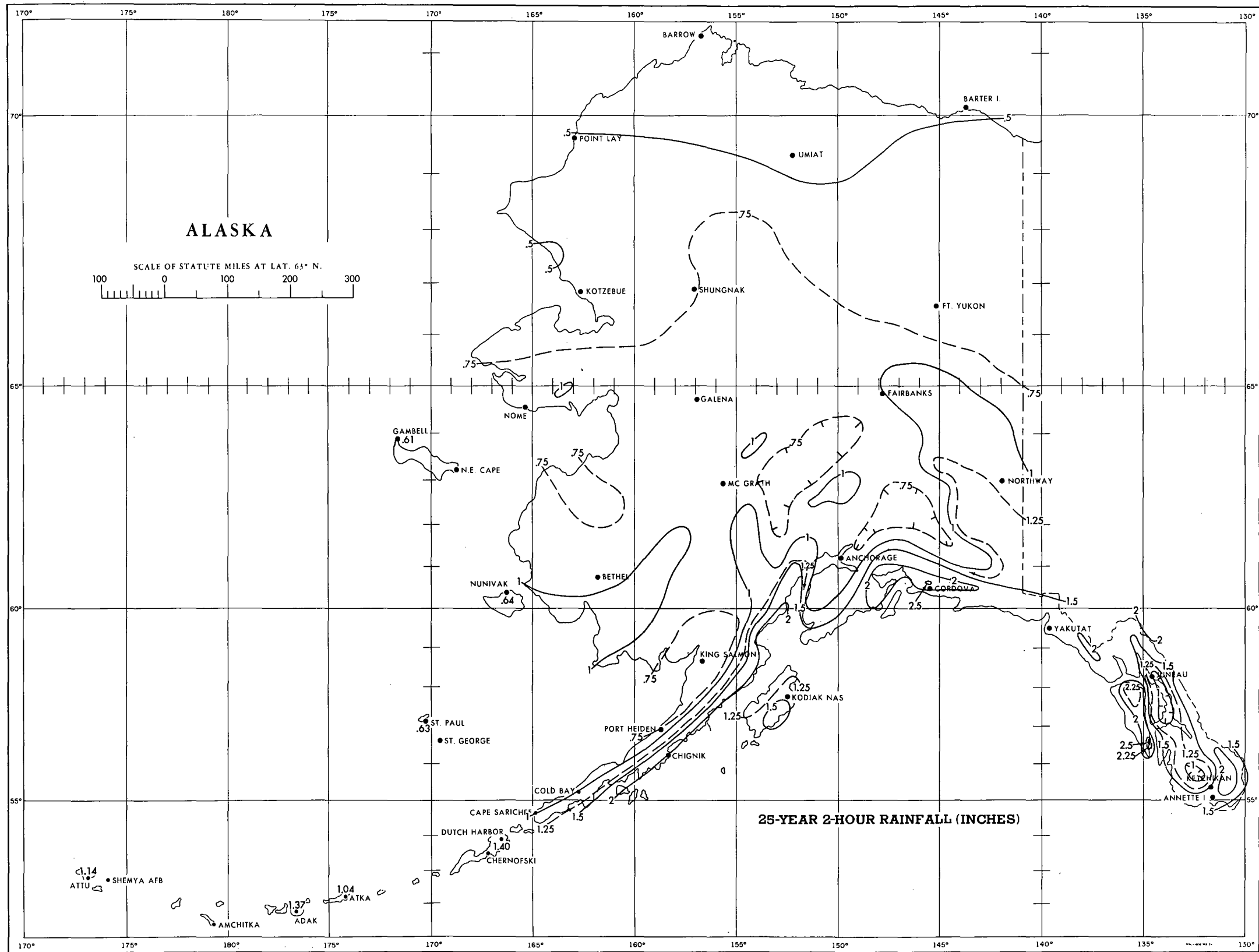


FIGURE 3-29.—25-yr. 2-hr. rainfall (in.).

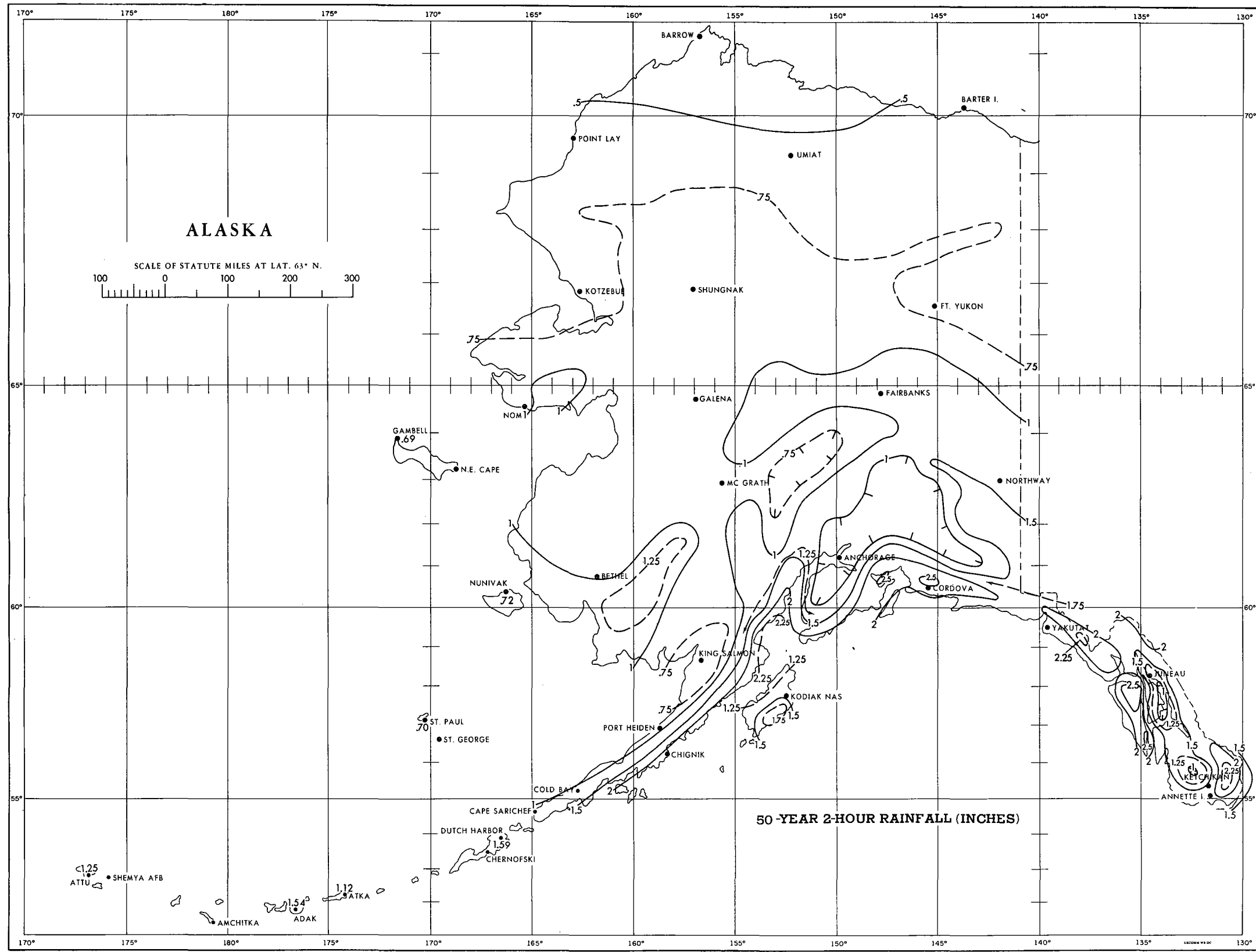


FIGURE 3-30.—50-yr. 2-hr. rainfall (in.).

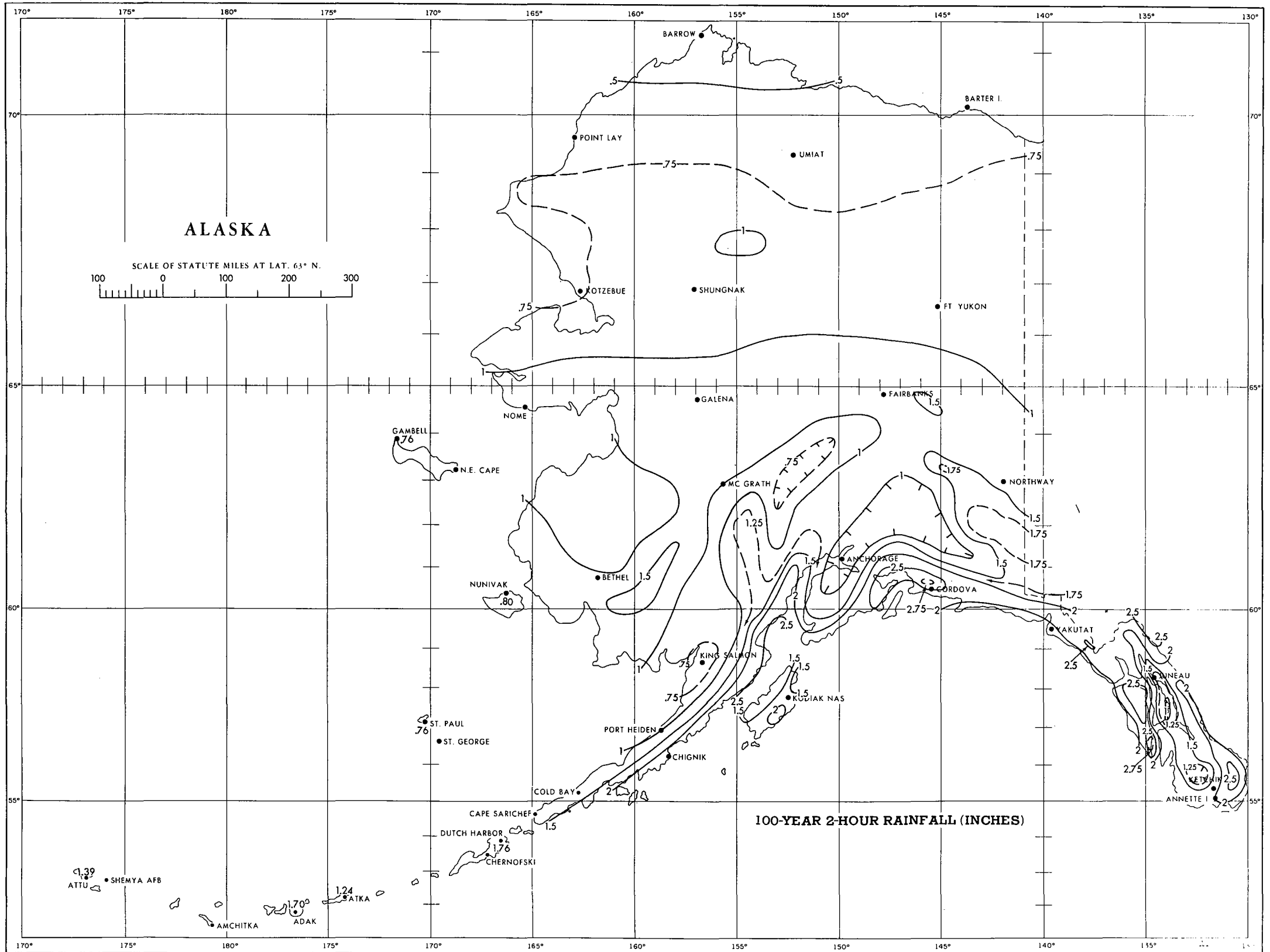


FIGURE 3-31.—100-yr. 2-hr. rainfall (in.).

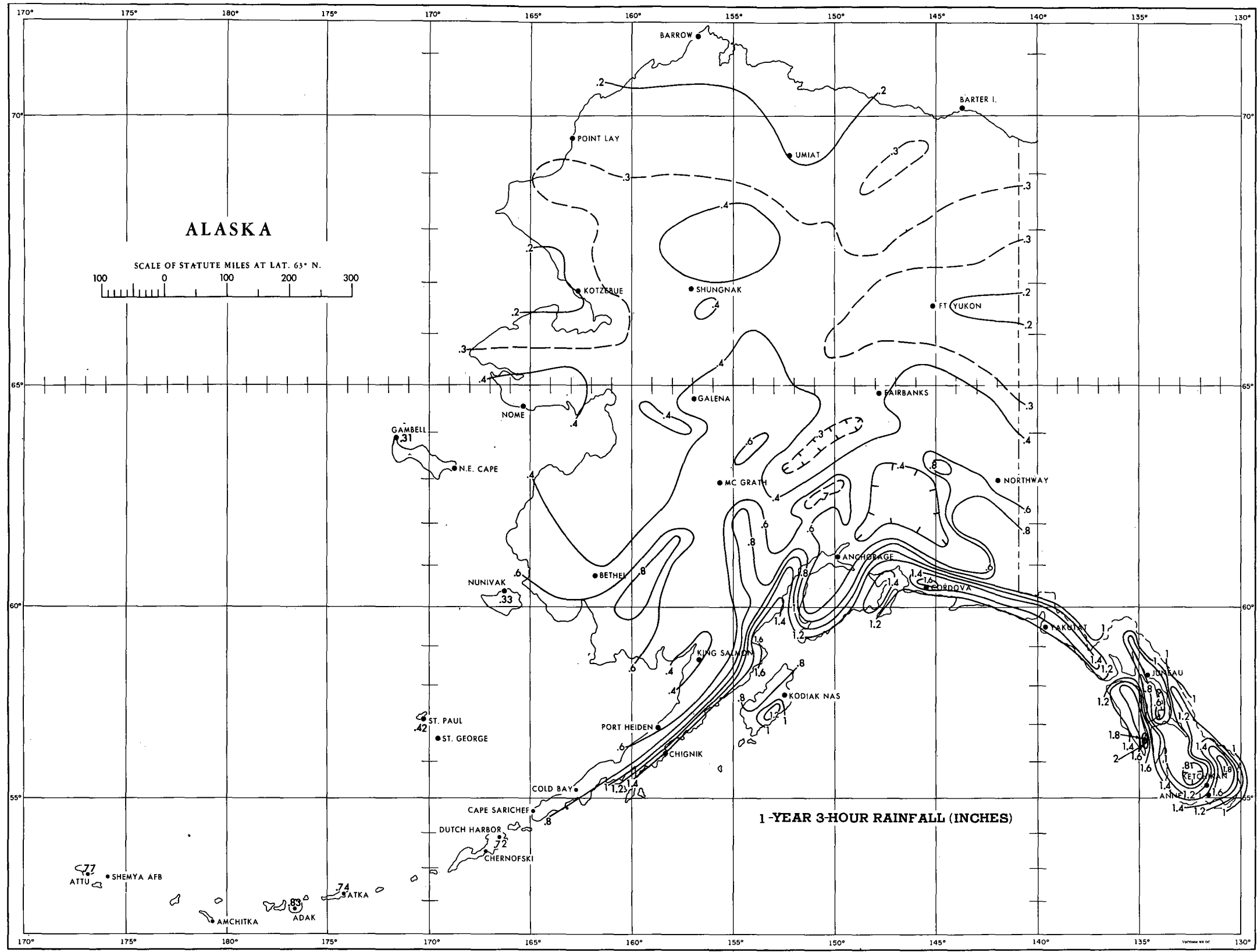


FIGURE 3-32.—1-yr. 3-hr. rainfall (in.).

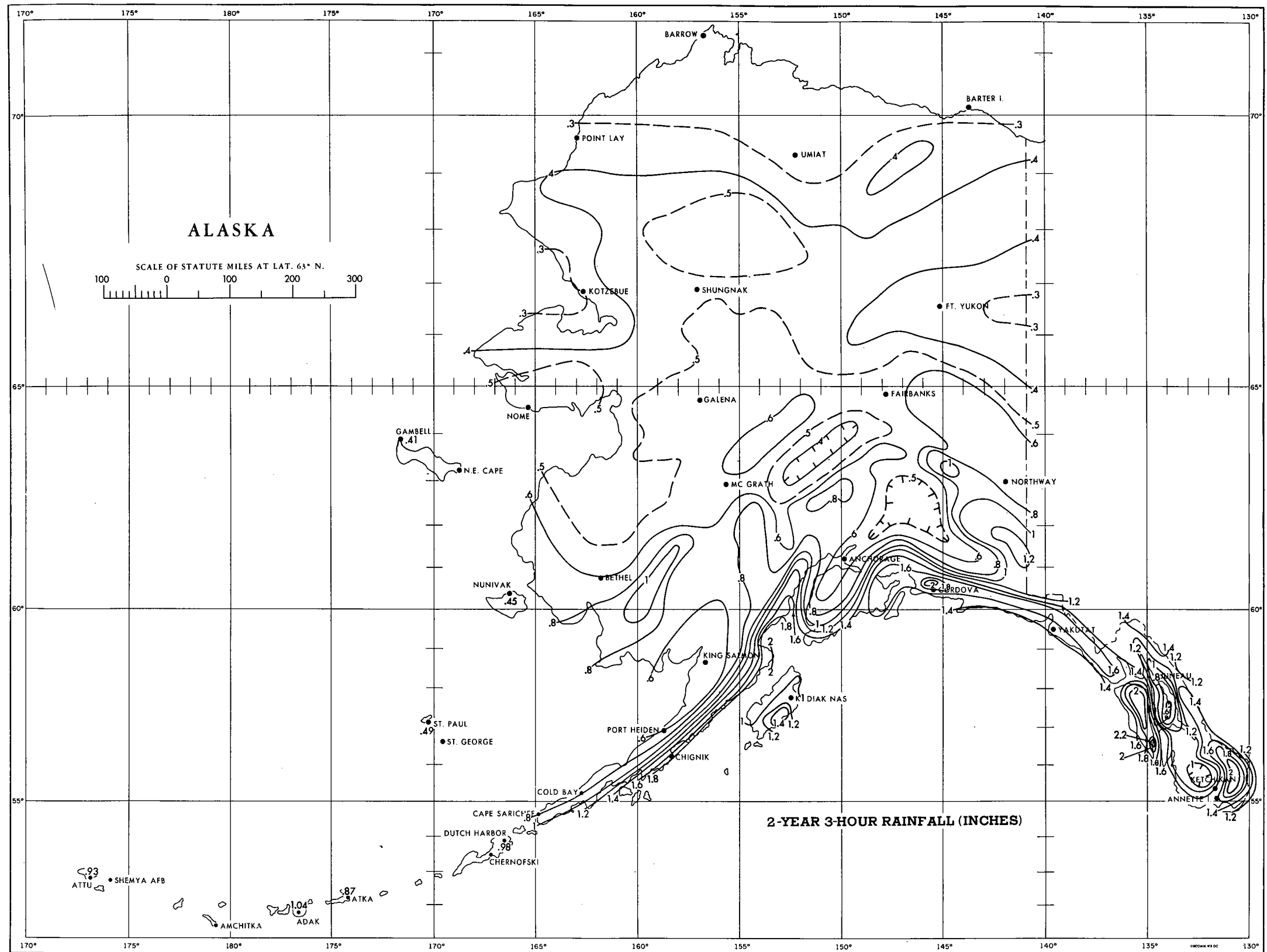


FIGURE 3-33.—2-yr. 3-hr. rainfall (in.).

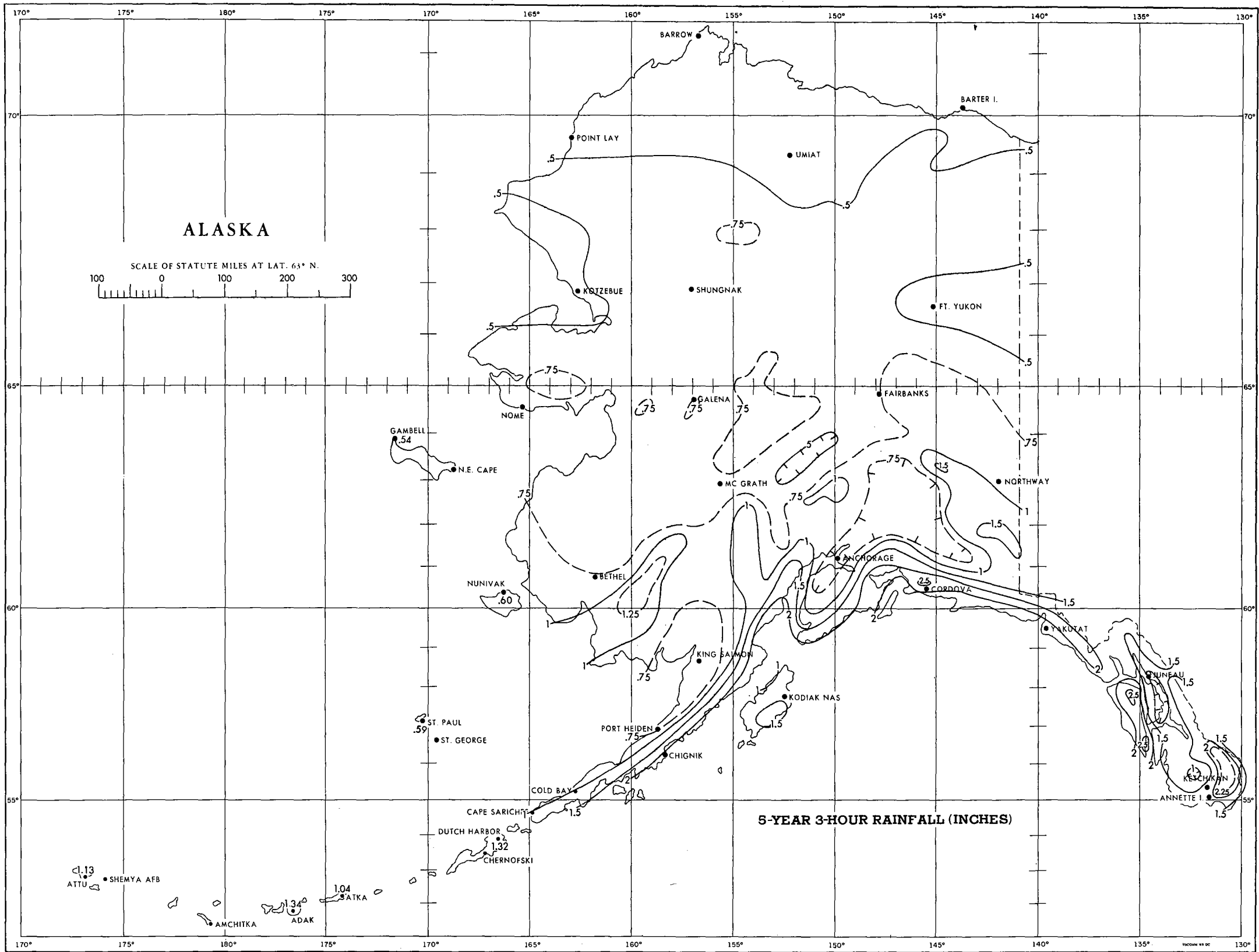


FIGURE 3-34.—5-yr. 3-hr. rainfall (in.).

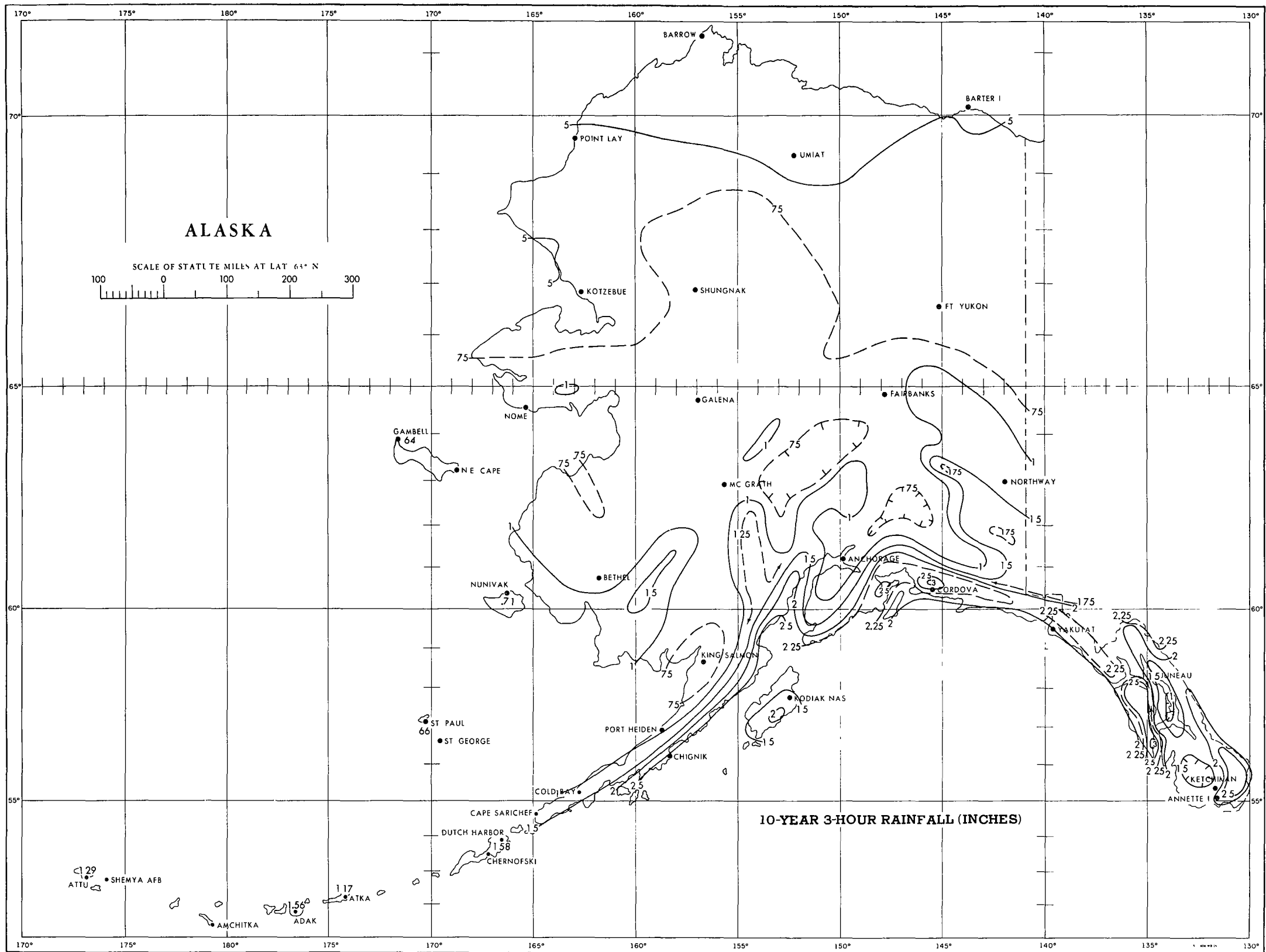


FIGURE 3-35.—10-yr. 3-hr. rainfall (in.).

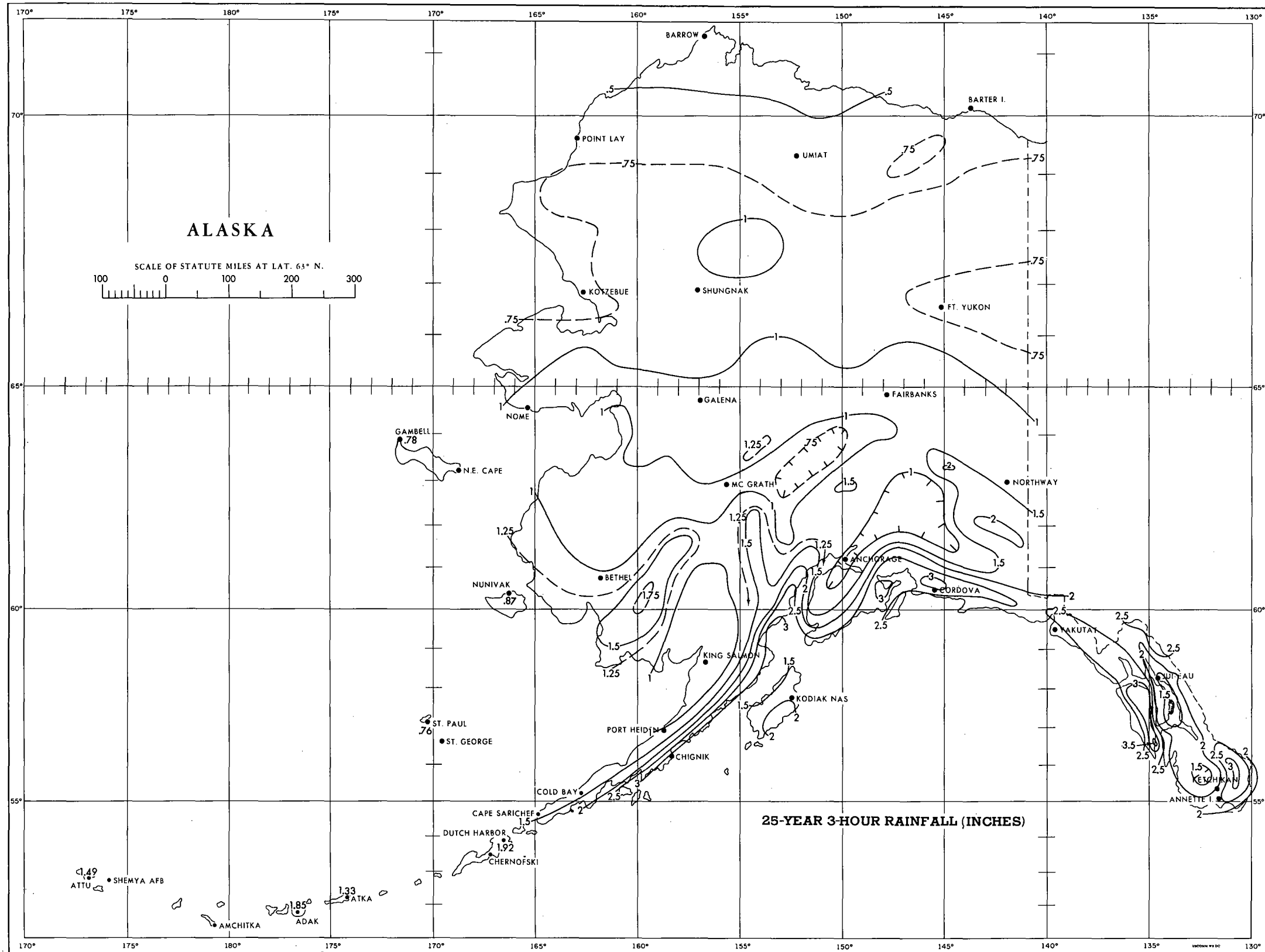


FIGURE 3-36.—25-yr. 3-hr. rainfall (in.).

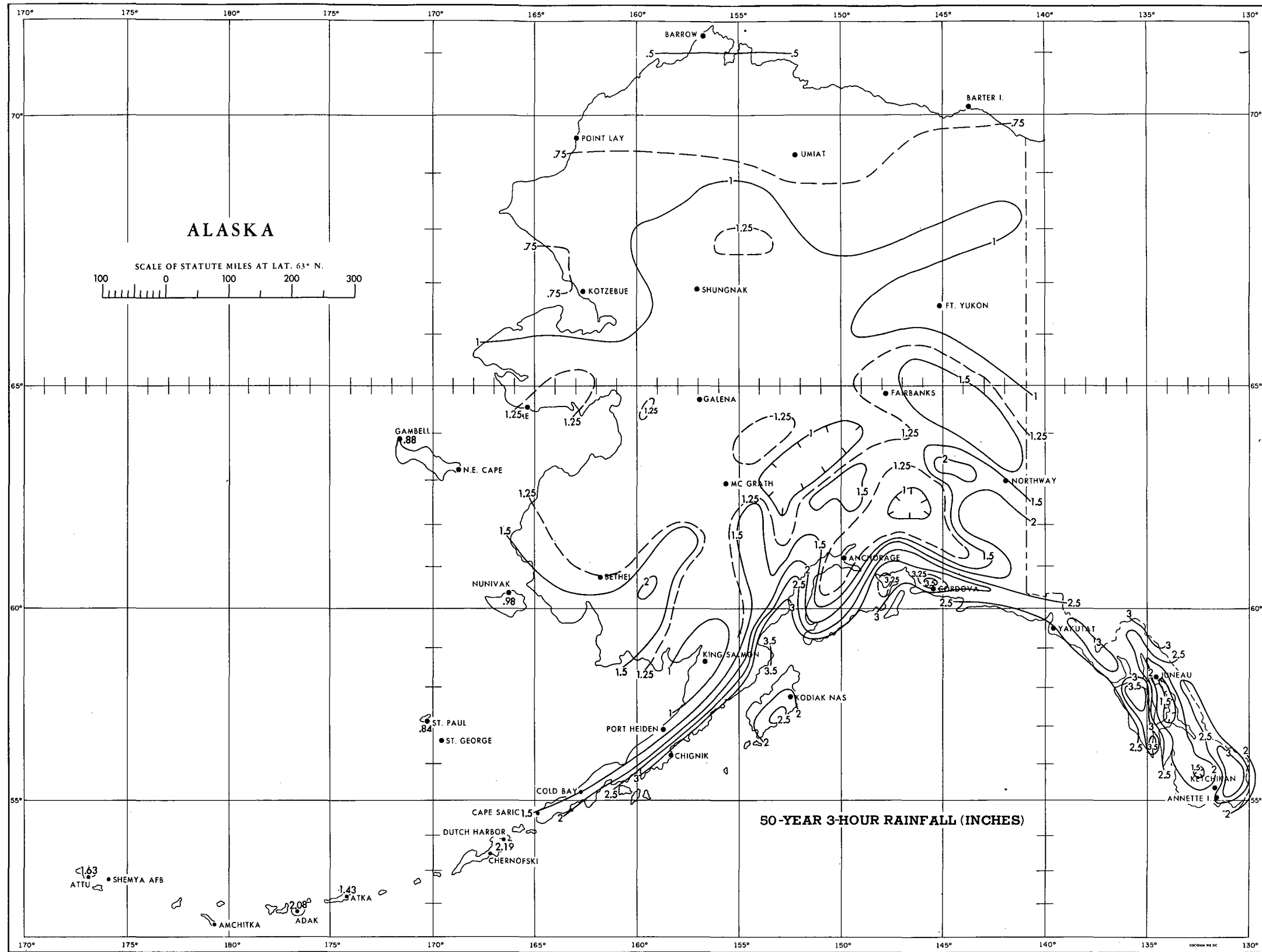


FIGURE 3-37.—50-yr. 3-hr. rainfall (in.).

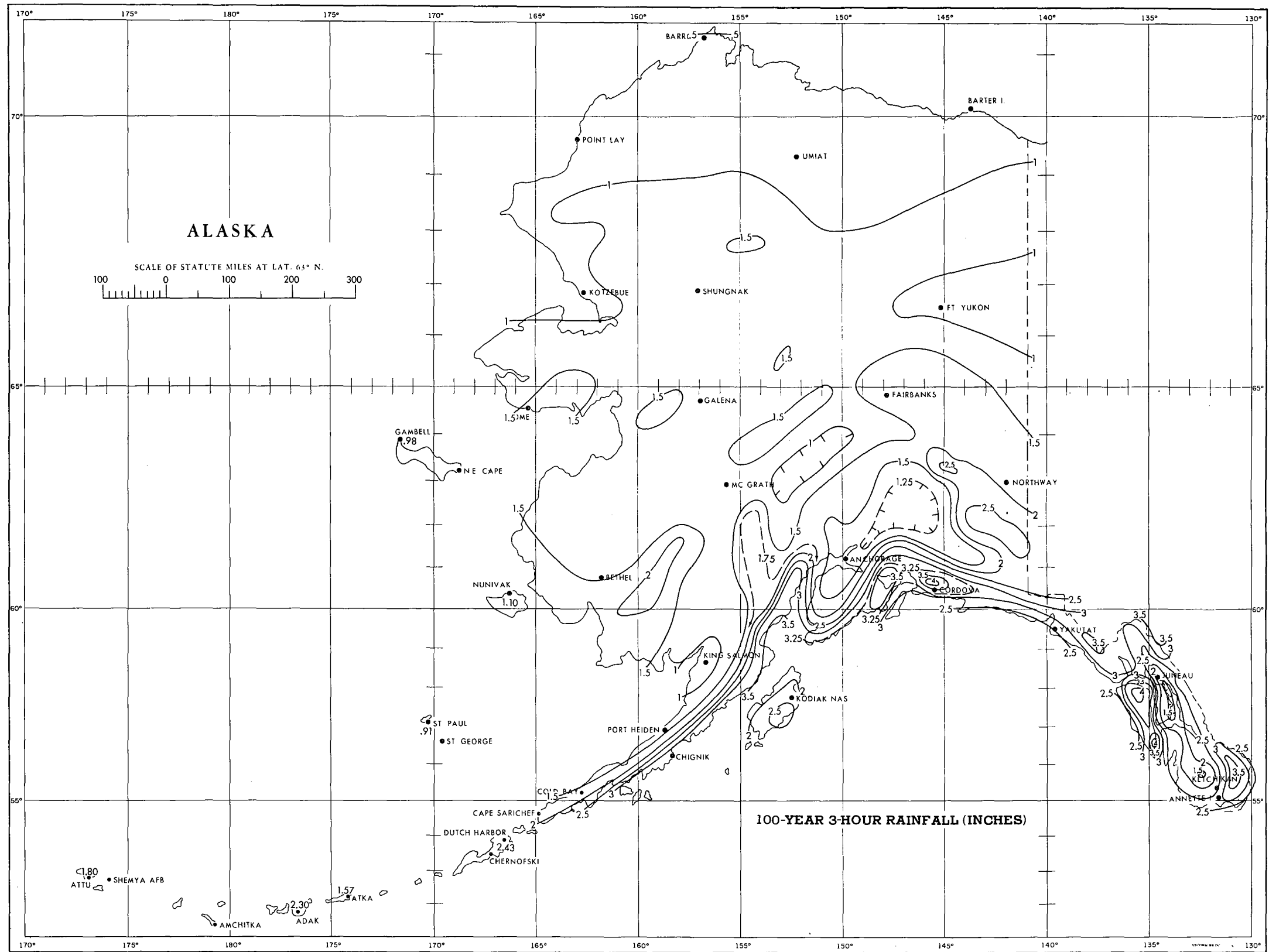


FIGURE 3-38.—100-yr. 3-hr. rainfall (in.).

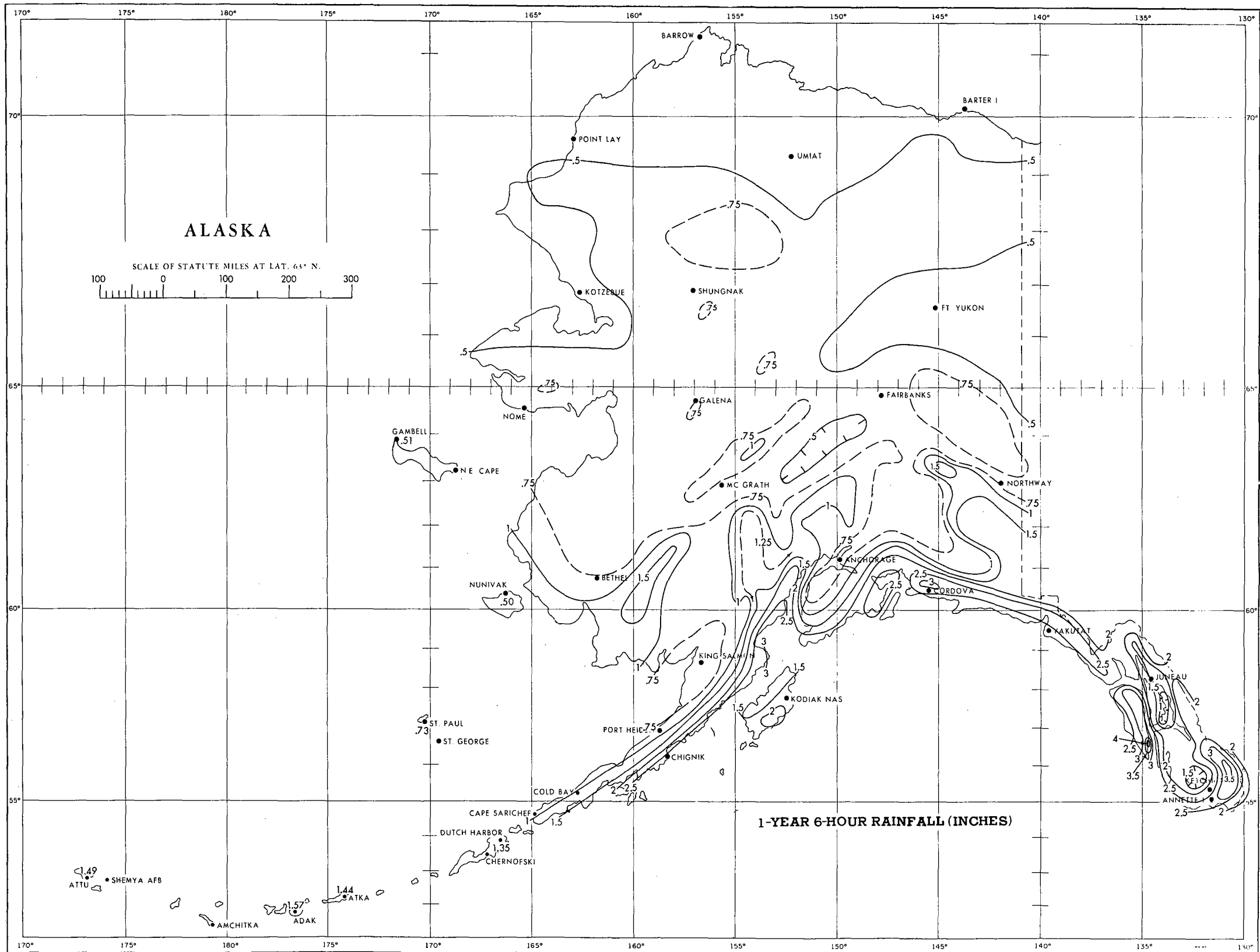


FIGURE 3-39.—1-yr. 6-hr. rainfall (in.).

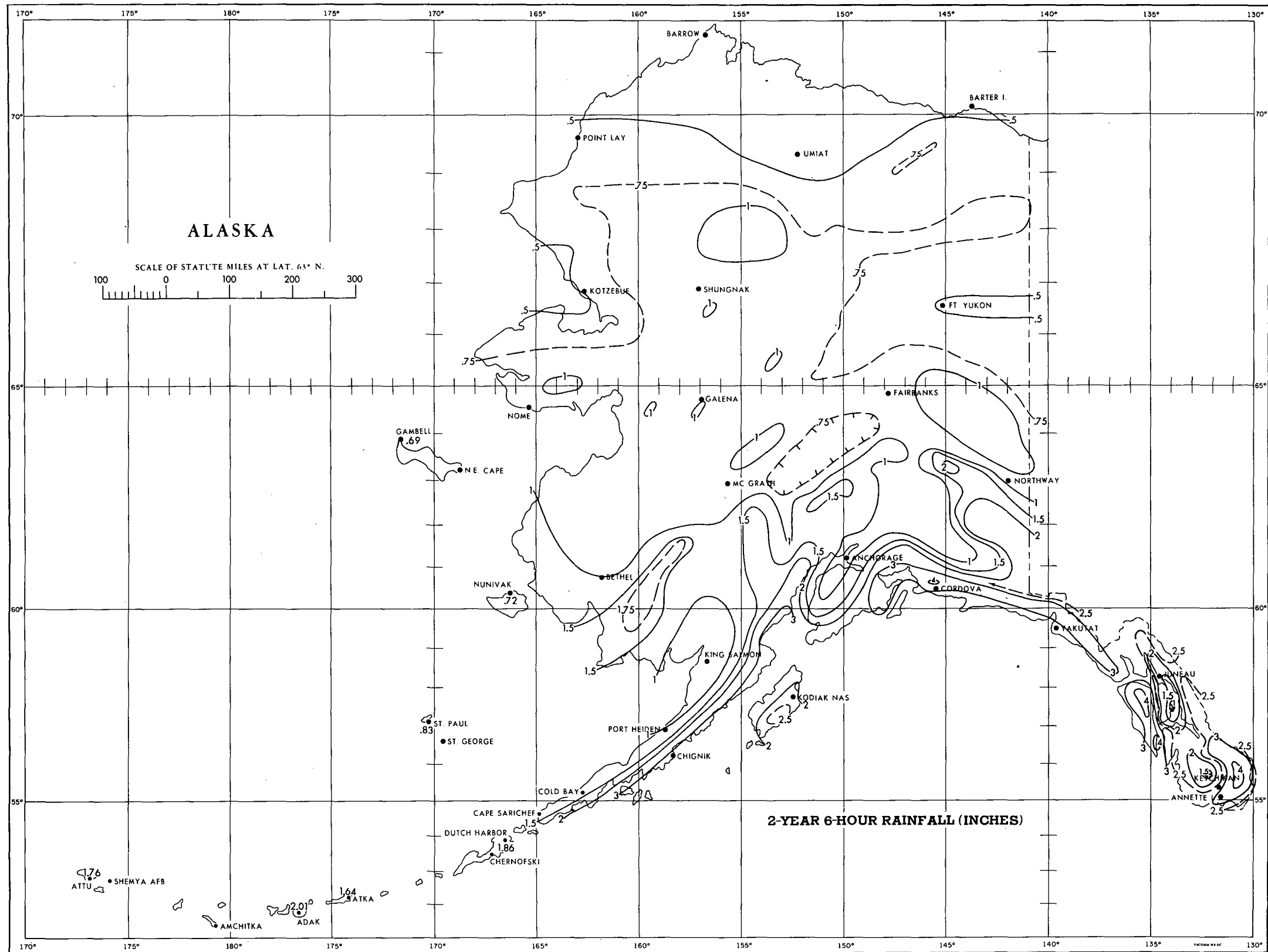


FIGURE 3-40.—2-yr. 6-hr. rainfall (in.).

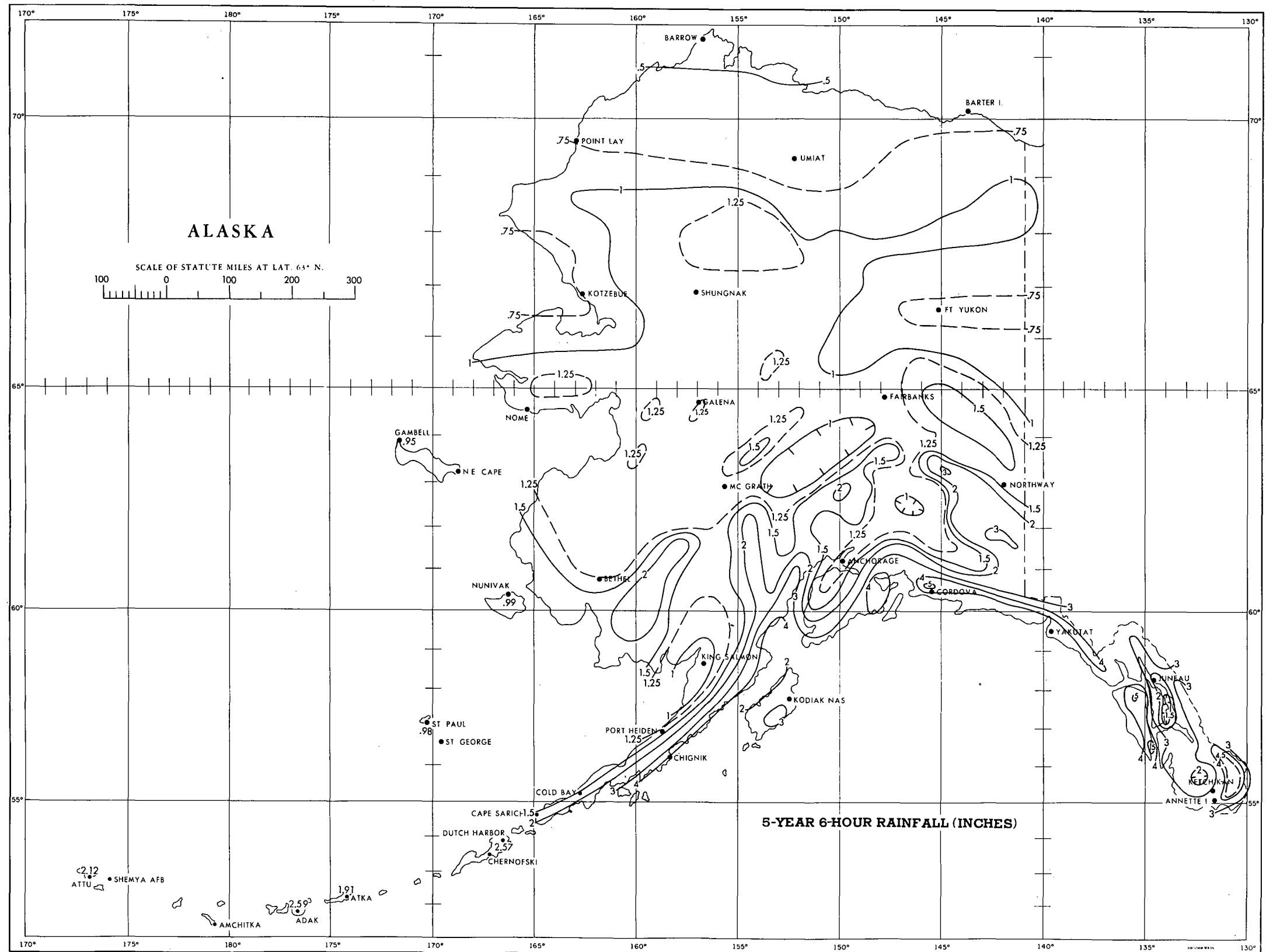


FIGURE 3-41.—5-yr. 6-hr. rainfall (in.).

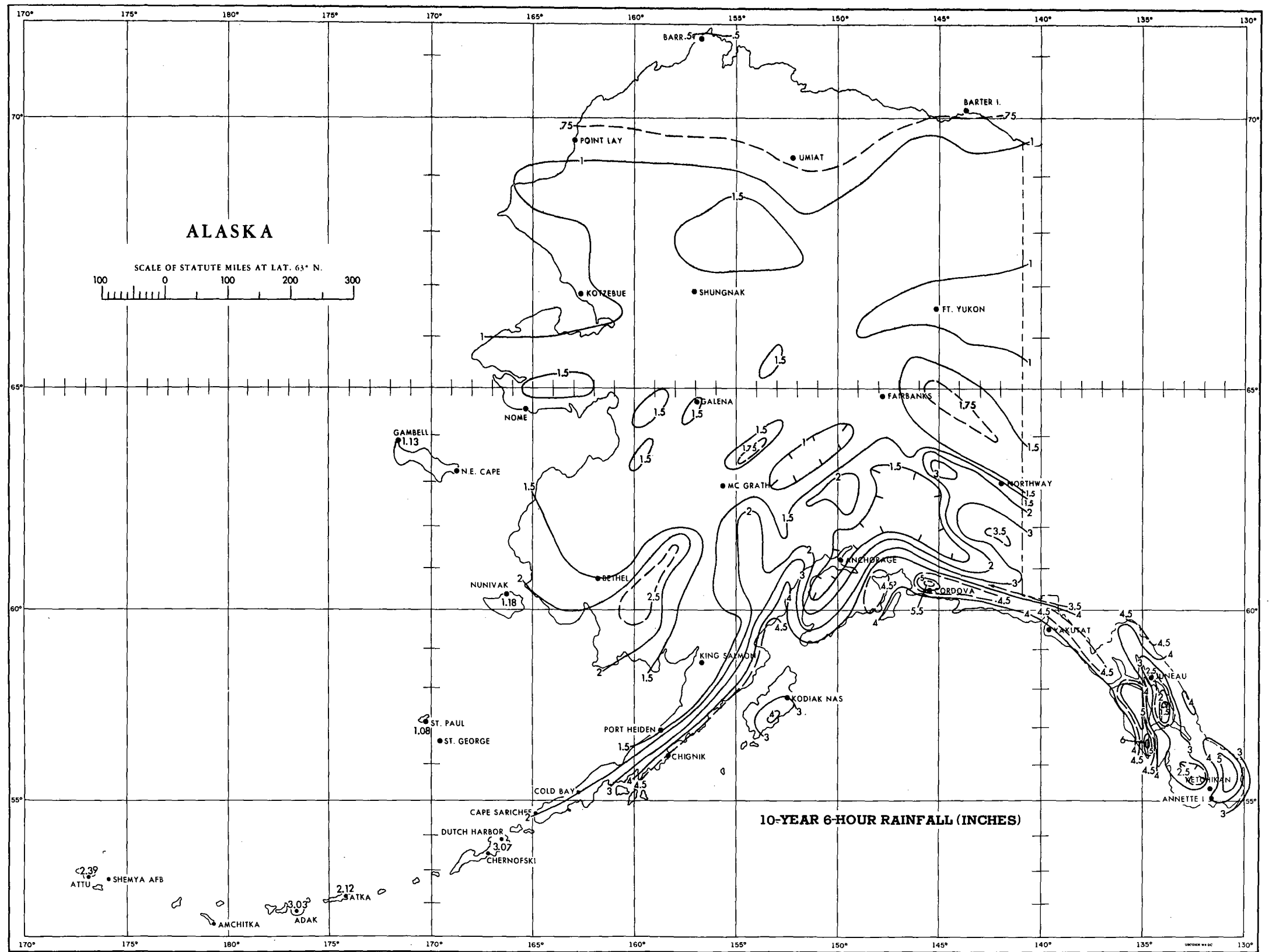


FIGURE 3-42.—10-yr. 6-hr. rainfall (in.).

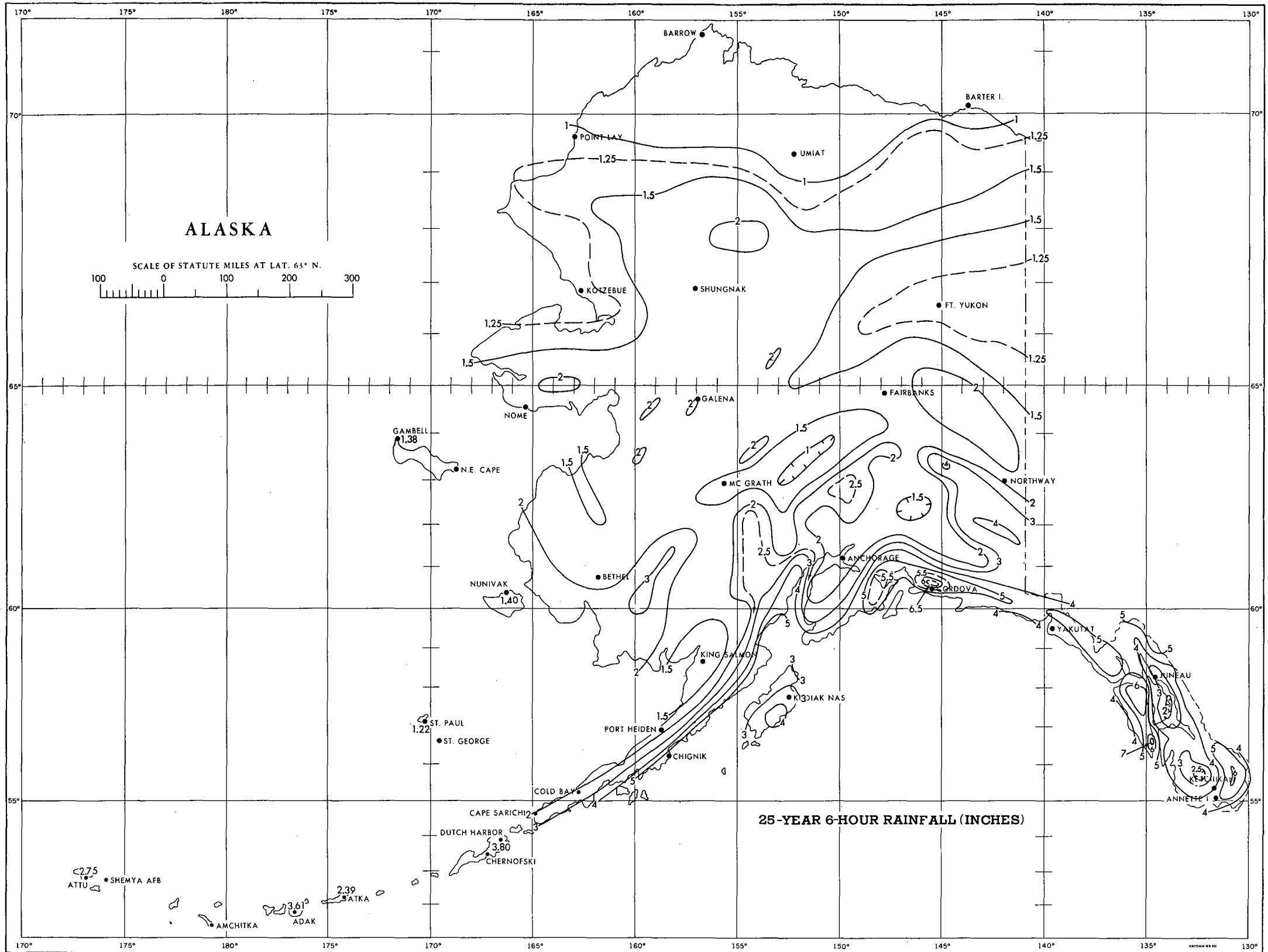


FIGURE 3-43.—25-yr. 6-hr. rainfall (in.).

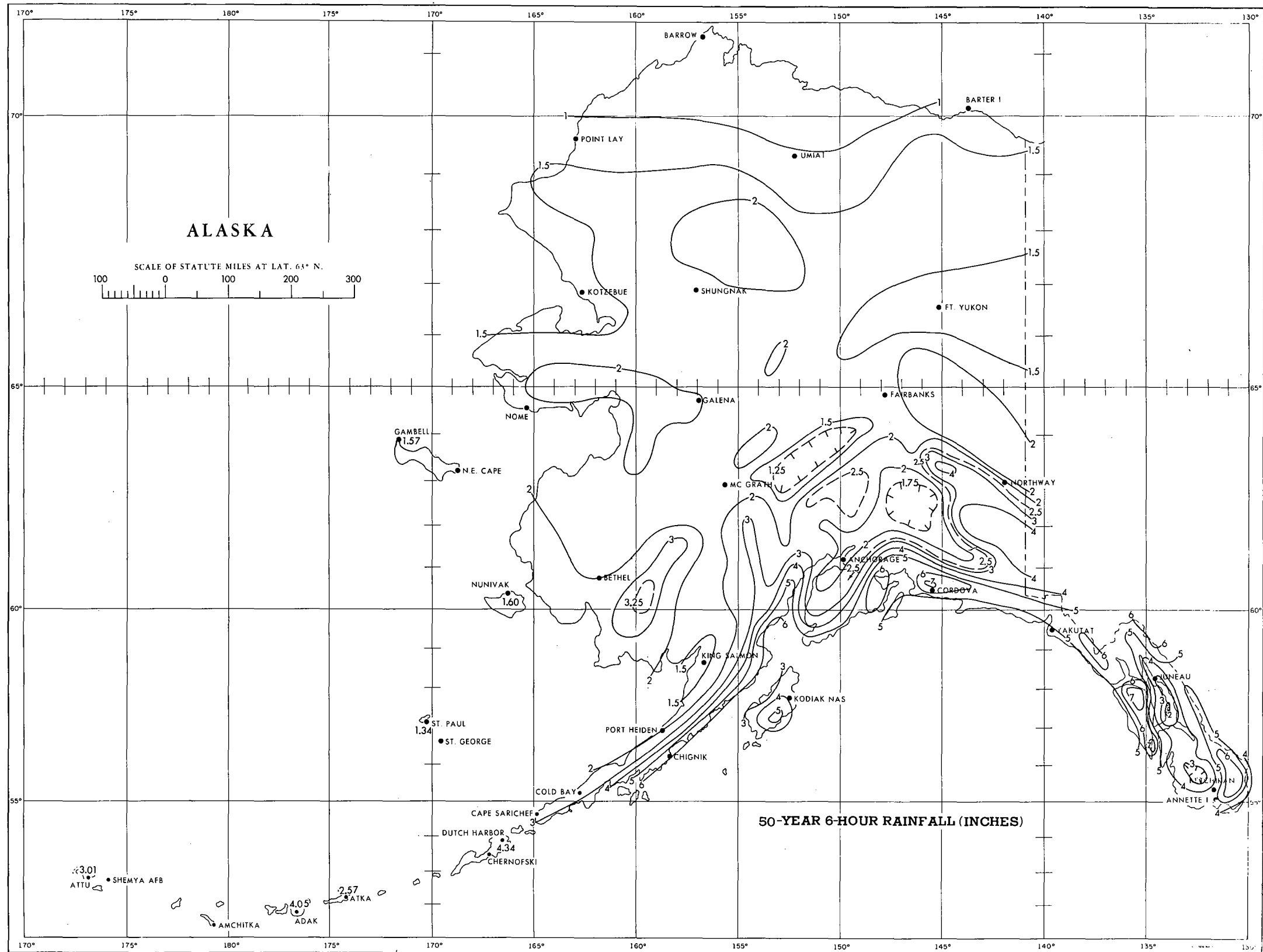


FIGURE 3-44.—50-yr. 6-hr. rainfall (in.).

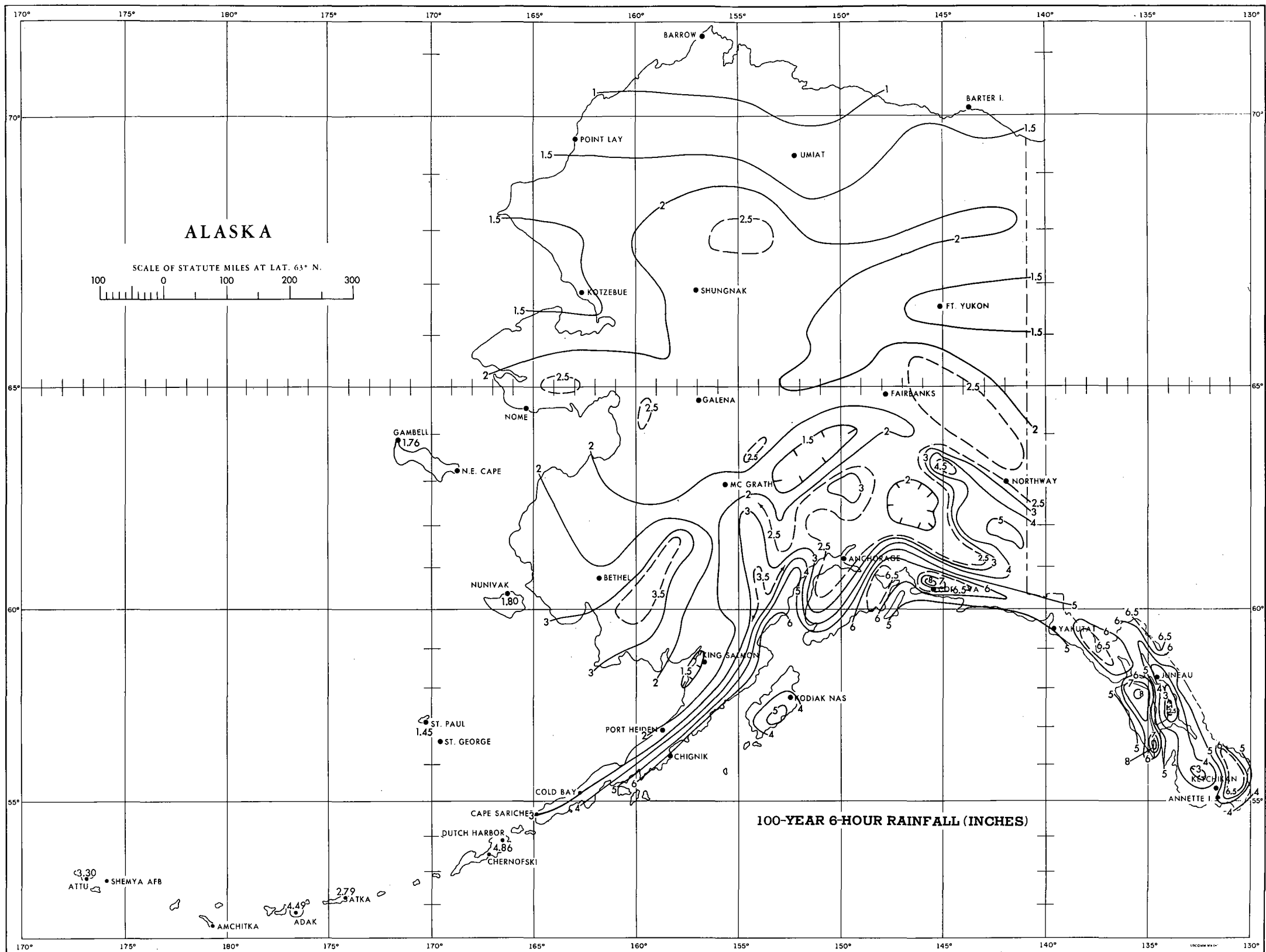


FIGURE 3-45.—100-yr. 6-hr. rainfall (in.).

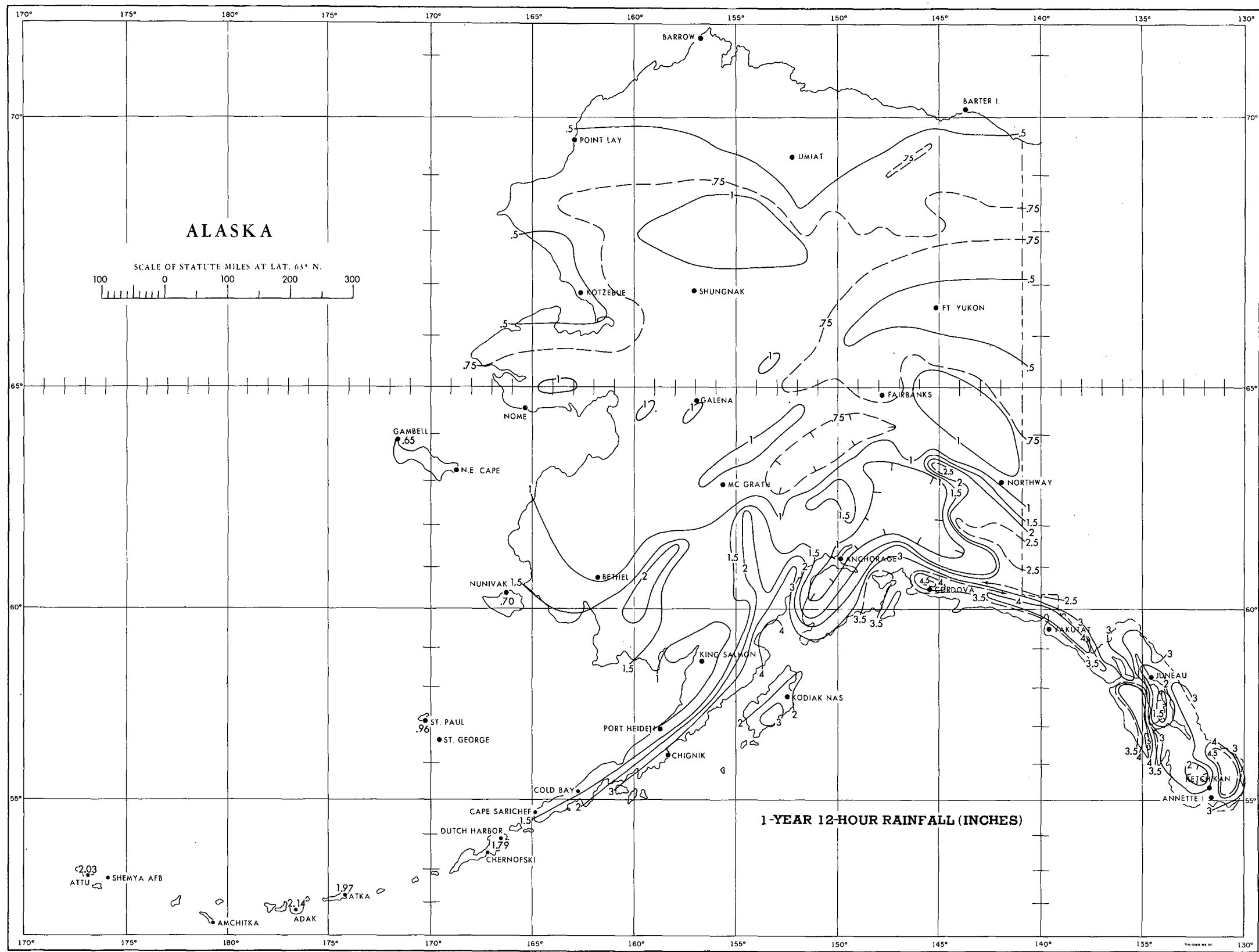


FIGURE 3-46.—1-yr. 12-hr. rainfall (in.).

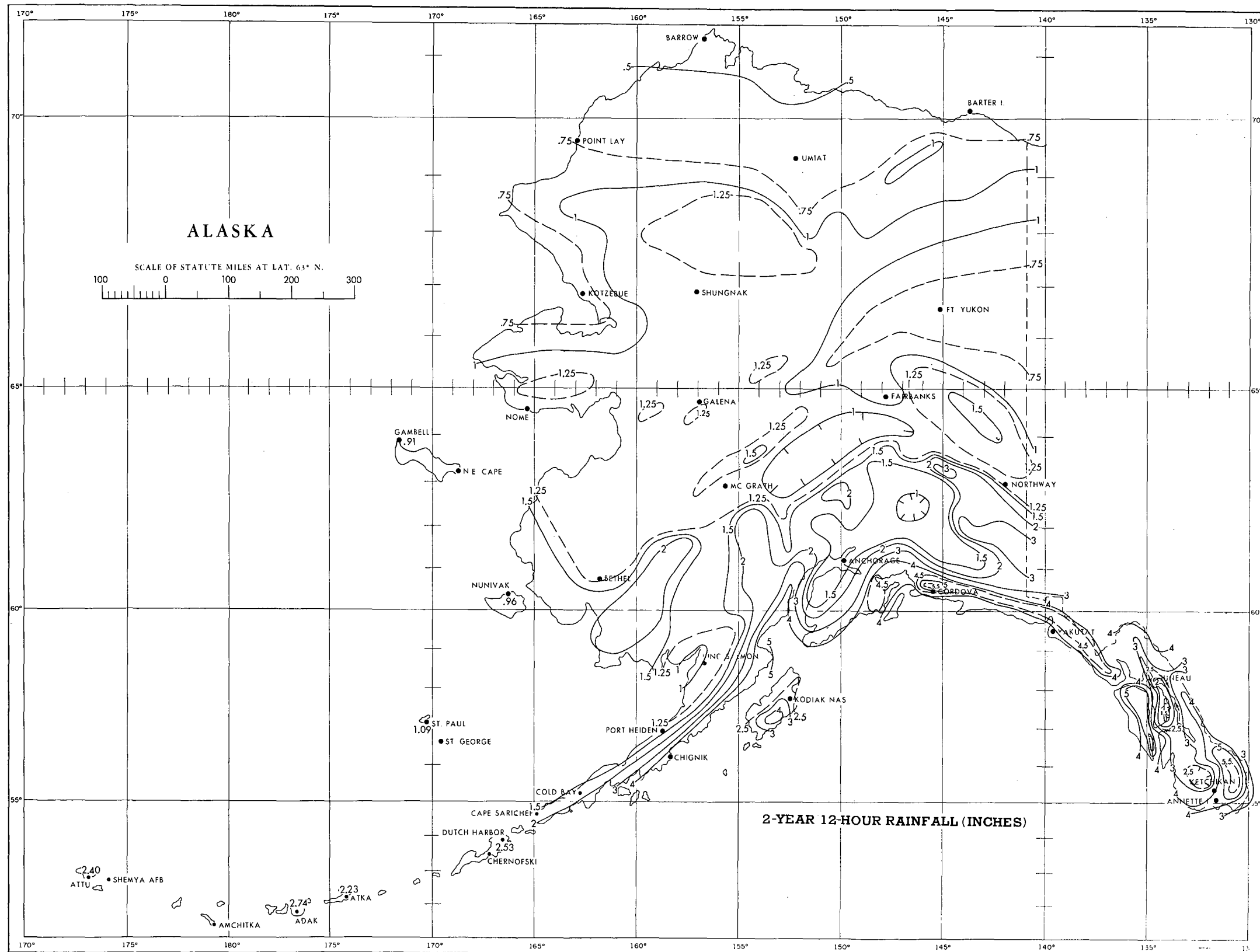


FIGURE 3-47.—2-yr. 12-hr. rainfall (in.).

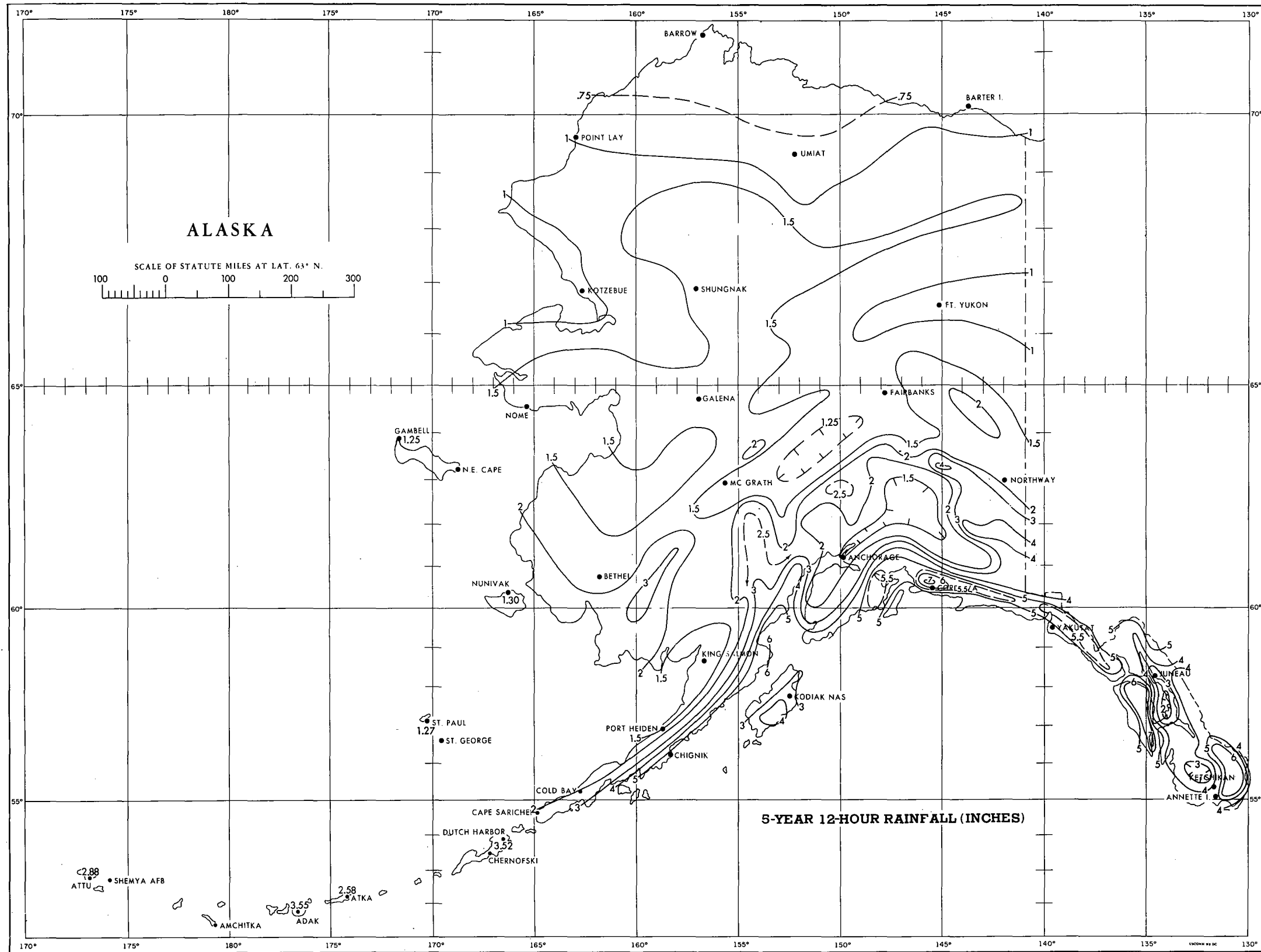


FIGURE 3-48.—5-yr. 12-hr. rainfall (in.).

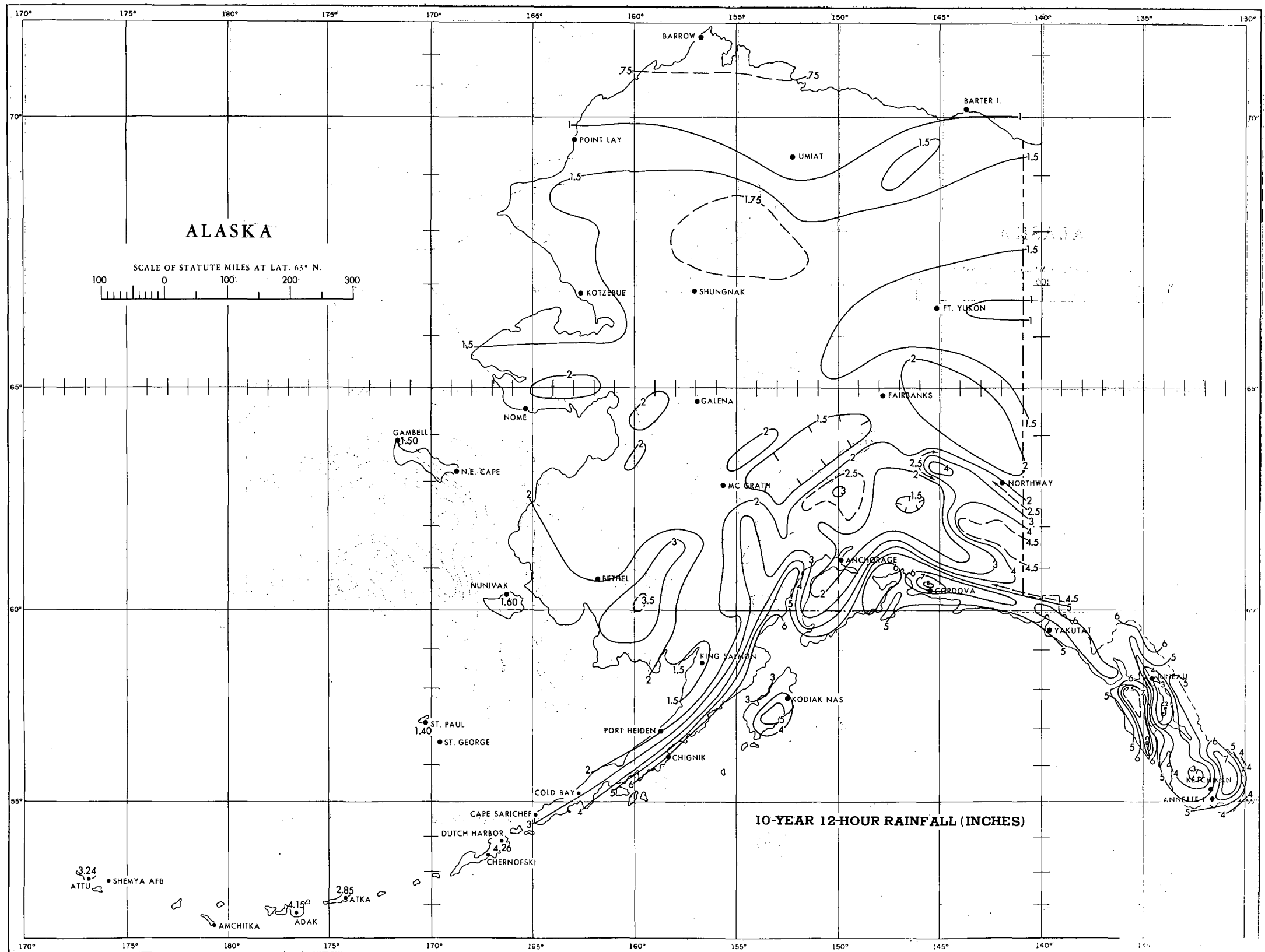


FIGURE 3-49.—10-yr. 12-hr. rainfall (in.).

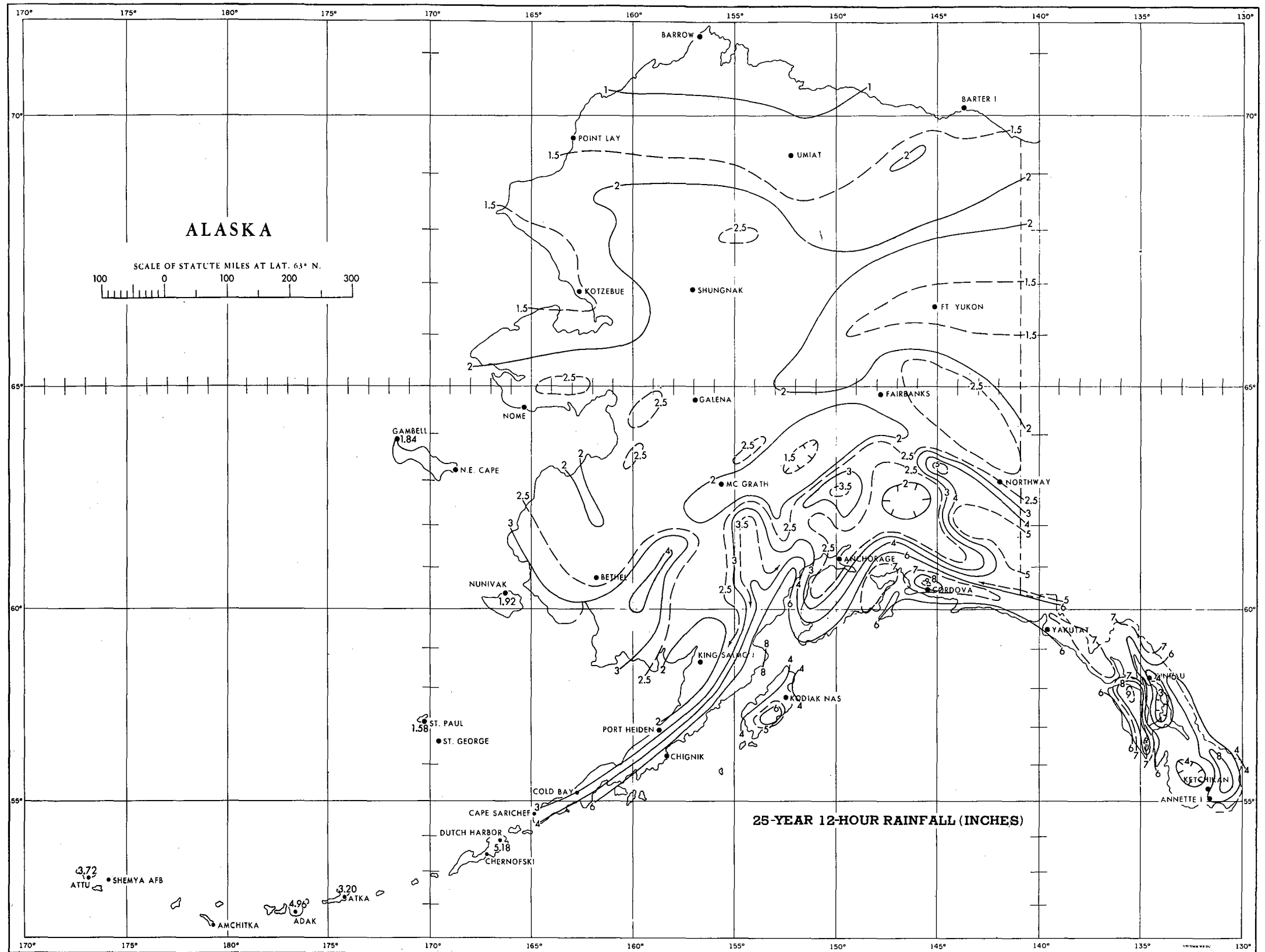


FIGURE 3-50.—25-yr. 12-hr. rainfall (in.).

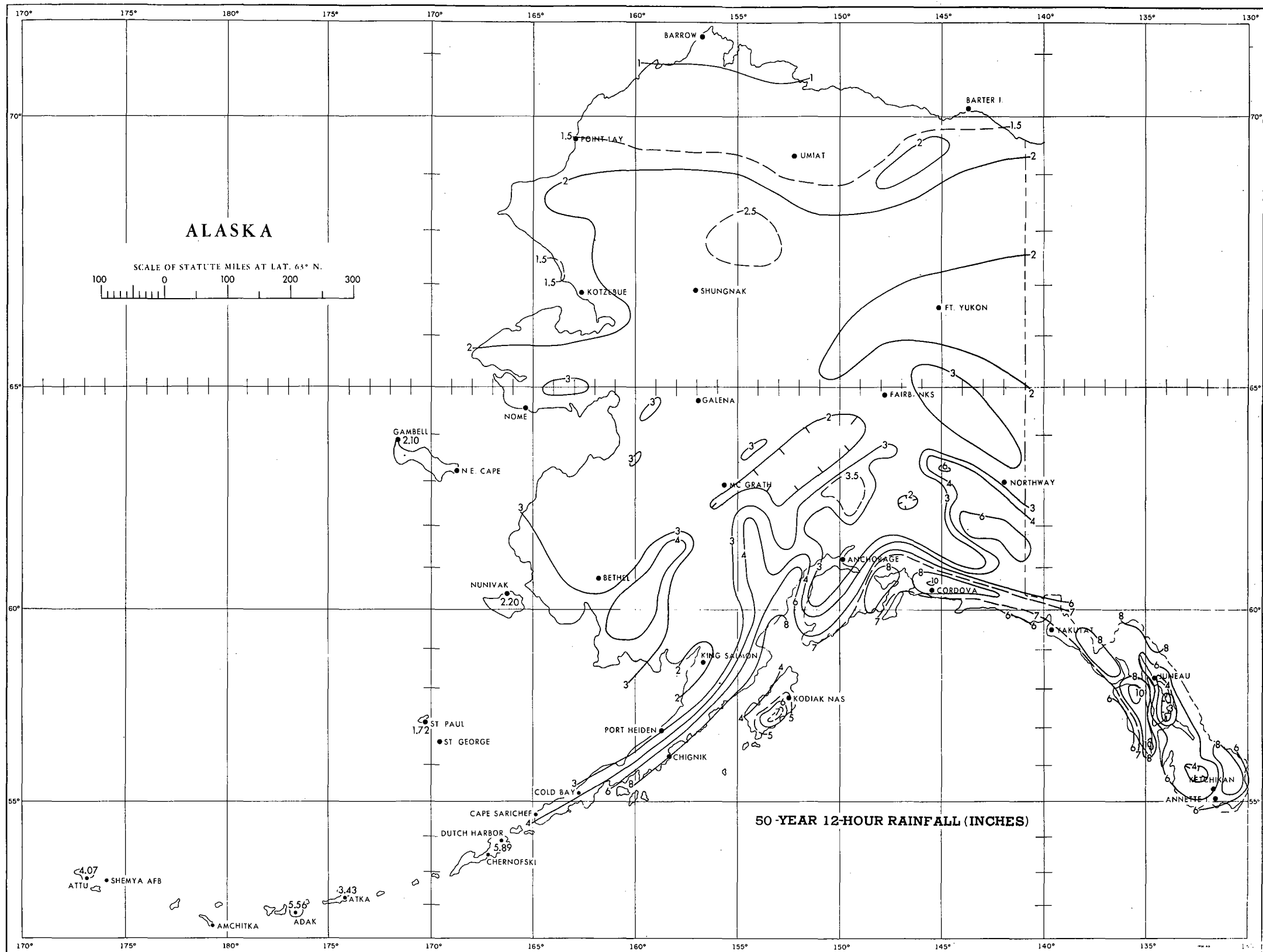


FIGURE 3-51.—50-yr. 12-hr. rainfall (in.).

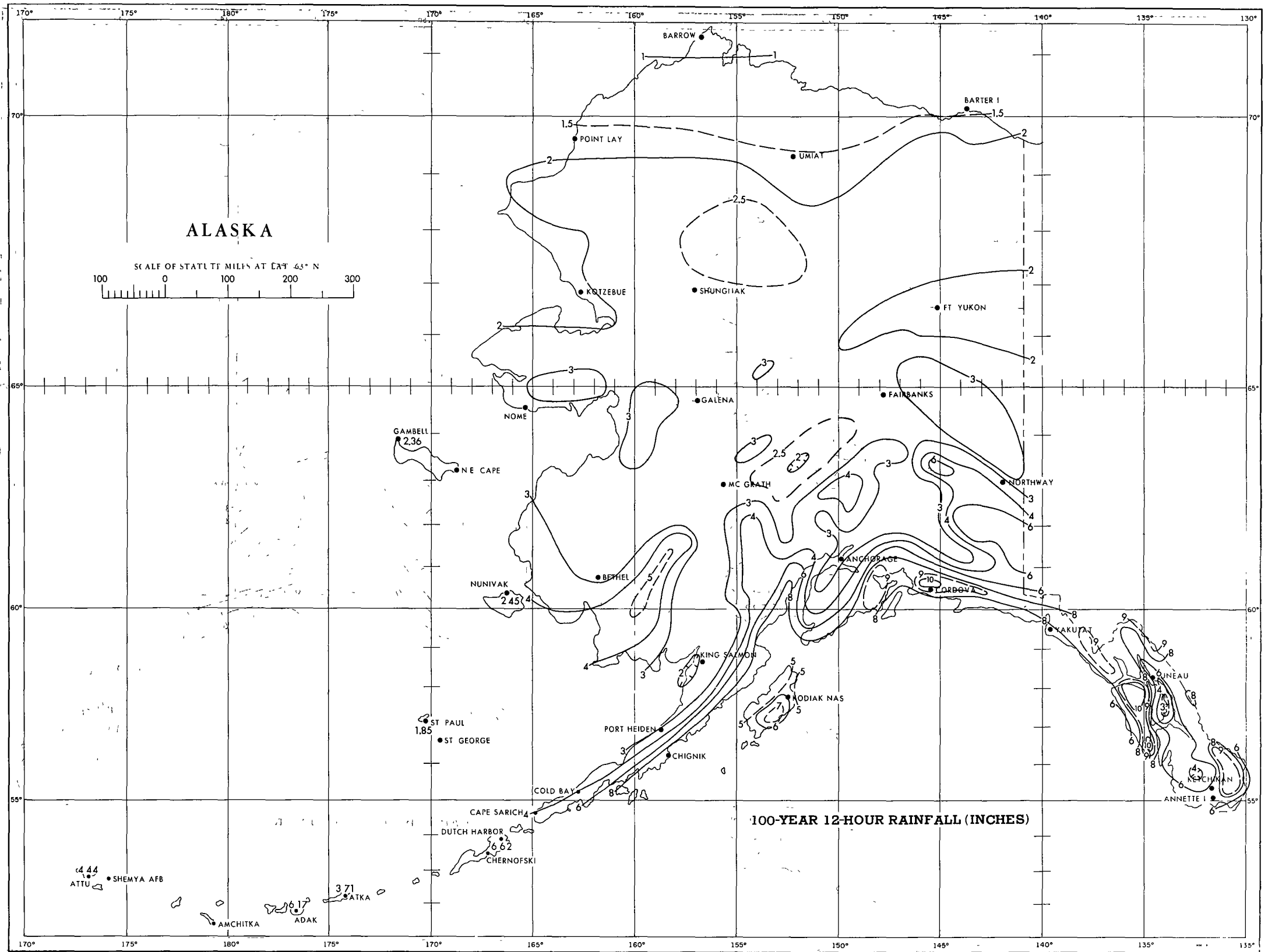


FIGURE 3-52.—100-yr. 12-hr. rainfall (in.).

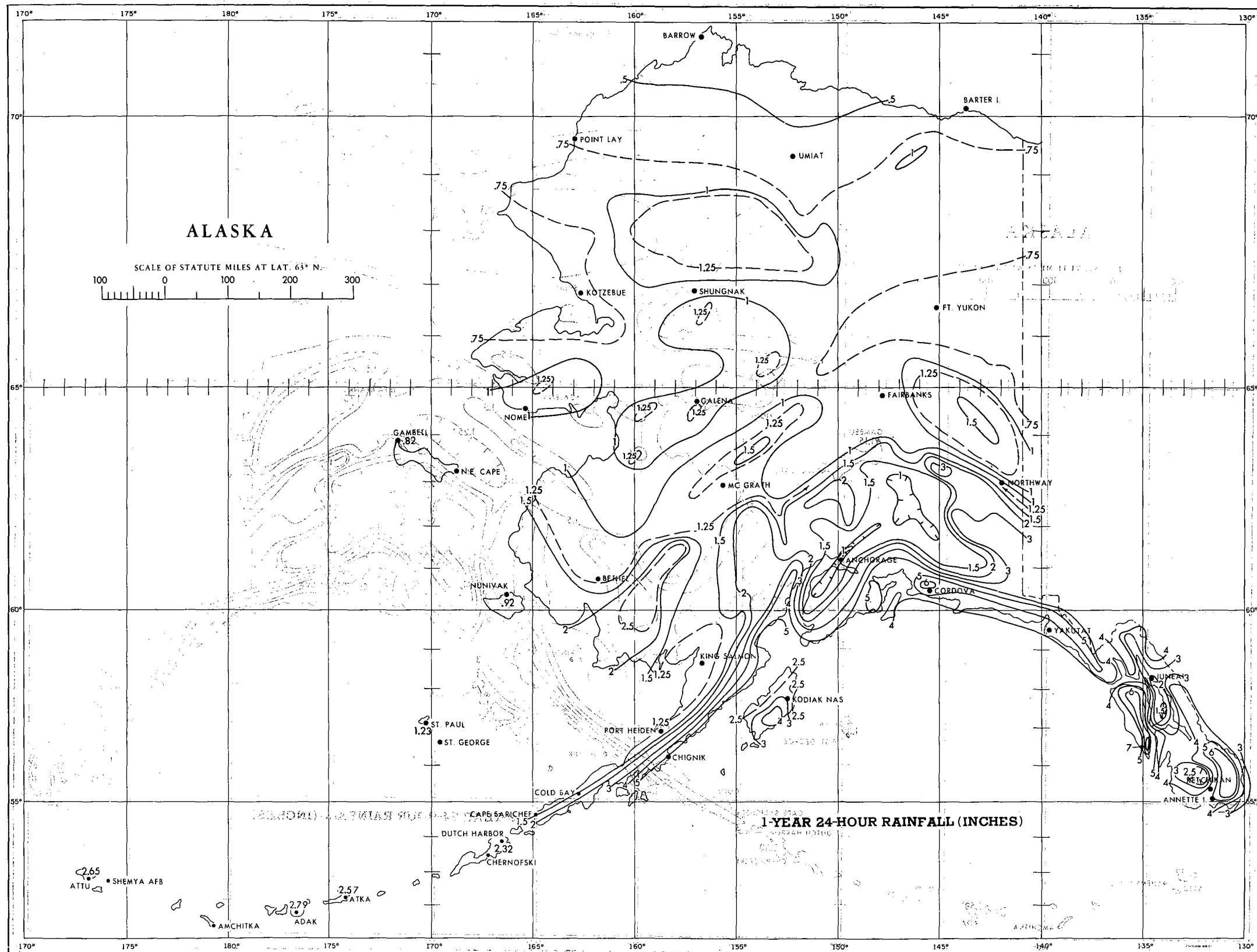


FIGURE 3-53.—1-yr. 24-hr. rainfall (in.).

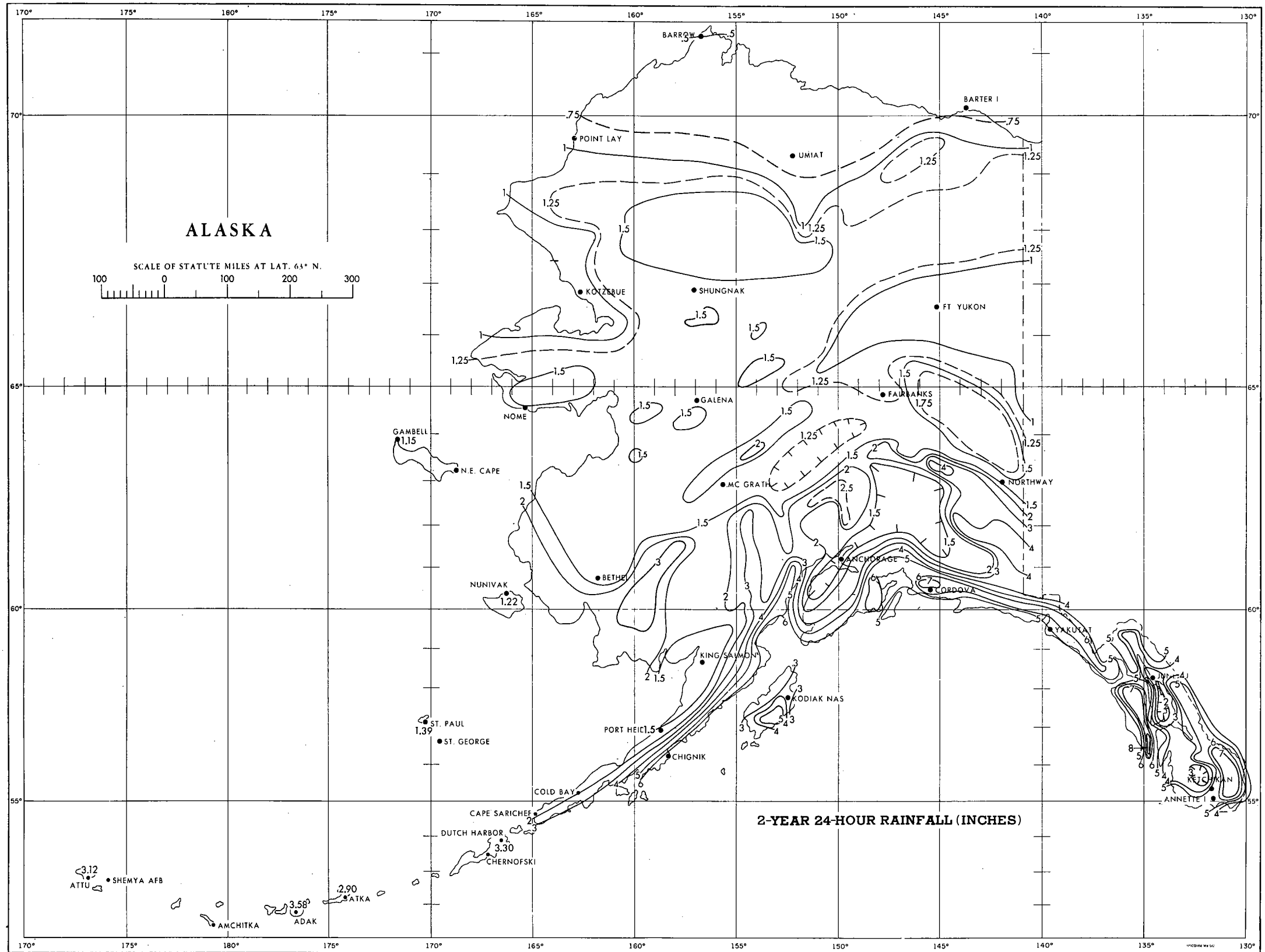


FIGURE 3-54.—2-yr. 24-hr. rainfall (in.).

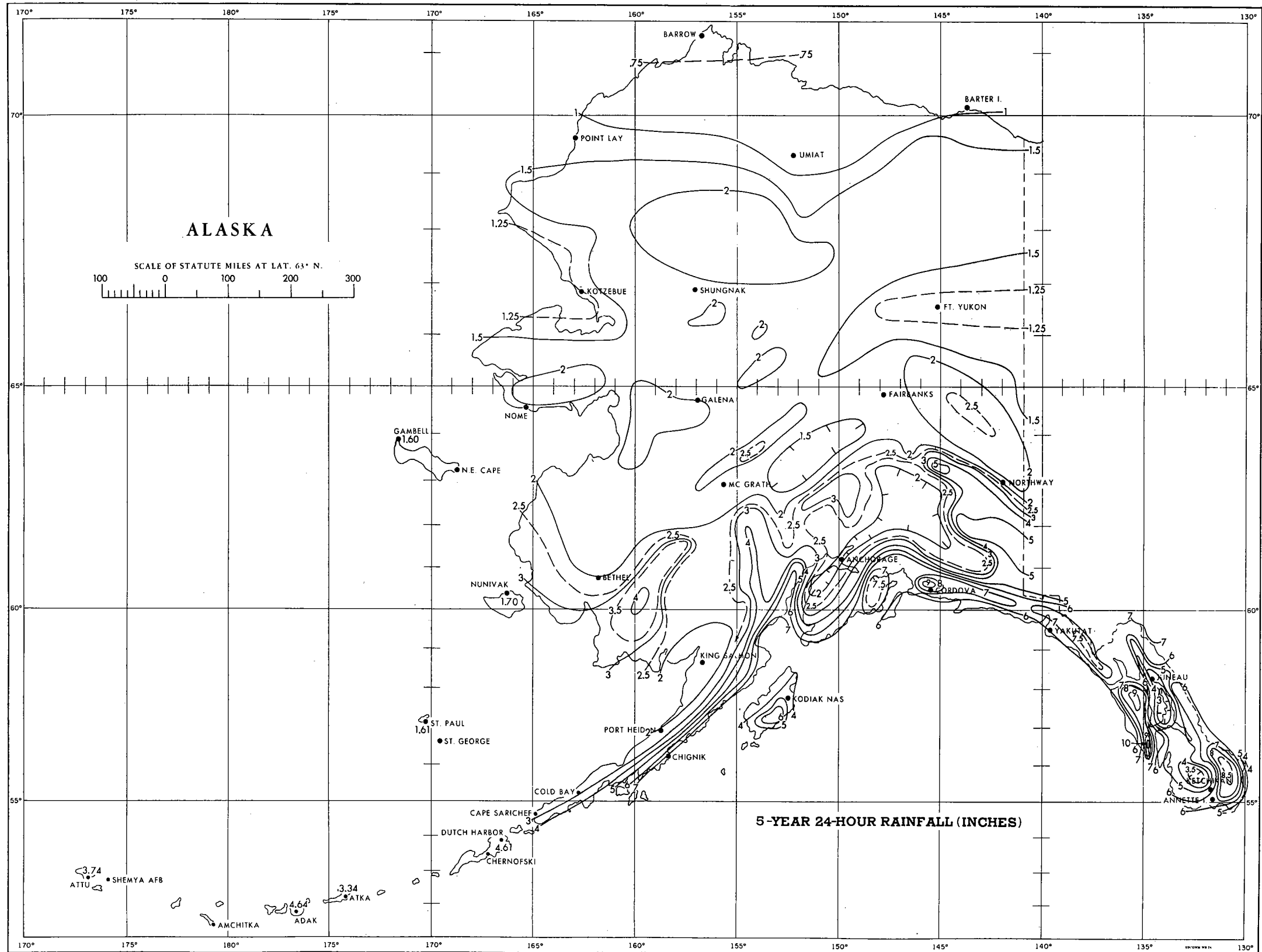


FIGURE 3-55.—5-yr. 24-hr. rainfall (in.).

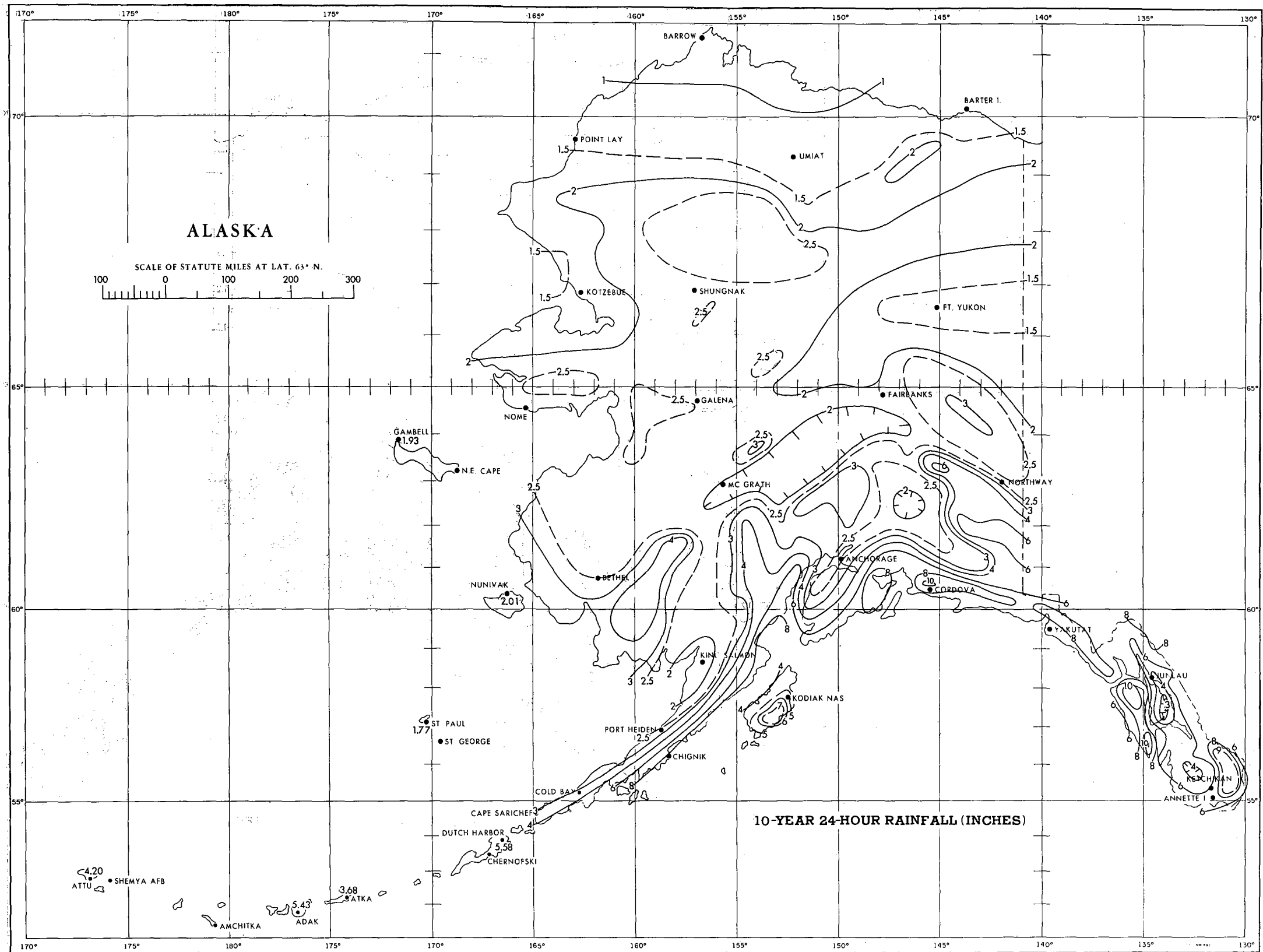


FIGURE 3-56.—10-yr. 24-hr. rainfall (in.).

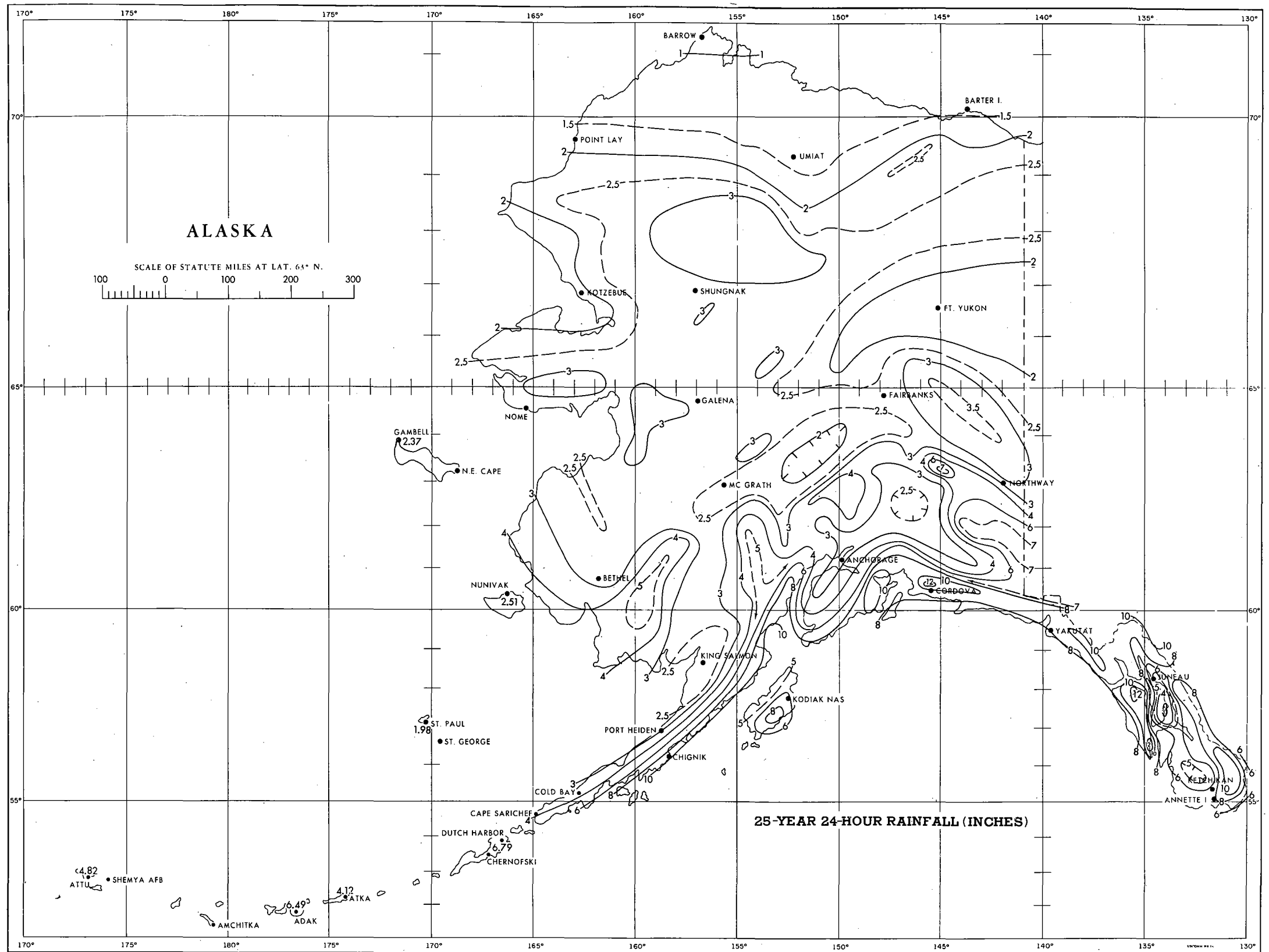


FIGURE 3-57.—25-yr. 24-hr. rainfall (in.).

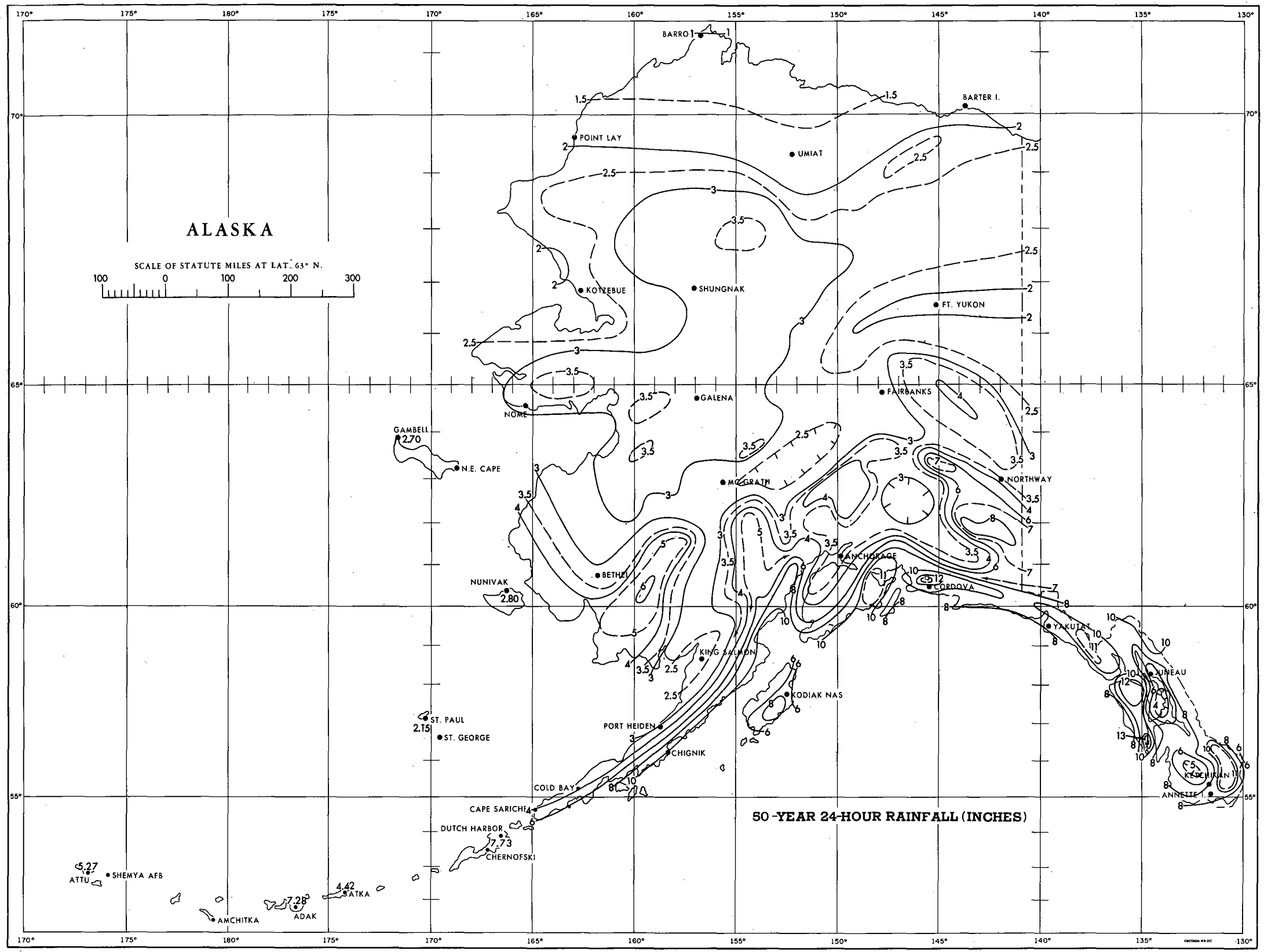


FIGURE 3-58.—50-yr. 24-hr. rainfall (in.).

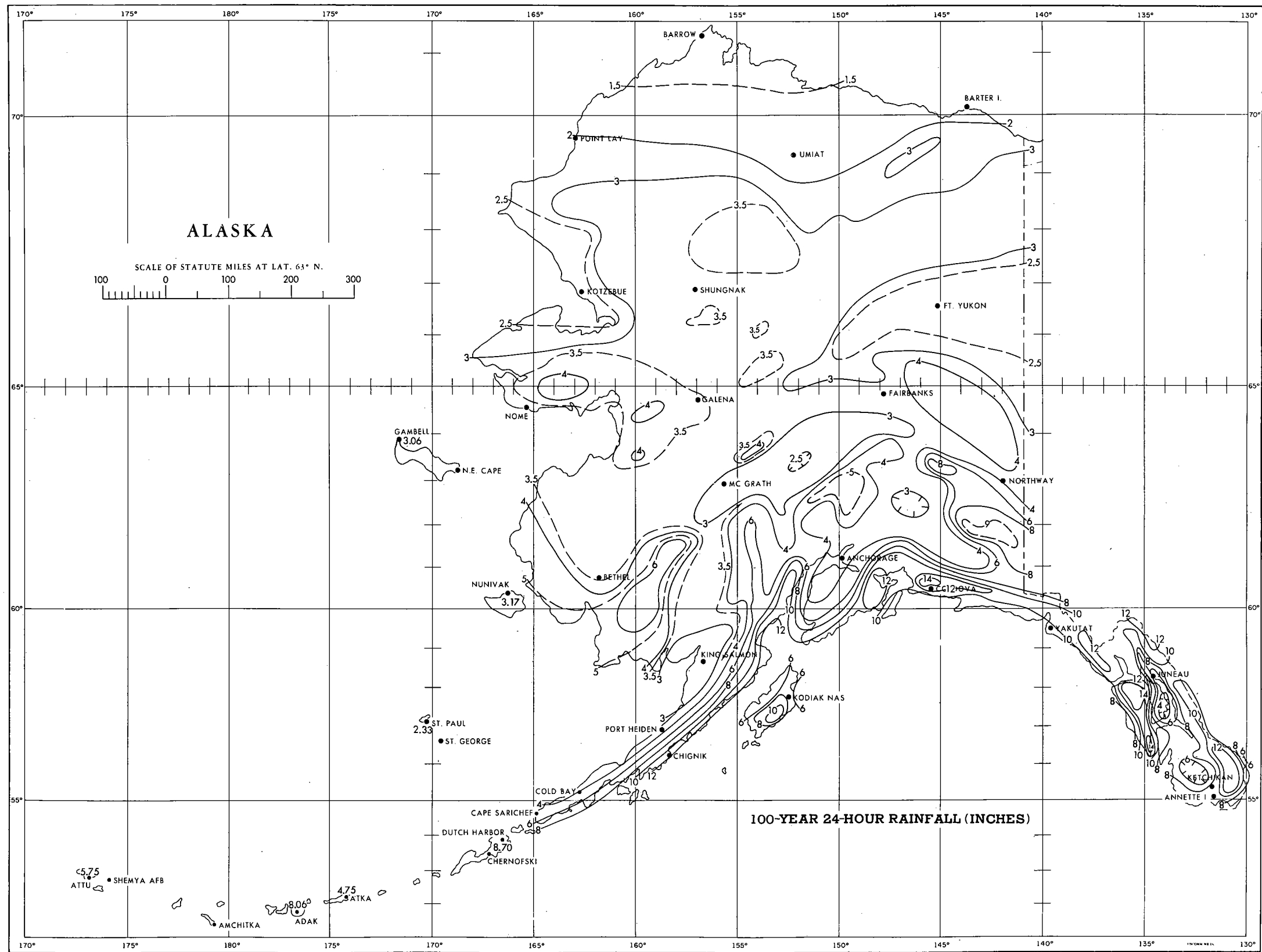


FIGURE 3-59.—100-yr. 24-hr. rainfall (in.).